B.A.R.C.-557

B.A.R.C.-557

GOVERNMENT OF INDIA
ATOMIC ENERGY COMMISSION

ANNUAL REPORT OF THE NUCLEAR PHYSICS DIVISION 1970

Edited by

P. K. Iyengar and N. S. Satya Murthy
Nuclear Physics Division

BHABHA ATOMIC RESEARCH CENTRE
BOMBAY, INDIA
1971

B. A. R. C. -557

B. A. R. C. -557

GOVERNMENT OF INDIA
ATOMIC ENERGY COMMISSION

ANNUAL REPORT
OF THE
NUCLEAR PHYSICS DIVISION
1970

Edited by
P. K. Iyengar and N. S. Satya Murthy
Nuclear Physics Division

BHABHA ATOMIC RESEARCH CENTRE
BOMBAY, INDIA
1971

FOREWORD

This is the second year that the activities of the Nuclear Physics Division are being documented in the form of a detailed,self-contained report. During this year various research programmes in Solid State Physics, Fission Physics and Low Energy Nuclear Physics have continued to make substantial contributions in the respective fields. The Seismology Section has not only established itself as a source of high quality seismic data but also used it in several studies in geophysics. There has been considerable progress in the work on the Zero Energy Critical Facility of the Pulsed Fast Reactor Project.

The staff strength of the Division has remained essentially the same as in the previous year. The number of different research and development activities have however increased.

I trust this report will prove a useful piece of document.

P.K. Iyengar

CONTENTS

A. NUCLEAR PHYSICS

The 5.5 MeV and the 400 keV accelerators at the Centre and the cascade generator at Tata Institute of Fundamental Research continue to be used in the investigations of nuclear reactions and nuclear spectroscopy. The experimental facilities now include a six-gap "orange" β -spectrometer for the measurements involving conversion electrons. A 4096 channel analyser with line printer units and a 1024 x 400 channel two parameter analyser have been installed during the year. These have been used in the experiments involving two-parameter analysis. Two Ge(Li) detectors, one of 30 cc volume - coaxial detector (Nuclear Diode Inc.) and another - a planar detector - 6 cc volume are also in use now.

The theoretical work in nuclear physics mainly centres on the study of nuclear structure through high energy reactions.

I. NUCLEAR REACTIONS AND SPECTROSCOPIC STUDIES

Reactions induced by protons on ^{32}Si, ^{64}Ni, ^{66}Zn and ^{72}Ge have been used to study the isobaric analogue states in compound nuclei. Isobaric analogue states in ^{36}Ar and ^{65}Cu have been identified in the reactions $^{35}Cl(p,p)^{35}Cl$ and $^{64}Ni(pn)^{64}Cu$. The γ -decay of the isobaric analogue state in ^{33}Cl to its antianalogue has been studied in $^{32}S(p,r)^{33}Cl$ reaction. Studies on the isobaric analogue states have been used as a spectroscopic tool to study the low lying energy levels of ^{67}Zn and ^{73}Ge. These studies include elastic scattering of protons on ^{66}Zn and inelastic scattering of protons on ^{72}Ge. The level structure of ^{75}Se has been investigated by detecting the conversion electrons and γ -rays from the excited states of ^{75}Se as produced in $^{75}As(p,n)^{75}Se$ reaction. Life times of levels in ^{75}Se, $^{103,105}Rh$, $^{107,109}Ag$, ^{111} have been measured.

Transient magnetic fields at ^{103}Rh nuclei recoiling into ferromagnetic materials have been investigated using recoil ion implation techniques.

1. A Study of the $^{64}Ni(p,n)^{64}Cu$ Reaction

(S.S. Kerekatte, S.K. Gupta and A.S. Divatia)

The (p,n) reaction on a ^{64}Ni target, has been investigated to identify the isobaric analogue resonances in the nucleus ^{65}Cu, corresponding to the parent nucleus ^{65}Ni. Recently, this reaction has also been studied by the Duke group[1] from E_p = 2.5 - 3.3 MeV. In the energy range E_p = 2.5 - 5.5 MeV scanned in the present investigation, strong resonances have been observed which are superimposed on the Ericson type statistical fluctuations.

A metallic ^{64}Ni target (enriched to 97%) was prepared by evaporating ^{64}Ni metal from a heated tungsten ribbon on to a tantalum backing foil. A 4π - geometry neutron counter was used to measure the yield of the reaction. The absolute cross-section has not been extracted. The relative cross-section is accurate to within ± 5%. The measured excitation function is shown in Fig. 1 and 2.

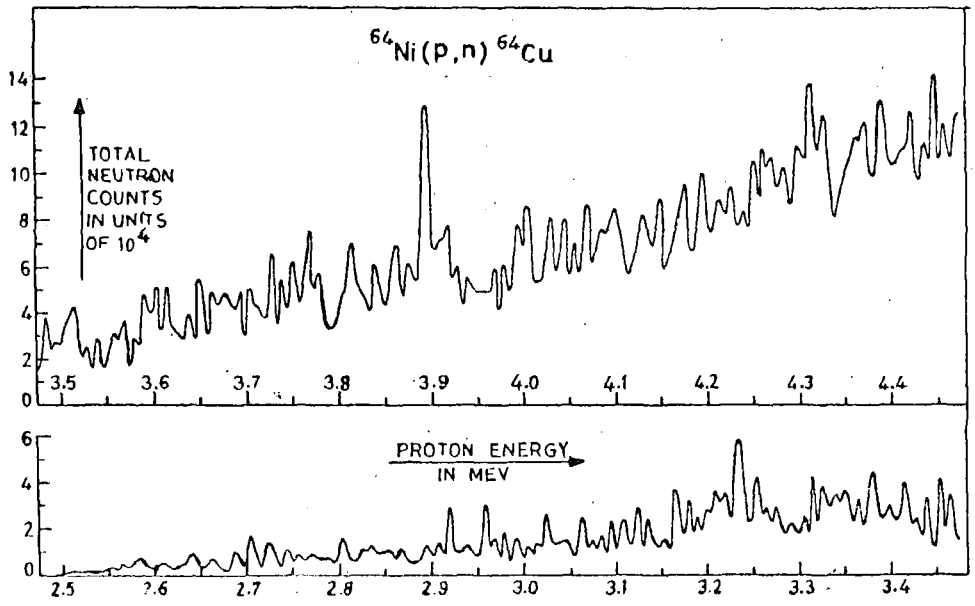

Fig. 1. Total neutron yield in the $^{64}Ni(p,n)^{64}Cu$ reaction for incident proton energies between 2.5 and 4.475 MeV.

The threshold of the reaction has been observed at E_p = 2.500 ± .005 MeV. The average cross-section gradually increases with the incident

proton energy due to the increase in the penetrability factor. The cross-section shows fluctuations. The average width of the compound

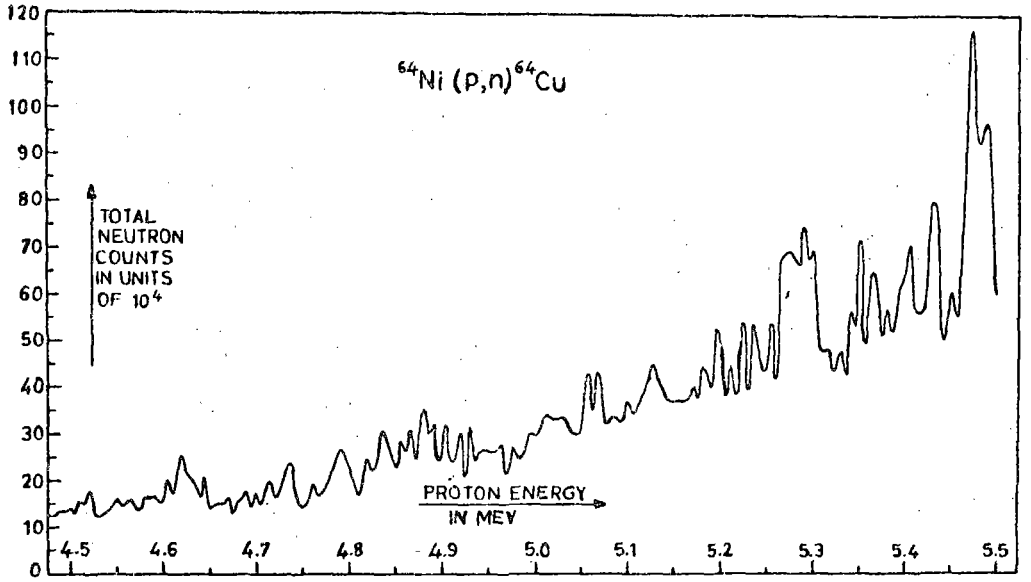

Fig. 2. Total neutron yield in the ^{64}Ni(p,n)^{64}Cu reaction for incident proton energies between 4.475 and 5.5 MeV.

nuclear levels is calculated to be $\sim 7 \pm 1.5$ KeV, using the peak counting method[2] and has been approximately corrected for the experimental resolution.

The ground state analogue of ^{65}Ni cannot be observed because it is due to $l_p = 3$. The Duke group observed the analogue of the first excited state at $E_p = 3.217$ MeV. Accordingly, the other analogue resonances are expected at $E_{p\ lab} = 3.471$, 3.861, 4.188, 4.591, 4.779, 4.968, 5.100 and 5.338 MeV. Out of these, on the basis of the spectroscopic factor for the parent states observed through the ^{64}Ni(d,p)^{65}Ni reaction[3] and the penetration factor criterion, the resonances at 3.861, 4.591, 4.779 and 5.338 MeV are strong. Experimentally, the strong resonances at $E_{p\ lab} = 3.895$, 4.620 and 4.790 MeV have been observed corresponding to the expected resonances. Strong resonances are also observed at $E_{p,\ lab} = 3.235$, 4.310 and 5.470 MeV which do not correspond to the known levels in ^{65}Ni. The resonance at $E_p = 3.895$

MeV is having the asymmetry predicted by Robson et al[4] in the (p,n) reactions.

---

1. J.C. Browne, H.W. Newson, E.G. Bilpuch and G.E. Mitchell, Nucl. Phys. A153,481(1970)

2. A. Van der Woude, Nucl. Phys. 80,14(1966)

3. R.H. Fulmer and A.L. McCarthy, Phys. Rev. 131,2133(1963)

4. D. Robson, J.D. Fox, H. Richard and C.F. Moore, Phys. Letters, 18,86(1965)

2. A Doorway State Observed as a Resonance in the $^{35}Cl(p,p_o)^{35}Cl$ Reaction

(S.K. Gupta, S.S. Kerekatte, S. Swami*, M.R. Dwarakanath**
K.K. Sekharan***, and A.S. Divatia)

The elastic proton scattering from the ^{35}Cl nucleus from $E_{p\ lab}$ = 2.380 MeV to 2.620 MeV has been studied to look for the isolated bound doorway states having a large coupling to the entrance channel. Doorway states were postulated to describe microscopically, the mechanism of nuclear reactions. So far the isobaric analogue states have been the only reported doorway states. The difficulties encountered in pinning down a doorway state of another type, experimentally and theoretically, are numerous. If the attention is concentrated on the bound isolated doorway states with a large decay width to the entrance channel, the experimental identification becomes definite. Payne[1] has theoretically investigated the elastic scattering of neutrons from the single closed shell even-even nuclei. His calculations, however, are approximate and are applicable to a very limited number of cases. The calculations for other cases are not actually available. The major difficulty in solving the doorway state problem theoretically is to deal with the complications of the nuclear structure as well as the nuclear reaction calculations.

The targets were prepared using NaCl having ^{35}Cl enriched to 99.32% on carbon backings. The scattered protons were detected using four solid states detectors at lab. angles of 98°, 113.8°, 138.5° and 155°. The data was taken in 2 keV steps. Bosnjakovic et al[2] have already investigated the $^{35}Cl(p,\alpha_o)^{32}S$ reaction in the same energy range. Fig. 3 shows their results along with the present data. A resonance at $E_{p\ lab}$ = 2.463 MeV

with a width of 16 keV appears only in the proton channel. As this resonance anomaly appears at all the four angles, it is consistent with an $\ell_p = 0$, $J = 2^+$ assignment. This assignment is not, however, unique.

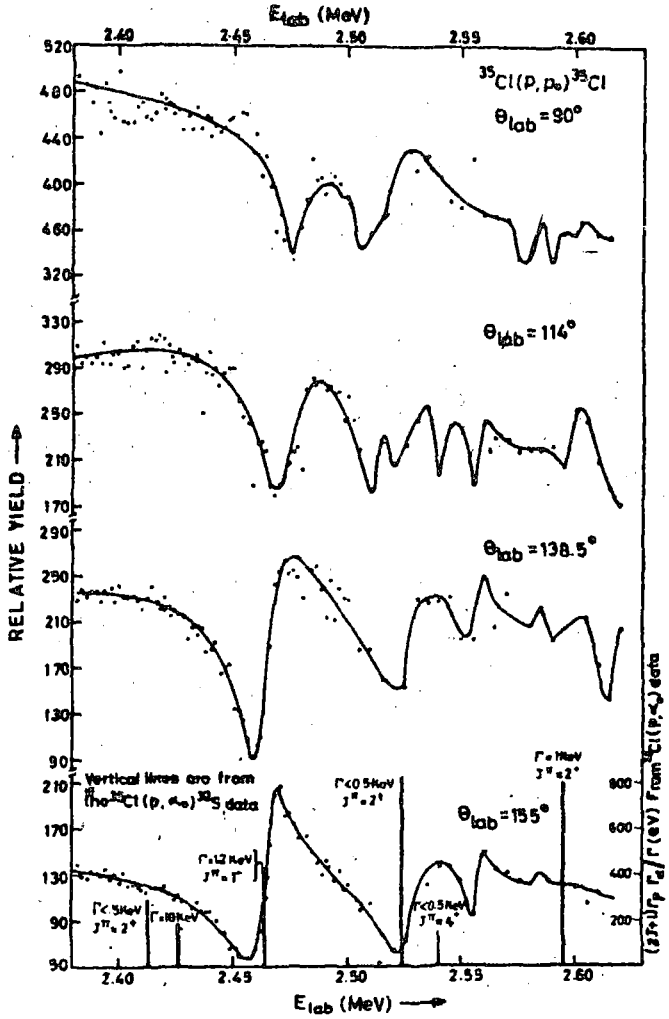

Fig. 3. Relative proton yield in the $^{35}Cl(p,p_0)^{35}Cl$ reaction. The data of Basnjakovic et al[2] is also shown for comparison.

The calculations of Payne[1] reveal that the isolated bound doorway states should appear at an incident energy of 2 to 3 MeV with a typical width of 50 - 100 keV in neutron elastic scattering. Taking into account the Coulomb effects, the width of the doorway state changes from 100 keV to 15 keV for $\ell_p = 0$ protons at $E_p = 2.0$ MeV. Glaudemans et al[3] have carried out bound state calculations within s-d shell

using an empirically determined residual interaction. In the configuration space made up of $s_{1/2}$ and $d_{3/2}$ subshells, the doorway states can have only $(s_{1/2})^3 (d_{3/2})^5$ or $(s_{1/2})^4 (d_{3/2})^4$ configurations. Glaudemans et al find a level at an excitation of 10.5 MeV with $J^\pi = 2^+$, T = 0 in ^{36}Ar with a 67% $(s_{1/2})^3 (d_{3/2})^5$ and a 11% $(s_{1/2})^4 (d_{3/2})^4$ configuration. The resonance observed here corresponds to a state in ^{36}Ar at 10.901 ± .005 MeV with a c.m. width of 15 keV. Thus these observations are consistent with the expected behaviour of the doorway states as calculated by Payne as well as the shell model calculations for bound states which will not differ substantially for the unbound states.

---

* Member of Indian Institute of Technology, Bombay.

** Now at the California Institute of Technology, U.S.A.

*** Now at the University of Kentucky, U.S.A.

1. G.L. Payne, Phys. Rev. 174,1227(1968)

2. B. Bosnjakovic, J. Bouwmeester, J. A. Van Best and H.S. Prays, Nucl. Phys. A114, 7 (1968)

3. P.W. Glaudemans, G. Wiechers and P.J. Brussard, Nucl. Phys. 56, 529(1964); 56,548(1964).

NC

3. Evidence for Doorway States in ^{29}Si(α,n)^{32}S Reaction

(M. Balakrishnan, M.K. Mehta and A.S. Divatia)

According to Feshbach et al[1] doorway states will be most readily observable if the number of open channels which are detected experimentally is small, so that total cross-section in a neutron induced reaction is least sensitive to the presence of doorway states. Hence the most suitable case for detection of doorway state is in the cross-section measurements for light nuclei at low energies, wherein the spreading width $\Gamma_{d\downarrow}$ can be relatively small. From this point of view the reaction ^{28}Si(α,n)^{32}S seems appropriate.

An examination of data reported earlier[2] and shown in Fig. 4 shows following details. (a) Resonances are about 10 keV wide, and $\langle\Gamma\rangle/\langle D\rangle > 0.3$ for the region of excitation around 10 MeV in ^{33}S.

This is in agreement with the widths and $\langle \Gamma \rangle / \langle D \rangle$ ratio known for ^{33}S in this region[3,4]. (b) There is an indication for the presence of gross structures, superposing the finer variations in cross-sections with energy. (c) The gross structures are not distributed at random, but there is a regularity in the

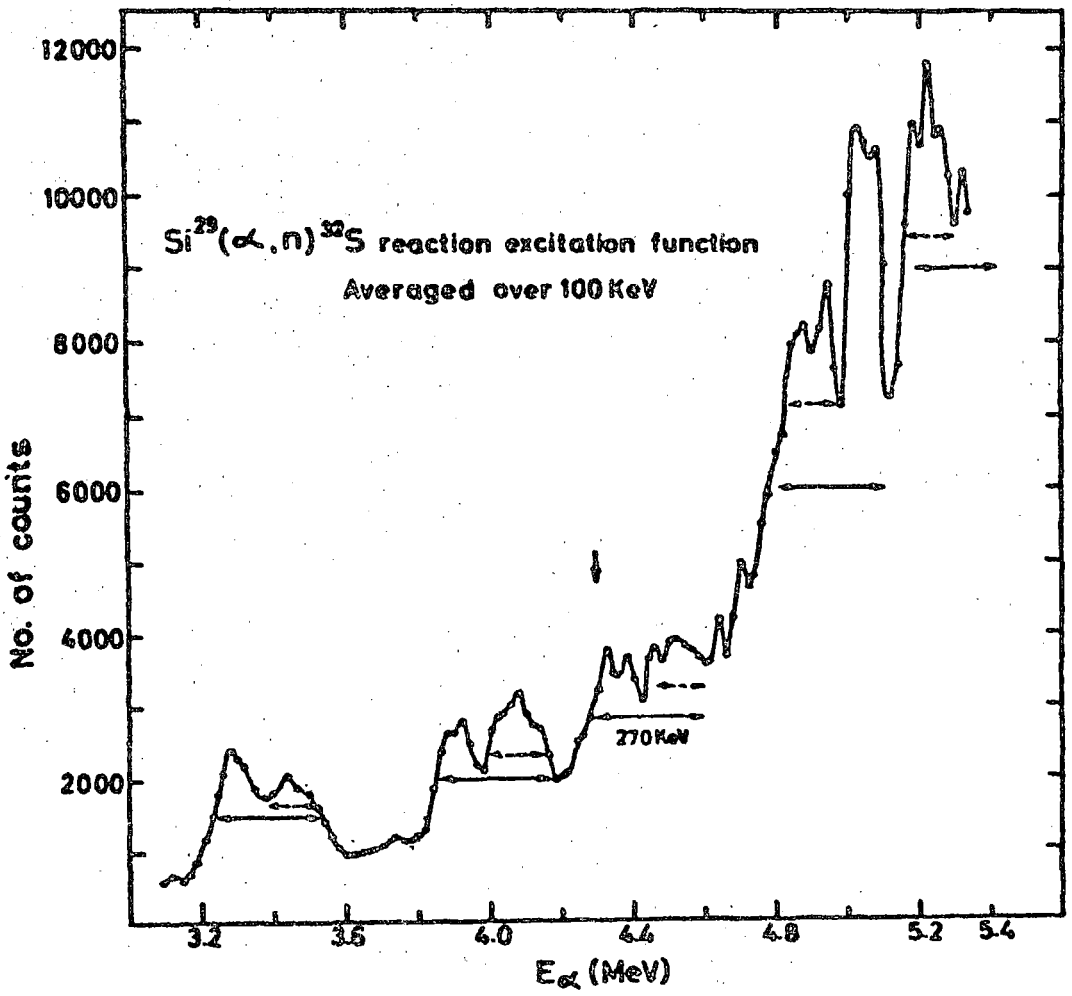

Fig. 4. The excitation function for the reaction $^{29}Si(\alpha,n)^{32}S$ showing the width of the resonances.

distribution of widths and energy spacings of these structures.

(d) The cross sections show more intense peaks within each of these broad structures than in between them.

The excitation function averaged over 100 keV are whown in Fig. 4, where structures of width around 270 keV with spacing of 500 keV are present. From observation (a), it can be seen that in this region of excitation Ericson fluctuations[5] are not valid. This is also supported by the fact that (n, α) and (n,p) correlation exists[6] in ^{32}S - and that compound nucleus cross-sections are not lumped. Hence accidental lumping of resonance states as discussed by Singh et al[7], wherein spurious "intermediate" like structures are built up, can be ruled out. For the region of excitation where $\langle\Gamma\rangle/\langle D\rangle$ is not too large and correlation exists between various entrance or exit channels, the structures have been qualitatively explained as due to statistical fluctuations in the average level densities of the compound nuclei involved[8]. From the observations (b) and (c) above, it is improbable that such an explanation can account for these structures.

A more realistic possibility is to explain these structures as due to simple modes of excitation of the compound nucleus. The reduced alpha width, for the single particle Wigner limit $\theta^2 = 3\hbar^2/2MR^2$ is 430 keV which is twice as great as the observed width 270 keV. Doorway states described as three quasiparticle states can account for a width of about 200 to 250 keV for nuclei in this mass region[1]. Shakin[9], Lande and Block[10] estimated that the number of three quasi-particle states that can occur per MeV energy spread is around three, in this region of excitation

for medium heavy nuclei. This is consistent with the separation of 500 keV observed for light nuclei as in the present experiment. Since each three quasi-particle states should be characterised by a unique angular momentum, it will be quite interesting to see the differential cross-sections for these structures, to check whether a unique angular momentum can be attributed to each of them. The expected spreading of the doorway states over many compound nuclear states (observation (d)) may make it more difficult to observe this.

---

1. H. Feshbach, A.K. Kerman and R.H. Lemmer; Ann. Phys. (N.Y.) 41, 230 (1967)
2. M. Balakrishnan, K.K. Sekharan, M.K. Mehta and A.S. Divatia, Proceedings of Nucl. Phys. & Solid State Phys. Symp., December 1968, p.57
3. P.M. Endt and C. Van der Leun, Nucl. Phys. A105,216(1967)
4. A.D. Carlson and H.H. Barschall, Phys. Rev.158,1142(1967)
5. i) T. Ericson, Phys. Rev. Lett. 5,430(1960)
   ii) T. Ericson, Ann. Phys. (N.Y) 23,390(1963)
6. A. Agodi, G. Pappalardo, R. Ricamo and D. Vinciguerra, Nuovo Cimento 23,1136(1962)
7. P.P. Sinha, P. Hoffman-Pinther and D.W. Lang, Phys. Lett. 23, 255(1966)
8. i) G. Calvi, R. Ricamo, A. Rubbino and D. Zubke, Nucl. Phys. 48,408(1963)
   ii) A. Agodi and G. Pappalardo, Nucl. Phys. 47,129(1963)
9. C. Shakin, Ann. Phys. (N.Y.) 22,373(1963)
10. A. Lande and B. Block; Phys. Rev. Lett. 12,334(1964)

4. Study of the Isobaric Analogue State in ^{33}Cl by the ^{32}S(p, γ)^{33}Cl Reaction

(M.A. Eswaran, M. Ismail, N.L. Ragoowansi and H.H. Oza)

Proton decay of the T = 3/2, T_z = - 1/2 states are energetically possible only to the T = 0 states in the neighbouring (A = 4n, Z = 2n) nucleus although such a breakup is isospin-forbidden. However, since

the only isospin-allowed decay is by gamma emission, even a slight violation of isospin conservation will permit proton emission to compete successfully. Hence the $T = 3/2$, $T_z = -1/2$ states can be formed by proton capture and the exit channel in which these states are most likely to be clearly exhibited is in the gamma channel since this is the only decay mode, that is not T-forbidden. In the present work the (p,γ) reaction has been used to study the lowest $T = 3/2$ state in ^{33}Cl.

A mechanically chopped proton beam ($\sim$ 1.5 μA) passed through thin ($\sim$ 200 $\mu g/cm^2$) natural Sb_2S_3 target evaporated on to a thick gold backing which was watercooled. The detector consisted of a 30 cm^3 Ge(Li) γ-ray detector with a single channel analyser set to select the pulses in the 511 keV annihilation radiation peak, generated by the annihilation of positrons, arising from the decay $^{33}Cl \rightarrow ^{33}S$ with 2.52 sec. half-life. The 511 keV peak pulses from the single channel analyser were fed into a pulse-height analyser operated in a multiscaler mode with 0.1 sec per channel. The operating cycle (bombard the target for 4 sec., and then count for 20 sec.) was repeated until a fixed charge was accumulated. The resultant time spectrum showed the expected 2.52 sec. activity plus a constant background. For obtaining the excitation function over the resonance, only the counts in the time spectrum corresponding to first two half-lives were taken after subtracting the constant background.

The delayed proton work[1] had found the lowest $T = 3/2$ level in ^{33}Cl at 5.556 $\pm$ 0.020 MeV, E_p(c.m.) = 3.266 $\pm$ 0.020 MeV. In agreement with this, a search through this region Fig. 5(a) located the resonance at E_p = 3.371 $\pm$ 006 MeV (E_p(c.m.) = 3.269 MeV). This corresponds to an excitation energy in ^{33}Cl of 5.559 $\pm$ .006 MeV. The slope of the yield curve at resonance could be entirely attributed to the energy spread in the proton beam. From this it is deduced that the total width of the level is less than 2.5 keV. The proton width Γ_p and the total width Γ for this resonance as determined from proton elastic scattering experiments have been reported[2] to be 125 eV.

The integrated yield over the (p,γ) resonance in the present has been found by comparison with the resonance in the same reaction at E_p = 2.547 MeV as well as from the comparison of the gamma ray yield at the E_p = 0.588 resonance. From these measurements preliminary value of the resonance strength and hence Γ_1 for the E_p = 3.371 MeV resonance has been obtained.

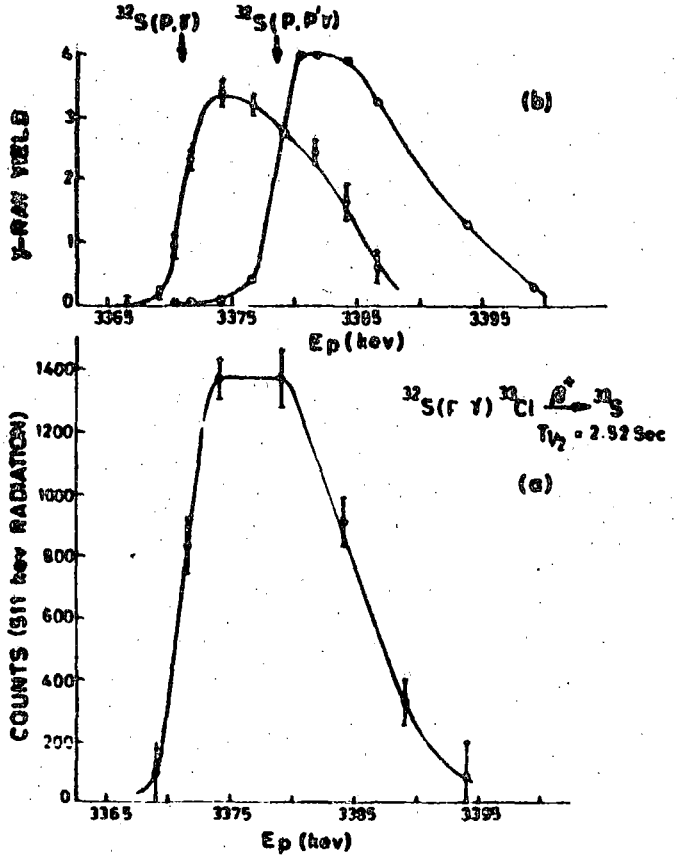

Fig. 5. The 511 keV γ yield as a function of proton energy in the reaction $^{32}S(p, \gamma)^{33}Cl$ showing the resonance at 3.371 MeV.

At this resonance the γ-spectrum has been measured with the 30 c.c. Ge(Li) detector and is shown in Fig. 6. For comparison, the gamma

spectrum taken at "off-resonance" is shown. These measurements show that the only significant transition from the resonance is to

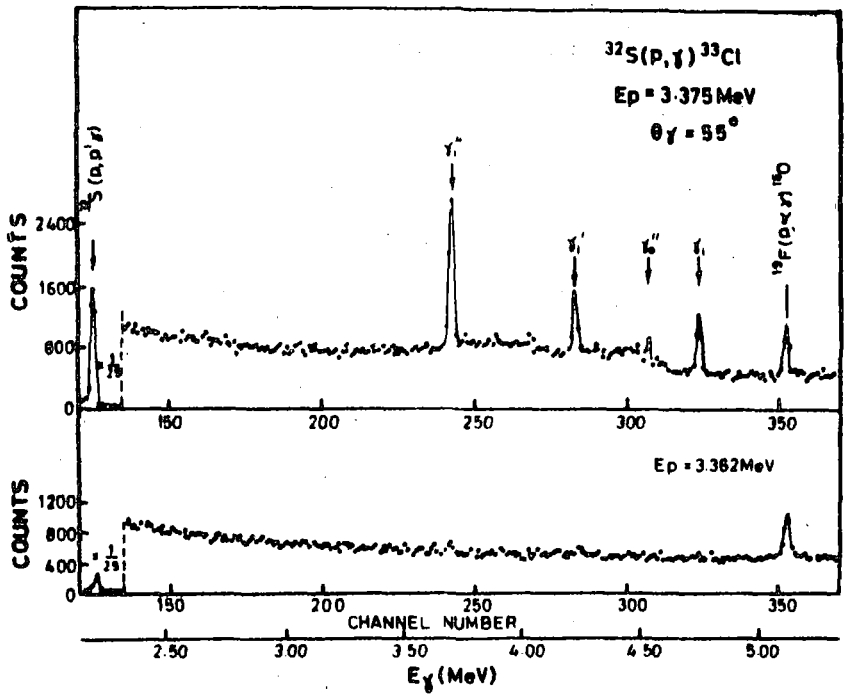

Fig. 6. The γ spectrum at the 3.371 MeV (Ep) resonance in the reaction $^{32}S(p,\gamma)^{33}Cl$. The off-resonance spectrum is also shown.

the 0.806 MeV($1/2^+$) first excited state in ^{33}Cl. This tansition from the 5.559 MeV (J = 1/2, T = 3/2) state in ^{33}Cl (which is the analogue of the ground state of ^{33}P) to the 0.806 MeV(J = 1/2, T = 1/2) state in ^{33}Cl is a pure M1 of moderate strength and can be conjectured to be the "analogue to the anti-analogue" transition. (Preliminary results of this work have been reported in reference(3))

---

1. A.M. Poskanzen, R. Mc Pherson, R.A. Esterlund and P.L. Reader, Phys. Rev. 152,995(1966)

2. G.M. Temmer in 'Nuclear Isospin' (Proc. Conf. on Nuclear Isospin, Asilomar, p. 87 (1969)

3. M.A. Eswaran, M. Ismail and N.L. Ragoowansi, Bull. Ann. Phys. Soc. 15,1689(1970)

5. Isobaric Analogue States in ^{67}Ga

(M.G. Betigeri, C.M. Lamba, N. Sarma
D.K. Sood and N.S. Thampi)

States at high excitation energy in ^{67}Ga are populated by the proton bombardment of ^{66}Zn and these are identified to be the isobaric analogues of the low lying states of ^{67}Zn. In the incident proton energy range of 2.9 MeV to 3.9 MeV, 5 analogue states corresponding to 93, 184, 390, 978 and 1142 keV level in ^{67}Zn have been identified. The states corresponding to the ground state and the 602 keV level in ^{67}Zn could not be observed because of high value of the orbital angular momentum involved. The theoretical analysis of the excitation functions at three angles 90°, 125° and 165° was carried out using the programme BRIGHT as modified for the CDC-3600 computer. The analysis yields values for the resonance parameters namely the resonance energy, the total width of the resonance, the partial width of resonance for decay back into the elastic channel and the value of the orbital angular momentum required to populate these levels. The results are tabulated in Table I.

Table I

Results of ^{66}Zn + p isobaric states in ^{67}Ga

Ep(meV)	E_{exc} in ^{67}Ga(MeV)	Energies of levels in ^{67}Zn(keV) present	^{66}Zn(d,p)	l	Γ keV	Γ_p keV
2.929	8.202	93	93	1	4.5	0.41
3.0210	8.294	184	184	1	3.62	0.04
3.227	8.500	390	389	1	4.0	
3.814	9.087	978	980	1	10.54	0.34
3.978	9.251	1142	1142	1	14.10	0.75

The l-values agree with those obtained from $^{66}Zn(d,p)^{62}Zn$ reaction[1]

except in the case of 978 keV level where the analysis assigns a value of l = 1 as against l = 2 in (d,p) study.

Efforts are in progress to calculate the spectroscopic factor for transition to these states in ^{67}Zn - as reflected through the partial width parameter for the various isobaric analogue resonances.

---

1. D. Von Ehrenstein and J.P. Schiffer, Phys. Rev. 164,1374(1967)

6. Spectroscopy of ^{73}Ge

(M.G. Metigeri, C.M. Lamba, D.K. Sood and N.S. Thampi)

The low lying levels of ^{73}Ge occur as isobaric analogue states in ^{73}As which can be studied as compound nuclear states in ^{72}Ge + p reaction. In the elastic scattering channel, these resonance are observed[1] as anomalies in the excitation function - because of their interference with the potential scattering. However, in a reaction, they are observed as resonances without any interference and hence the resonance energy determination is accurate. The reaction $^{72}Ge(p,p'e)^{72}Ge$ has been studied. Here the levels of ^{73}As found by ^{72}Ge + p decay inelastically to $^{72}Ge(0^+)$ at 690 keV. The observation of the inelastic group is difficult in view of the fact the elastically scattered particles off carbon cover this group. However, since the 690 keV 0^+ level decays to ground state 0^+ of ^{72}Ge by internal conversion process, the observation of the inelastic group is equivalent to observing the conversion electrons.

The electrons were detected by a six gap "Orange" beta-spectrometer with a transmission of 8%. The excitation function (Fig. 7) taken between incident proton energies of 3.30 to 4.8 MeV indicates 17 analogue states corresponding to various parent levels in ^{73}Ge in the energy range of 13 keV to 1310 keV and are listed in Table I. The

energy positions agree well with the results obtained from the reaction $^{73}Ge(pp')\ ^{72}Ge(d,p)$.

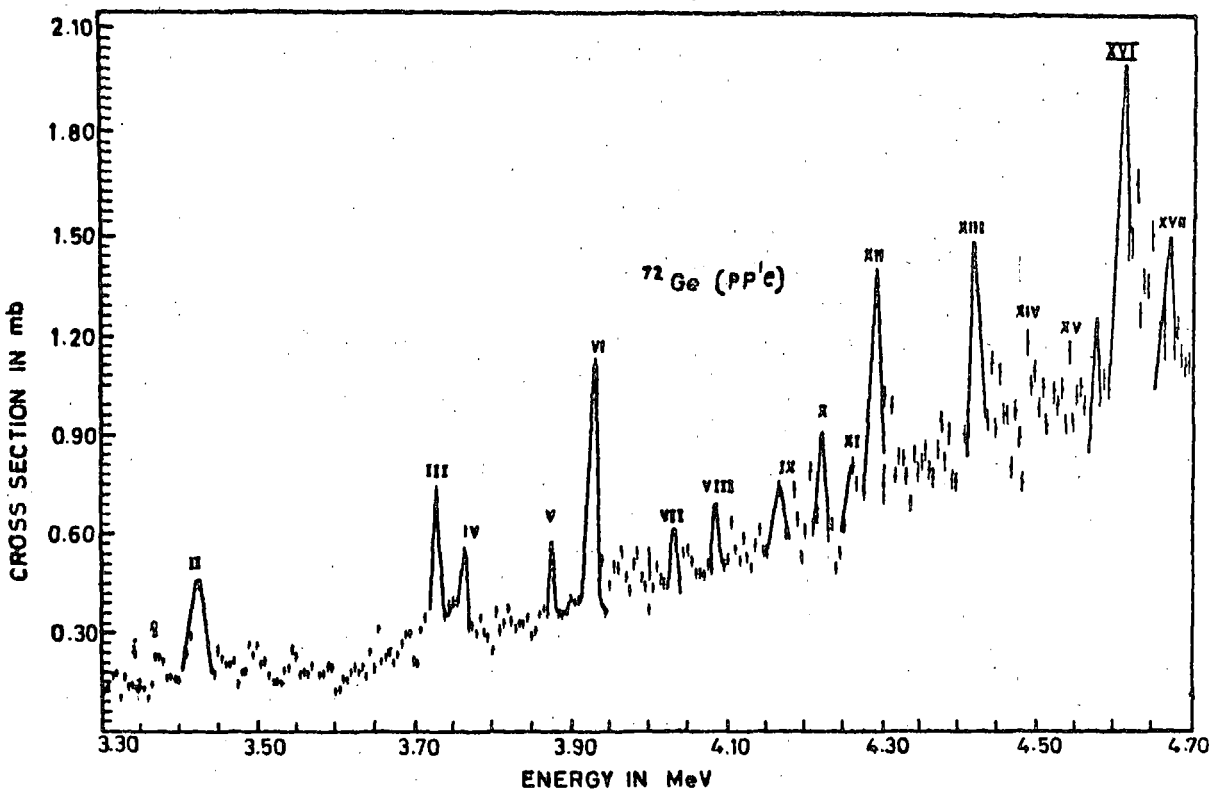

Fig. 7. The excitation function for the reaction $^{72}Ge(p,p'e)^{72}Ge$.

The results indicate that certain resonances which are strong in (pp'e) data are weak in (pp) data and vice versa. These strong

resonances in (pp'e) are expected to belong to configurations of the type $|\,^{72}Ge(0^+,690)$ + a neutron$\rangle$ whereas the strong resonances in (pp) data belong to $|\,^{72}Ge(0^+,$ g.s) + a neutron$\rangle$.

Table I

Sr.No.	$E_{exc.}$ in (keV) $^{73}Ge^*$	Energies as observed in $^{72}Ge(dp)$	$^{73}Ge(pp')$
1	13	13	-
2	65	67	67
3	370	368	-
4	400	396	-
5	515	512	498
6	570	563	551
7	673	666	656
8	725	727	-
9	805	-	825
10	860	864	867
11	900	904	-
12	930	926	918
13	1055	1051	1039
14	1130	1141	1132
15	1180	1176	-
16	1250	1274	-
17	1310	1322	1318

* assumes a coulomb energy displacement of 10070 keV.

7. Transient Fields on ^{103}Rh in Low Recoil Energies

(C.V.K. Baba, S.K. Bhattacharjee*, H.G. Devare*, H.C. Jain* and M.C. Joshi*)

Transient magnetic fields at nuclei recoiling into ferromagnetic materials in IMPACT experiments have been discussed by Grodzins[1]. In most of these experiments the recoil energy is about 10 MeV. Varga et al[2] made measurements on the 298 keV ($3/2^-$, τ = 9.1 ps) and 360 keV ($5/2^-$ τ = 85 ps) states in ^{103}Rh with a $Fe_{51.5}Rh_{48.5}$ alloy using Coulomb excitation by 2.5 MeV protons. They found the presence of large transient fields even for recoil energies below 100 keV.

^{103}Rh is a suitable case for studying transient field effects because it has two states easily excited in Coulomb excitation having half-lives differing by a factor of ten. Further, the core excitation model makes a prediction for the ratio of the g-factors of the two states. Here, results are presented on 5 at % Rh-Fe alloy using Coulomb excitation with 5.0 MeV alpha particles. Integral Reversed Field (IRF) measurements have been made with a polarising field of 1 kG using a 20 cc Ge(Li) detector. The rotation angle $\omega\tau$ in the angular distribution was measured for the 298 keV and 360 keV gamma rays. The values of $\omega\tau$ obtained are shown in Table I, together with the results of other workers.

Table I

Summary of angular precession ($\omega\tau$) results for ^{103}Rh in Fe

Energy (keV)	τ(ps)	present work[a]	$\omega\tau$(radians) Varga et al[b]	Roney et al[c]
298	9.1 ± 0.7[d]	+0.029±0.077	-0.017±0.004	-0.0004±0.0050
360	85.2 ± 6.1[d]	+0.108±0.014	+0.030±0.012	+0.099 ±0.007

a) 5 at.% Rh-Fe alloy; 5 MeV alpha particles
b) ref.2) $Fe_{51.5}$ $Rh_{48.5}$ alloy; 2.5 MeV protons
c) ref.5) IMPACT; ~ 30 MeV O^{16} ions
d) ref.6)

The sign of $\omega\tau$ is positive for both the states. If it is assumed that the g-factors of both these states are positive, this indicates

that no large transient fields are present as reported in ref.2).

Assuming that transient fields are absent and that only the static field H = -540 KG[3]) acts, it is found that g(298 keV) = 1.15 ± 0.31 and g(360 keV) = 0.48 ± 09. The ratio g(298 keV)/g(360 keV) = 2.4 ± 0.8 is in agreement with the value 1.7 ± 0.4 obtained by Miller et al[4] who used the method of recoil in gas. This ratio is also consistent with the value 1.8 expected on basis of the Core Excitation Model. Thus this experiment suggests that no appreciable transient fields are present in this case.

---

* Members of T.I.F.R.

1. L. Grodzins, Proc. Roy. Soc. A311,79 (1969)
2. L. Varga et al., Phys. Letters 29A,171(1969)
3. D.A. Shirley et al., Phys. Rev. 170, 363(1968)
4. T.R. Miller et al., Bull. Am. Phys. Soc. 14, 1172(1969)
5. W.M. Roney et al., (to be published)
6. F.K. McGowan P.H. Stelson, Phys. Rev.109,901(1958).

8. Study of Gamma-rays and Internal Conversion Electrons following the $^{75}As(p,n)^{75}Se$ reaction

(C.V.K. Baba, S.M. Bharathi*, B. Lal* and Baldev Sahai*)

In this work, the level scheme of odd neutron nucleus ^{75}Se has been studied using $^{75}As(p,n)^{75}Se$ reaction. According to the shell model, the neutrons in this region are expected to be filling $p_{\frac{1}{2}}$ and $g_{9/2}$ orbitals. Thus, low lying $1/2^-$ and $9/2^+$ states are expected. In many odd-neutron nuclei such states have been identified. States arising out of core excitation are also likely. The ground state of ^{75}Se has a spin of $5/2^+$ and has a large ($\sim$ 1.0b) quadrupole moment. The $9/2^+$ and $1/2^-$ states have not been identified so far.

The γ-ray and internal conversion electron spectra following the ^{75}Se reaction have been studied. The internal conversion electron

spectrum has been measured using a six gap 'orange' spectrometer set to 8% transmission at 1.2% momentum resolution. In addition to the transitions in ^{75}Se, some transitions in ^{75}As produced in $^{75}As(p,p^1)$ reaction were also seen. The 279 kev transition in ^{75}As was taken as a standard for conversion coefficient measurements. A 6 c.c. Ge(Li) detector could also be placed together with the spectrometer. A single γ -spectrum with such a detector was taken simultaneously with the internal conversion electron spectrum. A typical internal conversion electron spectrum taken at an incident proton energy of 4.5 MeV, is shown in Fig. 8. The target used was

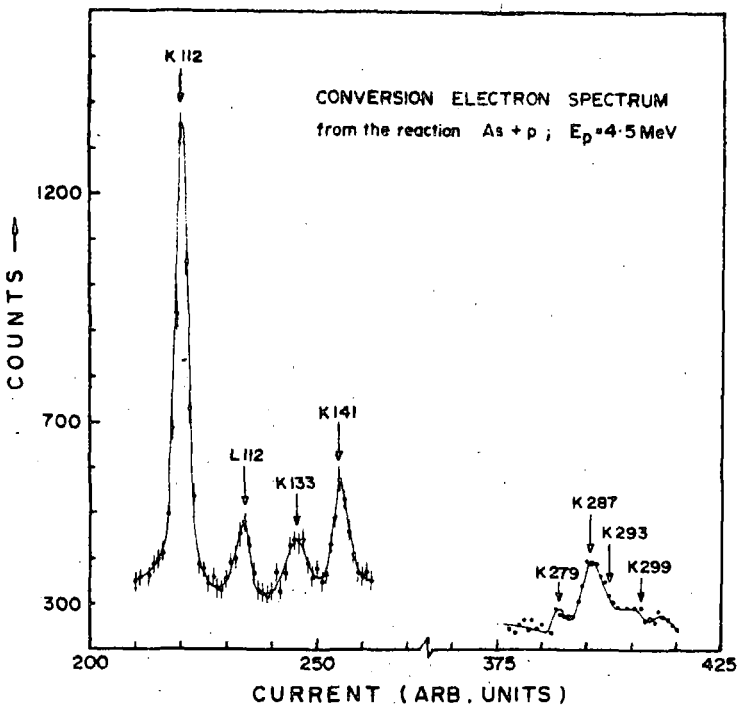

Fig. 8. The internal conversion electron spectrum at a proton energy of 4.5 MeV in the reaction $^{75}As(p,n)\ ^{75}Se$.

$\sim$ 50 $\mu g/cm^2$ of As deposited on a $\sim$ 100 $\mu g/cm^2$ C backing. The multipolarities of the transitions as determined from the present work are: 112 kev (M1), 133 kev (E2), 141 kev (M1), 287 kev (E1) and 377 kev (E2).

On the basis of the $\gamma - \gamma$ coincidence measurements, the following energy levels for ^{75}Se have been inferred: 0 kev ($5/2^+$), 112 kev ($7/2^+$)

133 kev ($9/2^+$), 287 kev ($3/2^-$) and 428 kev ($5/2^-$). The 133 kev ($9/2^+$) located in the present work probably corresponds to the single-particle, $g_{9/2}$ state; while the other positive parity levels are explainable as core excitation states.

A preliminary study of the half lives of the 112 kev, 133 kev and 287 kev levels was also made. The K-conversion electrons of either 112 kev, 133 kev or 141 kev focussed by the beta-ray spectrometer were detected in a plastic scintillator and the γ-rays feeding the levels were also detected in a 5 cm x 5 cm plastic scintillator, which could be placed at a distance of 4 cm from the target. No discrimination was made between γ-rays and the neutrons. The prompt width of the time spectrum was 3.0 ns. The preliminary values of the half lives measured are: 1.5 ± 0.3 ns for the 112 kev state, 5 ± 2 ns for the 133 kev state and 1.2 ± 0.3 ns for the 287 kev state.

---

* Members of T.I.F.R.

9. Life time Measurements in odd Mass Rh and Ag Nuclei

(C.V.K. Baba and H.C. Jain*)

The odd Z nuclei with Z between 40 and 50 show low lying $9/2^+$ and $1/2^-$ levels which are presumably the $g_{9/2}$ and $p_{1/2}$ single particle states. In addition, a $7/2^+$ state is seen very near the $9/2^+$ state; sometimes even lower than $9/2^+$ state in energy. Sherwood and Goswami[1] have explained the energy spacings of these levels on the basis of their 'Extended Quasiparticle Model'. In order to understand the nature of these levels in more detail, half life measurements of the $9/2^+ \rightarrow 7/2^+$ transitions in $^{103}_{Rh}$, $^{105}_{Rh}$, $^{107}_{Ag}$, $^{109}_{Ag}$ and $^{111}_{Ag}$ have been made. In these cases this M 1 transition is expected to be retarded.

In all these cases, the cascades of interest are of very low intensity and further the $9/2^+ \rightarrow 7/2^+$ transition energy is in the region of 30 - 100 kev. Pb loaded plastic scintillator were used to detect the low energy transition, while the higher energy transition was detected in a 5 cm x 5 cm plastic scintillator. Thick Pb absorbers (2mm to 1 cm) were placed in front of the thick plastic detector in order to minimise

the crystal-to-crystal scattering. A conventional time-to-amplitude converter was used to obtain the time spectra. The time resolutions (the full width at half maximum of the prompt curve) obtained varied from 0.7 ns to 2.5 ns depending on the energy of the low energy transition. The time calibration was measured both with delay cables and by measuring the half life of the 122 kev level in ^{152}Sm. As an example of the time spectra obtained, Fig. 9 shows the decay curve for the 126 kev $(9/2^+)$ state of ^{107}Ag, where the energy of the low energy transition is only 33 kev.

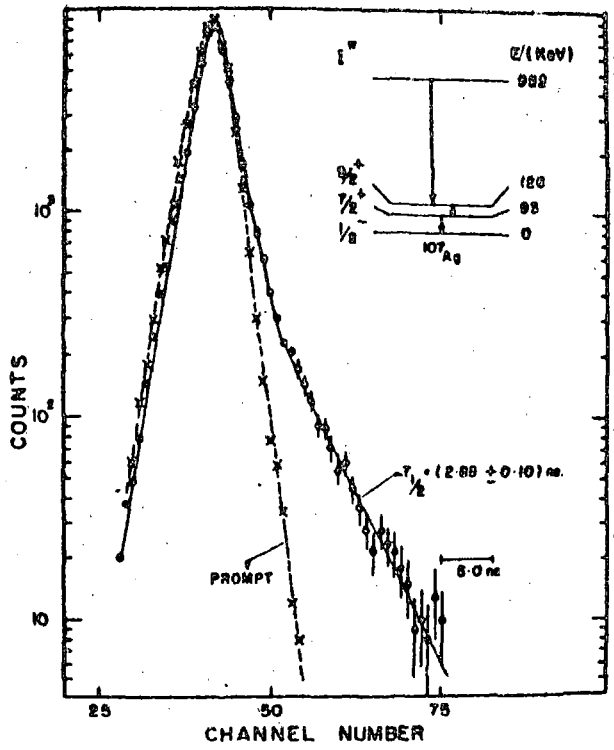

Fig. 9. The γ -decay spectrum of the 126 keV state of ^{107}Ag.

The half life of the states were obtained from a least-squares fit of the data. The results obtained are summarised in Table I. It is found that the M1 transitions are indeed retarded and the retardation factors are also listed in the table. The retardation factors are typically

$\sim$ 50. Similar M1 transitions between $h_{11/2}$ and the corresponding $9/2^-$ level in the odd mass Te isotopes show a retardations of $\sim$ 200.

Table I

Nucleus	Energy of $9/2^+$ Level (kev)	Energy of $9/2^+ \rightarrow 7/2^+$ transition (kev)	Measured T (ns)	M1 Retardation factor
^{103}Rh	93	53	1.13±0.03	20
^{105}Rh	150	150	0.3	60
^{107}Ag	126	33	2.85±0.15	45
^{109}Ag	132	44	2.60±0.12	50
^{111}Ag	130	60	0.95±0.06	30

The E2 admixture is not known in all the cases measured here. In those cases where the E 2 admixture is measured, the E 2 $\sim$ 5 transitions are enhanced by a factor of about 50, which is similar to the enhancement the $2^+ - 0^+$ transitions in the neighbouring even-even nuclei. This is consistent with the $7/2^+$ states being the core excited states.

---

* Member of T.I.F.R.

1. A.I. Sherwood and A. Goswami, Nucl. phys. 89,465(1966)

10. Operation and Maintenance of the Van de Graaff Accelerator.

The 5.5 MeV Van de Graaff Accelerator has worked for 5276 hours during the year 1970. A laboratory-fabricated beam steerer has been installed immediately before the beam switching magnet to facilitate beam alignment in all the five beam ports. Ion source assemblies used with the accelerator have been processed in the laboratory using the modified extraction canals*. Five ion sources have been used during

the year giving an average source life of 1055 hours. A number of replacement accelerator components are now fabricated in the laboratory. These include belt spacers, corona points, charge spray combs, high voltage bushings and resistor housing. The five-port switching magnet installed in 1969 has since been under continuous operation and is giving very satisfactory service. A new belt charge current control unit has been built in the laboratory and tested. This together with the 50 KV RF type D.C. power supply built by the Technical Physics Division constitutes a complete standby system for the accelerator belt charge supply.

The 400 keV PN 400 accelerator has been installed in the beam room of this laboratory and is being used for experiments.

---

* Van de Graaff Laboratory Progress Report, T.P. David, BARC 364(1968)

11. A Pre-Injection e/m Analyser System for use with Van de Graaff Ion Sources

(S.N. Misra and M.R. Dwarakanath*)

R.F. ion sources used in Van de Graaff accelerators produce ions in different charge states. These ions acquire different energies in falling through the same potential difference. There is often interest in ions which are produced in very small amounts in the ion source. In such cases it is necessary, in order to minimize electron loading and to improve the stability, to selectively inject only the required type of ions into the accelerating tube of the accelerator.

A test bench e/m analyzer system has been built and tested. It separates doubly charged helium ions from other ions coming out of the source and selectively injects them into the accelerating tube. This system when used with the 5.5 MeV Van de Graaff accelerator will produce helium ions of energies upto 11 MeV, thus enhancing the energy range of the accelerator considerably.

The pre-separation is achieved by a crossed field analyser in which the beam axis is unaltered and it coincides with the axis of the

accelerating tube. A fixed magnetic field of 900 gauss is produced across a pole gap of 3.5 cms. by a bank of 24 ceramic permanent magnet wafers and a continuously variable electric field is produced by applying 0-1600 volts across a pair of parallel plate electrodes kept 2.6 cms. apart. A 3 mm. acceptance aperture placed below the analyser, allows only the undeflected beam to enter the accelerating tube. Prefocussing of the divergent beam is best achieved by an Einzel lens which produces focussing without accelerating the ions and this immensely increases the resolving power of the analyser. The schematic of the system is shown in Fig. 10.

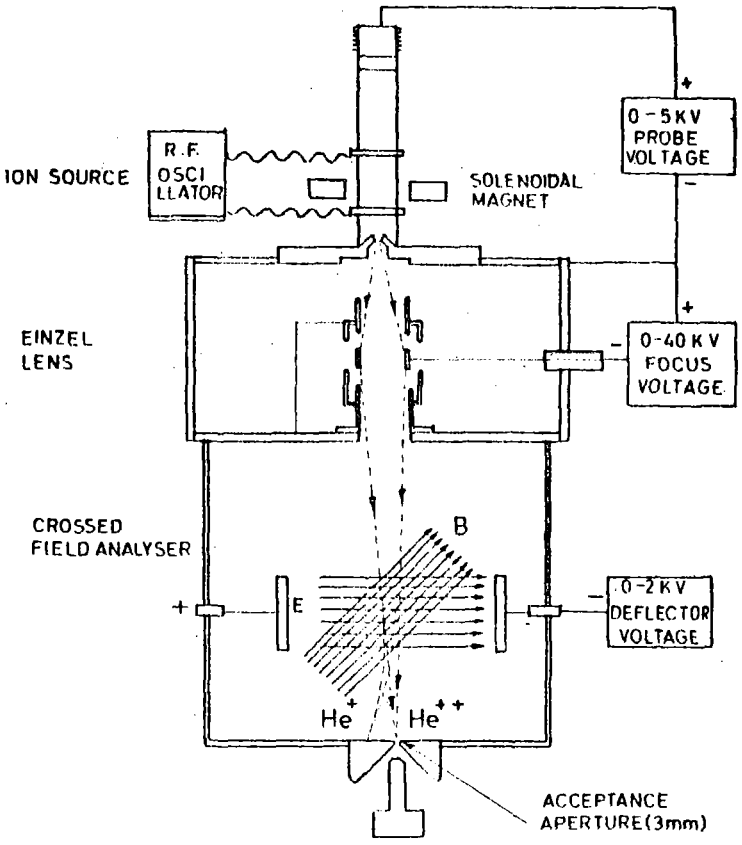

Fig. 10. Schematic diagram of the e/m analyser.

Ion current of the analysed beam can be monitored by connecting a Faraday cup to an ion current meter. Fig.11 shows a plot of the ion

current against deflector voltage by feeding ^{4}He, ^{3}He and ^{40}A gases into the ion source. Various peaks have been assigned on this

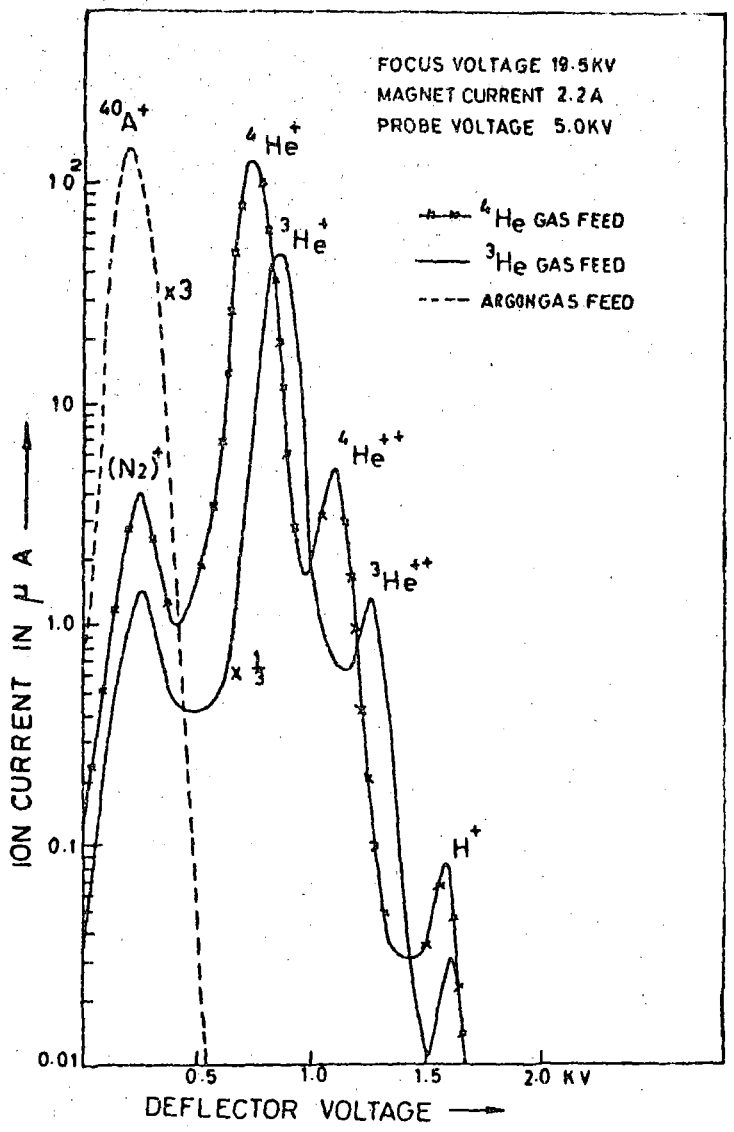

Fig. 11. Ion current for ^{4}He, ^{3}He and ^{40}Ar feed in the analyser as a function of deflector voltage.

graph and the deflector voltages were measured at which the peaks

appear. A graph of $\sqrt{Z/M}$ plotted against deflector voltage is shown in Fig. 12.

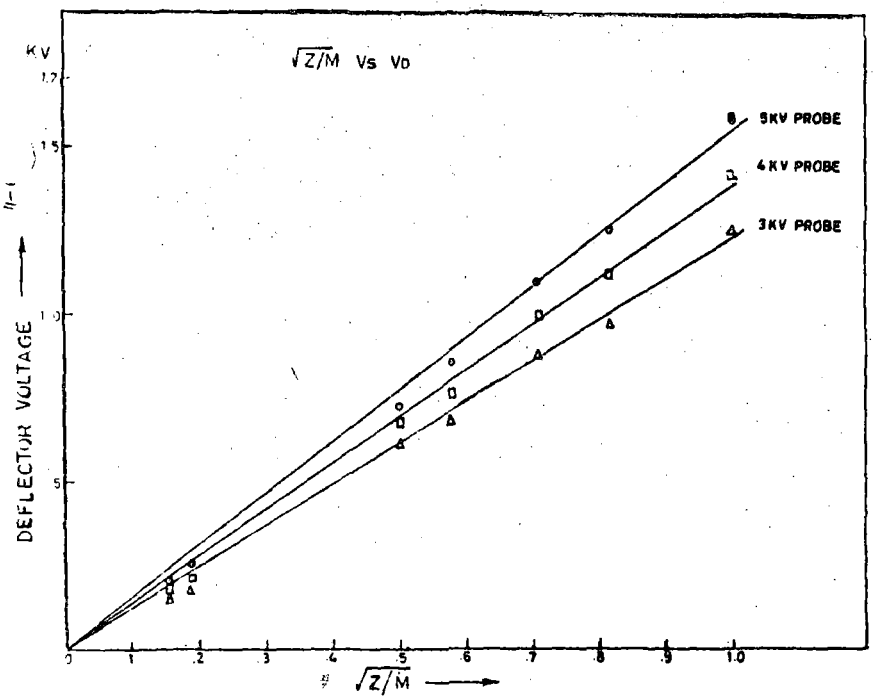

Fig. 12. Deflector voltage in analyser as a function of $\sqrt{Z/M}$

The closeness of experimental points to the straight line confirms the assignment for the various peaks. It can be seen that the He^{++} yield from the test bench assembly is 1 to 2 microamperes.

---

* Now at the California Institute of Technology, U.S.A.

12. Determination of the Efficiency of the 4π -Neutron Counter

(S.K. Gupta and S.S. Kerekatte)

The efficiency of the 4π-geometry neutron counter has been measured within an accuracy of ± 7%. This measurement supercedes

an earlier measurement[1] which was accurate to ± 12%.

Two accurately weighed LiF targets were used to produce the neutrons, using the $^{7}Li(p,n)^{7}Be$ reaction. The data was corrected for the dead time of the scalers, and the background. The estimates of errors were ± 1% for the beam current integrator, ± 4% for the reproducibility of the data and the target thickness and ± 5% for the $^{7}Li(p,n)^{7}Be$ cross section[2]. All these errors combine to give an r.m.s. value of ± 7%. The efficiency has been measured in the neutron energy range of 0.03 to 1.6 MeV and is shown in Fig. 13.

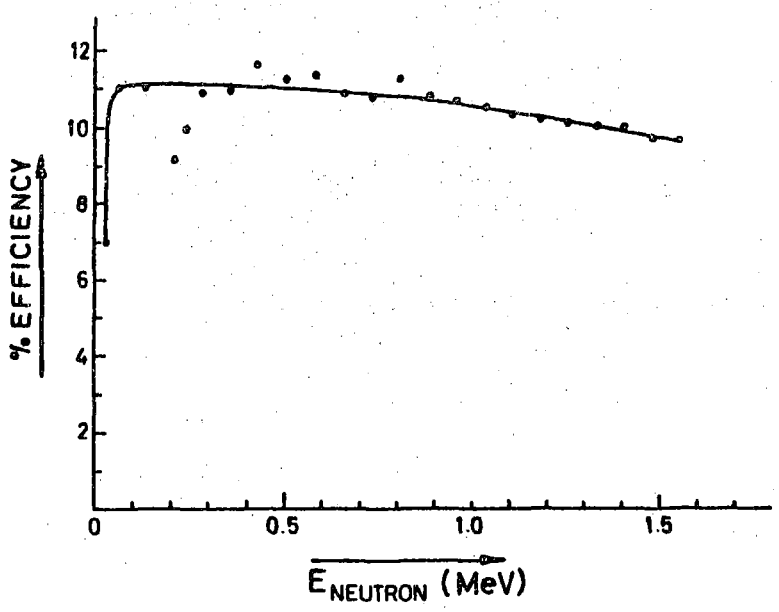

Fig. 13. The efficiency curve for the 4 π neutron detector.

The anomalous behaviour around the neutron energy of 0.2 MeV has already been explained[1].

---

1. K.K. Sekharan, M.Sc. Thesis, University of Bombay, (1965)
2. J.H. Gibbons and R.L. Macklin, Phys. Rev. 114, 571 (1959)

13. Efficiency Measurements of the 30 c.c. Ge(Li) Gamma Ray Detector

(M. Ismail and M.A. Eswaran)

Absolute efficiency measurements were made for the 30 c.c. coaxial Ge(Li) gamma ray detector for the energy range 0.2 to 6.13 MeV. For lower energies the radioactive sources ^{133}Ba, ^{137}Cs, ^{22}Na, ^{54}Mn and ^{60}Co were used and for the higher energies the nuclear reactions $^{27}Al(p,\gamma)^{28}Si$ (E_p = 0.992 MeV) and $^{19}F(p,\alpha\gamma)^{16}O$ (E_p = 1.375 MeV) were used which yield 1.78 MeV and 6.13 MeV gamma rays respectively. These measurements were made at a source-to-detector distance of 4.5 cm and the source strengths were calibrated using the known efficiency of the 7.6 cm x 7.6 cm NaI(Tl) crystal.

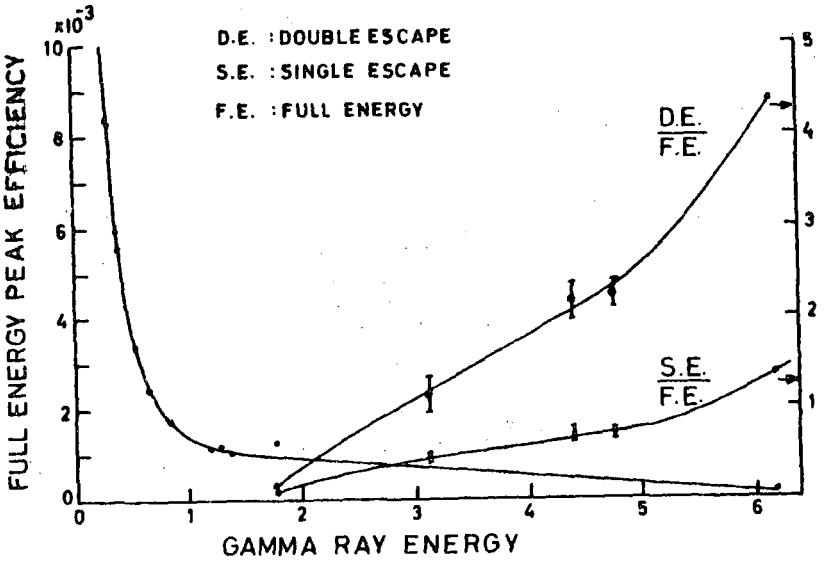

Fig. 14. The efficiency calibration for the 30 cc Ge(Li) detector for γ-rays.

Fig.14 shows the results, for the full energy peak efficiency. The ratios, double escape peak to full energy peak are also shown in the figure which were obtained for gamma rays produced in the above

mentioned reactions as well as in $^{32}S(p,\gamma)^{33}Cl$ and $^{34}S(p,\gamma)^{35}Cl$ reactions.

14. Systematics of Ground State Spins of Light Odd-Odd Nuclei

No

(S.K. Gupta)

A coherent survey of the rules predicting ground spins of the odd-odd nuclei upto A~60 has been carried out. The odd-odd nuclei in which the valence nucleons under j-j coupling shell model are filling different subshells are divided into five categories. Two of these obey strong rules while two out of the remaining three obey weak rules.

For the odd-odd nuclei when the valence nucleons are filling the same subshell, two new empirical rules have been found. All the nuclei except ^{34}Cl and the $f_{7/2}$ subshell nuclei obey the first rule. The second rule is applicable to the nuclei excluded by the first rule. Both the rules coincide for $T_Z = 1$ cases. In order to understand these rules the separation between the T = 0 lowest and T = 1 states in $T_Z = 0$ odd-odd nuclei has been plotted. This plot indicates an oscillatory behaviour in the nature of the two body residual interaction. For the $f_{7/2}$ shell nuclei an empirical formula has been found to describe the separation between the lowest $T = T_Z$ and $T = T_Z + 1$ states. This formula resembles the second rule for the ground state spins of the odd-odd nuclei in which the valence nuclei are filling the same subshell.

15. Distorted Wave Analysis of Deuteron Knockout from ^{6}Li Nucleus

No

(A.K. Jain, N. Sarma and B. Banerjee*)

The existence of nucleon clusters in atomic nuclei has been under discussion in recent years. Light nuclei in particular, have been known to exhibit features typical of clustering. Direct observation of such clustering effects should be possible through knock-out reactions such as (p,pd), (p,pα) and (α,2α). The ^{6}Li nucleus is a particularly

interesting case because on the basis of the conventional shell model, it is difficult to explain consistently both the $^{6}Li(p,2p)^{5}He$ reaction and the electron scattering data. The cluster model on the other hand gives satisfactory agreement in both the cases. $^{6}Li(p,pd)^{4}He$ reaction is analysed using this model. The earlier estimates of this reaction were not good enough to infer about the clustering, the localization and even to explain the angular correlation distribution. The discrepancies arise mainly because of using unantisymmetrized ^{6}Li wave functions in the cluster model, using plane waves in place of distorted waves for the scattering states and using an asymptotically incorrect wavefunction. All these factors have been corrected in this analysis.

Using the knock-out approximation the matrix element can be written as

$$t_{fi} = t_{pd}(q) \left\langle \Psi_f^{(-)} \middle| \delta(\underset{\sim}{r}_o - \underset{\sim}{r}_d) \middle| \Psi_i^{(+)} \right\rangle \qquad (1)$$

where $t_{pd}(q)$ is the free p-d scattering amplitude $\underset{\sim}{r}_o$ and $\underset{\sim}{r}_d$ are the space coordinates of the incident proton and the struck deuteron respectively. The eigen states $\Psi_f^{(-)}$ and $\Psi_i^{(+)}$ are the solutions of the unperturbed Hamiltonian H_i and H_f. $\Psi_i^{(+)}$ will have the bound wavefunction of ^{6}Li. There have been two sets of bound wave functions, one of these by Tang et al[1] has the intercluster wave function (R) containing one Gaussian, W1, while the other one by Schmid et al[2], contains two Gaussians W2. These intercluster wave functions have been matched by exponentials corresponding to the separation energy of the α-d clusters in ^{6}Li; let these be represented by W1T and W2T.

The calculations have been carried out for an incident proton energy of 155 MeV and the results are compared with the data of Ruhla et al[3].

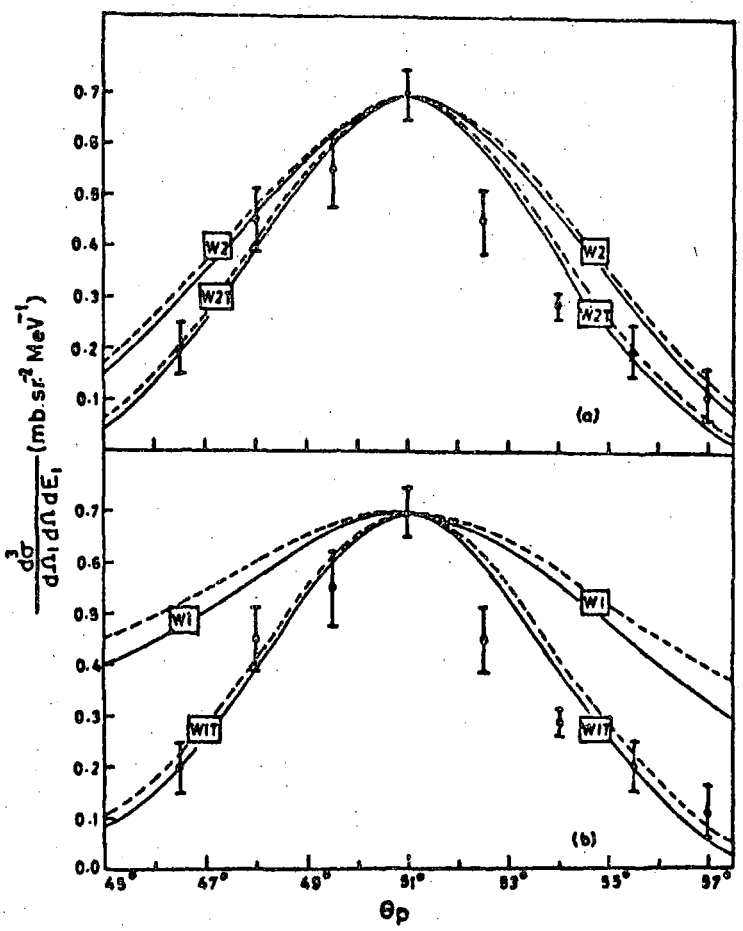

Fig. 15. Cross section calculated in plane wave impulse approximation (PWIA) with (dashed line) and without (solid line) the effects of antisymmetrisation.

In Fig. 15 are plotted the results for these wavefunctions in plane wave impulse approximation (PWIA) and it is found that the shape of the angular correlation curve is fitted nicely by both the modified wavefunctions W1T and W2T, while the unmodified ones W1 and W2 give a rather broad pattern. It is also noticed that in the case of modified wave

functions antisymmetrization effects are very small. The results of the distorted wave (DWIA) calculations compared with PWIA results in Fig.16.

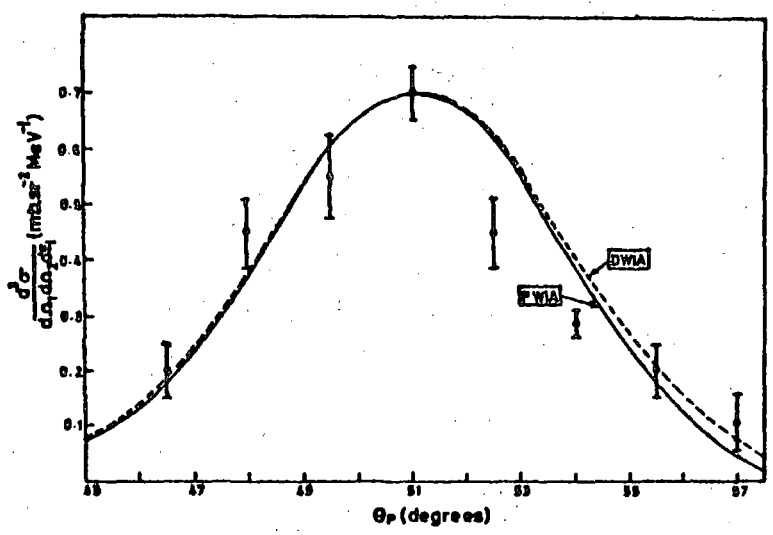

Fig. 16. The angular correlation as calculated in the DWIA and PWIA for the modified wave function W2T. The calculated curves are normalised to experiment at 51°.

Comparison shows that the inclusion of distortions does not affect the shape of the angular correlation except at higher correlation angles.

The absolute magnitude of the cross section has been calculated in the PWIA and DWIA. It is found that (see Table I) the calculations including distortions agree very well with the experimental value, (at $\theta_p = 51°$, the computed cross section is 0.53 while the experimental value is 0.7 ± 0.1 mb Sr^{-2} MeV^{-1}). This indicates that the p-d angular

correlation in the reaction $^{6}Li(p,pd)^{4}He$ can be described resonably well in terms of the cluster model provided the intercluster wave

Table I

Cross sections and ratios of exchange matrix elements at $\theta_p \approx 51°$

Wave function	$\frac{d\sigma}{d\Omega_1 , d\Omega_2 dE_1}$ (mb $sr^{-2}MeV^{-1}$)	(SE/NE)	(DE/NE)
W1, plane wave	0.120	0.350	0.470
W1, distorted wave	0.044	0.316	0.404
W1T, plane wave	0.891	0.130	0.180
W1T, distorted wave	0.384	0.095	0.120
W2, plane wave	0.675	0.100	0.148
W2, distorted wave	0.347	0.063	0.089
W2T, plane wave	1.190	0.075	0.110
W2T, distorted wave	0.533	0.054	0.072

function is modified to have the correct asymptotic behaviour. The antisymmetrization and distortions affect only the magnitude of the cross-section.

---

* Member of T.I.F.R.

1. Y.C. Tang, K. Wildermuth, L.D. Pearlstein, Phys. Rev. 123,548(1961)

2. E.W. Schmid, Y.C. Tang and K. Wildermuth, Phys. Lett. 7,263(1963)

3. C. Ruhla, M. Riou, M. Gusakow, J.C. Jacmart, M. Lin and L. Valentin, Phys. Lett. 6,282(1963)

16. Charge Form Factor and Quadrupole Moment of ^{6}Li Nucleus

(A.K. Jain and N. Sarma)

The structure of the ^{6}Li nucleus is very interesting because the ground state shows nucleon clustering effects symptomatic of long range correlations. It has been shown that the differential cross-section for the reaction ^{6}Li(p,pd) ^{4}He can be predicted accurately using a modified α-d cluster model wave function for the ^{6}Li nucleus. However, the kinematics and the nature of the reaction are such that it is the asymptotic behaviour of the intercluster wave function rather than the structure of the cluster themselves that is explicitly examined. High energy elastic lectron scattering experiments on the other hand examine the interior of the nucleus. The charge form factor must therefore contain information about the structure of the clusters themselves.

The important drawbacks among the calculations done earlier are that, in the shell model ad-hoc short range correlations have to be incorporated along with large configuration mixing effects. In the case of the cluster model have been neglecting the antisymmetrization as well as the rather important asymptotic behaviour of the intercluster wave function have been neglected by other workers.

Here the cluster model wave function has been used as follows:

$$\psi(^{6}\mathrm{Li}) = \mathcal{A}\left\{\psi(\alpha)\,\psi(d)\,\psi(R)\right\} \quad \text{---} \quad (1)$$

Here $\mathcal{A}$ is the antisymmetrizer.

The alpha and deuteron wave functions are Gaussians for each nucleon around its centre of mass. There are two forms for the intercluster wave function ψ (R), first form suggested by Tang et al[1], has a single Gaussian, the second one suggested by Schmid et al[2] contains two Gaussians. These wave functions have been modified to show the correct asymptotic behaviour corresponding to the α-d separation energy. The α and deuteron wave functions have been deformed to obtain the quadrupole moment as suggested by Cohen[3]. First the

charge density distribution $\rho(r)$ has been obtained and then its Fourier transform gives the charge form factor F(q). We have

$$F(q) = F_{proton}(q) \cdot \frac{1}{Z} \int f(\underset{\sim}{r}) \exp(-i \underset{\sim}{q} \cdot \underset{\sim}{r}) \, d\underset{\sim}{r} \qquad (2)$$

For the quadrupole moment (QM) we have

$$Q = \int f(\underset{\sim}{r}) (3z^2 - r^2) \, d\underset{\sim}{r} \qquad (3)$$

F(q) and Q for the wavefunctions quoted above have been calculated. It is found that corrected one-Gaussian intercluster wave function (WIT) can explain the charge form factor and QM. A unique fit to the form factor gives that the deuteron cluster in ^{6}Li does not behave as a free deuteron but is shrunk in its size. The alpha particle remains like a

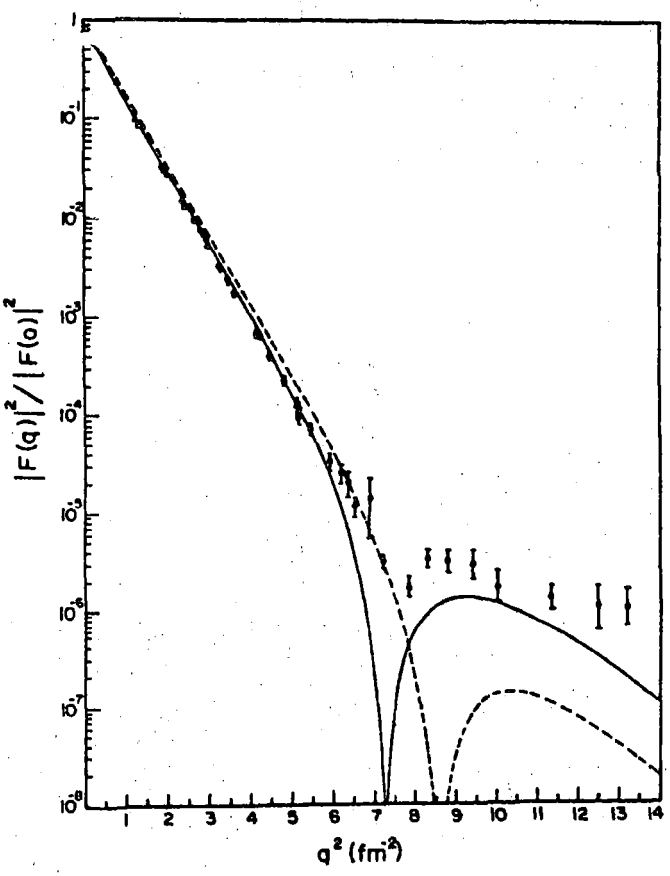

Fig. 17. The charge form factor as measured and as calculated. The continuous curve represents the full calculation while the dotted curve shows form factor using an unantisymmetrised wave function; $\alpha = 0.514$ fm^{-2}, $\alpha = 0.74$ fm^{-2} for both these curves.

free alpha. The form factor fitting is shown in Fig. 17. The dotted

curve indicates the results of an unantisymmetrized wave function.

The fitting of the QM ($Q = -0.08$ fm^{+2}) indicated that a 16% deformation of both the α and d clusters is necessary. If the alpha cluster is assumed spherical then the deuteron cluster deformation is unusually large. A neglect of exchange terms leads to an incorrect value of $Q = -0.175$ fm^{+2}.

Thus it is concluded the practice of neglecting antisymmetrization in the cluster model calculations leads in turn to incorrect information about the cluster structure of the nucleus. The second maximum in the form factor can be reproduced using antisymmetrized cluster model for ^{6}Li without introducing the ad-hoc short range correlations in the shell model representations.

---

1. Y.C. Tang, K. Wildermuth, L.D. Pearlstein, Phys. Rev. 123,548(1961)

2. E.W. Schmid, Y.C. Tang and K. Wildermuth, Phys. Lett. 7,263(1963)

3. IL-T. Cheon, Phys. Lett. 30B, 81(1969)

17. Triton Knock-out From ^{7}Li Nucleus

(A.K. Jain and N. Sarma)

Knock-out reactions provide information about the momentum distribution of the particles within the target nucleus. Direct observation of the clustering effects in nuclei should therefore be possible through knock-out reactions such as (p,pd), (p,pt), (p,pα) and (α,2α) reactions. The analysis of the reaction ^{6}Li(p,pd)^{4}He in terms of the cluster model of ^{6}Li has been very successful[1] and encourages the analysis of the ^{7}Li(p,pt)^{4}He reaction using a (α+ t) cluster model of ^{7}Li. Data on the ^{7}Li(p,pt)^{4}He reaction is available at 156 MeV incident energy from Bachelier et al[2] and at 55 MeV incident energy from Hendrie et al[3]. These results have been analysed using a plane wave impulse approximation but a detailed analysis has to be carried out before a

definite statement can be made about clustering in ^{7}Li. Such a detailed analysis requires firstly, the antisymmetrization of the target wave function. Secondly, as has been pointed out in many discussions, the intercluster wave function should have the correct asymptotic behaviour. A wave function with the correct asymptotic behaviour has been used in this work and it is of great importance in the determination of the angular distributions of the emitted particles. However the use of such correct wave functions creates computational difficulties. Finally the interaction of the incident and emergent particles with the initial and final nuclei has to be included through the use of distorted waves (i.e., DWIA). The DWIA matrix element for the transition is then given by

$$t_{if}(\underline{q}, \underline{k}_3) = t_{pt}(q) \langle \Psi_f^{(-)} | \delta(\underline{r}_0 - \underline{r}_t) | \Psi_i^{(+)} \rangle$$
$$= t_{pt}(q)\, g_{if}(\underline{q}, \underline{k}_3)$$

$t_{pt}(q)$ is the free p-t scattering amplitude and is a function of the momentum transfer q while $g_{ig}(\underline{q},\underline{k}_3)$ is the momentum transform of the overlap integral of the final state with the initial state and is a function of $\underline{q}$ and the recoil momentum $\underline{k}_3$. The initial and final state wave functions $\Psi_i^{(+)}$ and $\Psi_f^{(-)}$ are given as follows,

$$\Psi_i^{(+)} = N_i \Phi_A(1234;567)\, \chi_1^{(-)}(\underline{k}_{0A}, \underline{r}_{0A})$$

$$\Psi_i^{(-)} = N_f \Phi_\alpha(1234)\Phi_t(567)\, \chi_1^{(-)}(\underline{k}_{0\alpha}, \underline{r}_{0\alpha})\, \chi_2^{(-)}(\underline{k}_{t\alpha}, \underline{R})$$

The χ 's here are the distorted waves and Φ's are the wave functions of the bound systems. The wave functions of the target nucleus are given by

$$\Phi_A(1234;567) = \mathcal{A}\left\{\psi_A(1234;567)\, \xi_A(1234;567)\right\}$$

ξ and ψ are respectively the spin and space parts of Φ and $\mathcal{A}$ is the antisymmetrizer. The space part ψ_A is expressed in the cluster model as a product of the internal wave functions of the clusters and the intercluster wave function. The form of ψ_A as given by Tang et al[4] is

$$\psi_A(1234;567) = \exp\left\{-\frac{\alpha}{2}\sum_{i=1}^{4} e_i^2 - \frac{\beta}{2}\sum_{j=5}^{7} e_j^2\right\}\phi R$$

e's are the coordinates of the particles with respect to the centres of mass of the clusters, and $\phi(R)$ has the form R^3 exp $(-\frac{6}{7}\gamma R^2)\, Y_1^M(\hat{R})$. The parameters α, β and γ were obtained by variational calculations. Using a partial wave expansion for χ's and summing over all the spin functions and integrating over internal coordinates,

$$g_{if}(\underline{q}, \underline{k}_3) = \int \chi_{q,k_3}(R)\left\{B_{NE}(R) - 3B_{SE}(R) + 3B_{DE}(R) - B_{TE}(R)\right\} dR$$

Here $X_{\underline{q}',\underline{k}_3}(R)$ comes from the three distorted waves and $\hat{\underline{R}}$ part of bound wave functions on summing over the partial waves. The subcripts NE, SE, DE and TE correspond to no, single, double and triple exchange of particle coordinates in the alpha and triton cluster wave function of the target nucleus.

To obtain the correct asymptotic behaviour, an intercluster wave function has been used

$$\varphi(R) = R^3 \exp\left(-\frac{6}{7}\gamma R^2\right), \quad R \leq 3.53 \text{ fm}$$

$$= \left(\frac{1}{fR} + \frac{1}{f^2R^2}\right)\exp\left(-fR\right), \quad R \geq 3.53 \text{ fm}$$

The parameter $f\left\{= (2\mu_{t\alpha} E_{t\alpha}/\hbar^2)^{\frac{1}{2}}\right\}$ corresponds to the α-t separation energy $E_{t\alpha}$ = 2.47 MeV, $\mu_{t\alpha}$ is the reduced mass. In order to evaluate the exchange terms, it is found necessary to expand this correct intercluster wave function in terms of a series of Gaussians.

The numerical evaluation of the results is in progress for the 156 MeV data[4] and 55 MeV data[2].

---

1. A.K. Jain, N. Sarma and B. Banerjee, Nucl. Phys. A142,330(1970)
2. D. Bachelier et al., High energy Phys. and Nucl. Structure, ed. S. Devons, page 318(1971)
3. D.L. Hendrie, M. Chabre and H.G. Pugh, UCRL report, 16580, page 146
4. Y.C. Tang, K. Wildermuth and L.D. Pearlstein, Phys. Rev. 123,548(1961)

18. Formalism for the Study of Two Hole States in Nuclei with the $(\bar{\pi},NN)$ Reaction

(B.K. Jain)

It is known that due to the kinematic considerations the process of the absorption of negative pions by nuclei are very suitable for the study of short range correlations in nuclei. With this purpose many detailed calculations of this process have been carried out recently[1]. These calculations use the ps-pv pion nucleon interaction and employ for the initial nucleus the Justrow type wave function. The results of these calculations are generally in accord with experiments. But due to the importance of the mutual scattering of nucleons in final state it has prooved rather difficult to extract precise and quantitative information about the two body correlations in nuclei.

There is, however, another aspect of this process. The emission of two nucleons following the absorption of a bound pion creats a two hole state in the residual nucleus. This is similar to the creation of one hole states in the (p,2p) reaction. From the successful use of the (p,2p) reaction to study one hole states in nuclei it seems logical to use the $(\bar{\pi},NN)$ reaction to investigate two hole states in nuclei. This potentiality of pion absorption studies was pointed out by Ericson[3] and has been emphasised recently by Wilkinson[4]. However, no serious attempts have been made so far to use this process to study two hole states in nuclei. There is, therefore, a motivation to develop a formalism for the reaction and to use it to investigate systematically two hole states in nuclei. Since the details of this formalism have already been published separately[5] only the essential points of it are mentioned here.

Since the purpose is to study the two hole states, a semi phenomenological approach has been used to describe the pion nuclear interaction. This avoids both the explicit introduction of a correlation function in the initial wave function and the treatment of the N-N-scattering in final state. In this approach, pion capture in nuclei is assumed to proceed through the elementary reaction

$$\pi + NN \longrightarrow N + N \qquad (1)$$

For the effective interaction Hamiltonian for the process (1) the one developed by Eckstein[6] is used. The parameters of this interaction are determined by the analysis of data on the elementary reaction. The effective interaction thus contains within it the effect of the two nucleon correlations in the initial and in the final state.

For the nuclear state wave function the shell model wave functions have been used. These wave functions should be good as they are needed to consider only the long range behaviour of the wave function correctly.

Since in the final state only the scattering of the outgoing nucleons with the residual nucleus has to be considered, the problem is simplified a lot. This scattering is incorporated by the use of optical model potential. The solution to the optical potential is sought in the partial wave analysis.

For the pion wave function the hydrogenic wave function has been used.

The formalism contains the absorption of pions from its 1s and 2p orbits. It is known from the pi-mesic X-ray data[7] that higher pionic orbits do not contribute to the absorption to the absorption process.

---

1. E.H.S. Burhop, High Energy Physics, Vol. III (Academic Press, New York, 1969)
2. B.K. Jain and D.F. Jackson, Nucl. Phys. A99,113(1967)
3. T. Ericson, Phys. Lett. 2,278(1962)
4. D.H. Wilkinson, Proc. Int. Conf. on Nucl. Structure Tokyo (1967)469; Comm. in Nucl. and Part. Phys. 2,83(1968)
5. B.K. Jain, BARC report, 512
6. S.G. Eckstein, Phys. Rev. 129,413(1963)
7. S. Berezin et al., Nucl. Phys. B16,389(1960)

19. Study of the Two Hole States in ^{12}C Nucleus with the (π^-,nn) Reaction

(B.K. Jain)

With a view to study the two hole states in atomic nuclei with the (π^-,NN) reaction a formalism has been developed to study these reactions. Using the simplified version of this formalism, the recent available data on ^{12}C (π^-,nn) reaction has been analysed.

^{12}C nucleus in its ground state has iso-spin, $T_i = 0$ and spin, $J_i = 0^+$. The simplified expressions are therefore directly applicable to it. Recently Cheshire and Sobottka reported the (π^-,nn) reaction on ^{12}C. In this experiment they observe the peaks in the excitation energy spectrum of ^{10}B corresponding to the emission of nucleons from $(1p)^2$, (1s,1p) and $(1s)^2$ configurations. The emission from $(1p)^2$ configuration. Using the wave function of Boyarkina for ^{12}C and ^{10}B the relative strengths of the peak cross-section to various excited states of ^{10}B are as follows:

Exc. Energy (MeV)	0	0.717	1.74	2.15	3.59	4.72	5.16	5.53
J_f, T_f	3^+0	1^+0	0^+1	1^+0	2^+0	3^+0	2^+1	2^+1
Relative Strength	1	25	45	108	0	0	0	2

From this it is clear that a good resolution experiment should show the structure of three peaks in the observed one $(1p)^2$ peak corresponding to the first three excited states of ^{10}B. Their strength would roughly be in the ratio of 1:2:4. In the present analysis the experimental cross-section is compared with the summed cross-section for these three states. This is shown in Fig. 18. The agreement is satisfactory. In order to estimate the effect of distortion of outgoing neutrons by the residual nucleus also plotted in Fig. 18, is the result from a plane wave analysis. The introduction of distortions

reduces the peak cross-section by a factor of 2.6.

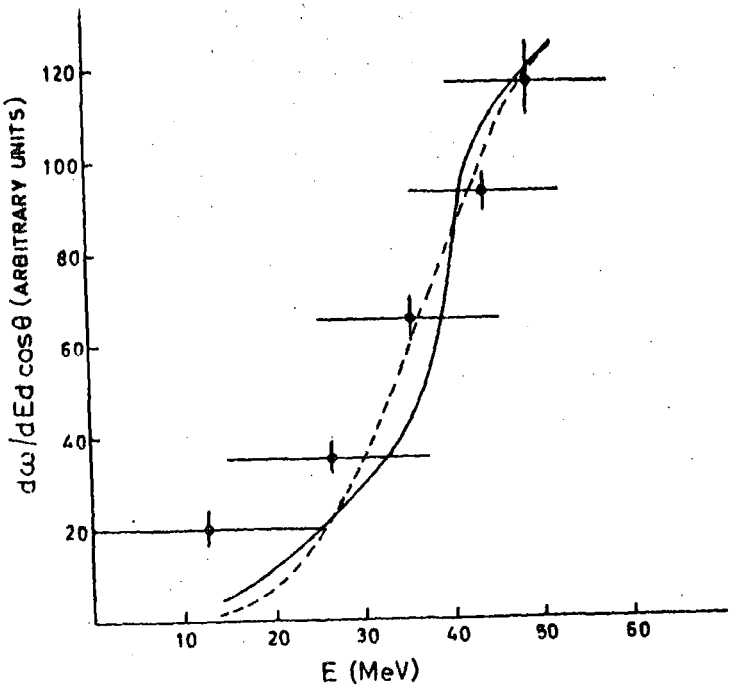

Fig. 18. Comparison of the experimental cross section for the ^{12}C (π^-,nn) reaction with calculations by (a) plane wave analysis and (b) summation for three outgoing states.

It is important to note the agreement between experiment and the present results which consider absorption from only the 1s orbit is in contradiction to the inference from pi-mesic x-ray data. The x-ray data suggest that the absorption from 1s and 2p pionic orbit is comparable in ^{12}C. While analysing their ($\bar{\pi}$,nn) data Cheshire and Sabottka also reached the same conclusion. They were, however, not confident of their findings as the scattering of outgoing neutrons by the residual nucleus could not be computed in their formulation. In order to estimate the quantitatively the fractional contribution of 2p orbit to ($\bar{\pi}$,nn) reaction, calculations are in progress.

20. Analysis of $^{12}C(p,2p)$ and $^{12}C(e,e'p)$ Reactions at High Energies

(R. Shanta and B.K. Jain)

It has been known for quite sometime that the (p,2p) and the (e,e'p) reactions can be used to study the single particle aspect of atomic nuclei. It is also believed that if the multiple scattering of

the unbound protons in the two reactions are properly taken into account, these two reactions should yield identical information about the bound state of protons in nuclei. A detailed analysis of the (p,2p) reaction data on the 1p shell nuclei has been carried out by Jain and Jackson. They conclude in their work that if the distortion of the incoming and outgoing protons is taken into account properly, the bound state wave functions which fit the elastic electron scattering data also fit the (p,2p) reaction on the same nucleus. Using the same approach, the experimental data on the (e,e'p) reaction have been analysed by Ciofi delgi Atti[1], Boffi et al[2] and Epp and Griffy[3]. Unlike the (p,2p) reaction they observe that the bound state wave function which fits the elastic electron scattering data does not fit the (e,e'p) data on the same nucleus. This seems a little surprising. It may be noted though, that the analysis of Jain and Jackson of the (p,2p) reaction was restricted to the experimental data in the incident proton energy range of 155-185 MeV. Therefore, this analysis is subject to all the uncertainties normally encountered in the theoretical treatment of the (p,2p) reaction; due to the multiple scattering of the incoming and outgoing protons, the offshell nature of the two body t-matrix and the three body nature of the final state. The effect of these uncertainties, however, becomes unimportant as the incident proton energy becomes greater than about 400 MeV.

Recently Simpson et al[4] have reported (p,2p) data on ^{12}C at 1 GeV. Data at 460 MeV incident energy are already available in literature from Tyren et al. Here these high energy (p,2p) data on ^{12}C have been analysed along with the (e,e'p) data around 600 MeV of Amaldi et al[5]. For the bound proton the Woods-Saxon wave function of Elton and Swift and the projected radial Hartree Fock wave function of Boffi et al., which fit the ^{12}C(e,e) data have been used.

From this analysis it is concluded that

i) Keeping in view the uncertainties due to the lack of detailed information about the optical model potentials and the unavailability of the angular distribution for the 1s knock-out at 460 MeV, the phenomenogical Elton-Swift wave functions reproduce the (p,2p) distributions at 460 MeV and 1 GeV.

ii) The projected radial Hartree-Fock wave functions which are obtained by minimizing the total energy of the nuclei, reproduce the shape as well as the magnitude of the 1s distribution and the shape of the 1p distribution of the (p,2p) reaction at 1 GeV.

iii) Both these wave functions (i.e. Elton and Swift and PHE) reproduce the shape of the 1s distribution of (e,e'p) reaction. For the 1p knock-out the computed distribution peaks at higher momentum than the experimental distribution. The FWHM for the 1p knock-out, however, is approximately the same for the experimental and computed distributions.

iv) In the (e,e'p) reaction the distortion of the outgoing proton not only reduces the magnitude of the cross-section, but also shifts the momentum distribution towards the high momentum side. The peak cross section is reduced by a factor of 0.614 and its position is shifted by about 0.05 fm^{-1} (i.e. 10 MeV/c).

---

1. C. Ciofi delgi Atti, Nucl. Phys. A106,215(1967)
2. S. Boffi et al., Nucl. Phys. A120,135(1968)
3. C.D. Epp and T.A. Griffy, Phys. Rev. C1,1633(1970)
4. W.D. Simpson et al., Nucl. Phys. A140(1970)201
5. U. Amaldi, Jr. et al., Phys. Rev. Lett. 13,141(1964); Phys. Lett. 25B,24(1967)

21. Ray tracing Calculations on a Magnetic Spectrograph

(S. Das and N. Sarma)

A general equation of motion of a charged particle in the median-plane through a magnetic field has been derived. This equation has been solved numerically with the following geometry of the split-pole magnetic spectrograph.

Source distance (l_1')	= 60.8 cm.
Entrance angle (E_1^I)	= 37°
Radii of curvature of (R'	= 19.7 cm.
The circular sector (R'	= 54.1 cm.
Uniform magnetic field inside the pole gap (B_o)	= 10 kOe.
Magnetic field in the split	= 0.134 B_o

This geometry gives an energy range of 5 to 40 MeV for protons and alpha particles.

i) Sharp cut-off approximation calculation for the fringing field gives virtual image distances(produced by circular sector) and final image distance in good agreement with earlier calculations.

ii) Calculations using fringing field of the extended type give the focal plane, dispersion, magnification, momentum resolution, aberration and a correction for "kinematic" line broadening. The results compare well with those of Spencer and Enge[1]

---

1. J.E. Spencer and H.A. Enge, Nucl. Inst. and Methods, 49,181(1967).

II. FISSION PHYSICS STUDIES

1. Excitation Energy Dependence of Shell and Pairing Effects on Nuclear Level Densities and Fission

(V.S. Ramamurthy, S.K. Kataria, S.S. Kapoor and R. Ramanna)

The influence of the nuclear ground state shell structure, pairing interactions, angular momentum and deformation on the excitation energy dependence of nuclear level densities were investigated. Microscopic calculations of nuclear level densities were carried out using the formulation of statistical thermodynamics and the single particle eigenvalues in a deformed harmonic oscillator potential. The results regarding shell effects on level densities can be summarized as follows: For small excitation energies E_x (< 30 MeV), not only is the level density parameter $\underline{a}$ shell and excitation-energy-dependent, but in addition E_x has to be measured from a reference energy surface which itself depends on E_x. In the asymptotic limit of $E_x \gtrsim 30$-40 MeV, it is found that this reference surface coincides with the liquid drop model mass surface, and $\underline{a}$ is independent of shell effects. This implied that, contrary to general belief, shell effects on nuclear level densities disappear even at medium excitation energies of 30 - 40 MeV. The results of the present calculations carried out for the model single particle level scheme of Kahn and Rosenzweig[1] are in agreement with their closed expressions. However, their interpretation regarding shell effects on the entropy in

the asymptotic limit of large E_x are in apparent contradiction with the present conclusions. This descrepancy has been resolved and calculation show that the reference energy surface for the calculation of the ground state shell correction should be identified with a continuous uniform single particle level scheme and not with a discrete one. Regarding the pairing interactions, the present calculations show that at all energies except those very near the ground state, a constant addition term to E_x is required for all types of nuclei including odd-odd, to take into account the pairing effects on level densities. The results of microscopic calculations have been shown to produce a good fit with the measured level densities for Fe^{56} and Mn^{55}. The results of calculations for deformed nuclear shapes have thrown new light on the interpretation of the transition state of fissioning nuclei with double-humped barrier and on the interpretation of fragment angular distributions in these cases[2]. The implications of the rapid washing out of shell effects on the statistical properties of nuclei are also being worked out with particular emphasis on the production possibility of superheavy nuclei by heavy-ion bombardment.

The present investigations of the shell effects on the statistical properties of nuclei have also been extended to an interpretation of the fragment mass and charge division in fission, wherein the scission is treated as a stochastic process. The asymmetric division of mass and charge is shown to result from the requirement that during the division process, the chemical potentials and the temperatures of the nacent fragments tend to equalize.

---

1. P.B. Kahn and N. Rosenzweig, Phys. Rev. 187,1193(1970)

2. V.S. Ramamurthy, S.S. Kapoor and S.K. Kataria, Phys. Rev. letters. 25,386(1970)

2. Studies of the Time of Emission and Multiplicities of K x-rays from Fission Fragments of Specified Atomic Numbers+

No 4

(S.S. Kapoor, S.K. Kataria, S.R.S. Murthy, D.M. Nadkarni, V.S. Ramamurthy and P.N. Rama Rao)

The average emission times of the K x-rays emitted from ^{236}U fission fragments of specified atomic numbers and the multiplicities of

K x-rays from ^{252}Cf fission fragments of specified atomic numbers have been determined in two separate experiments using high-resolution Si(Li) x-ray Spectrometers. In the first series of experiments the average emission times of K x-rays emitted from ^{236}U fragments were determined by detecting the x-rays in the two cases of the emitting fragments moving towards and away from the x-ray detector. Information regarding the presence of any significantly delayed components in the x-ray emission from heavy fragment group was also obtained by recording the spectra of K x-rays emitted from these fragments in the time ranges of 110 nsec and 1000 nsec after fission. The most striking delayed K x-ray emitter is found to be $_{52}Te$, where the fraction of the K x-rays emitted in the time interval 110-1000 nsec is found to be $(79 \pm 5)\%$. In the second series of experiments, information about the cascade emission of K x-rays from fission fragments of specified atomic numbers was obtained by measuring the energy spectra of coincident K x-rays with two Si(Li) x-ray spectrometers operated in coincidence with each other and with fission.

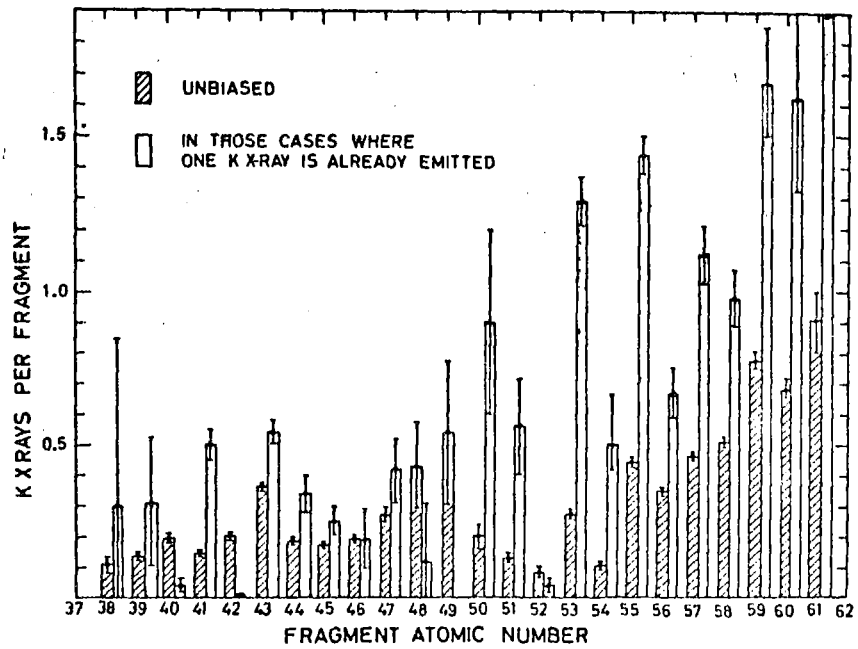

Fig. 19. The unbiased average K x-ray yield per fragment is compared with the yield of the additional K x-rays per fragment when one K x-ray is known to have been already emitted fragments of specified atomic numbers.

From the analysis of these spectra both the first moment ($\bar{n}$) and the

second moment (n^2) of the x-ray emission distribution function $f_z(n)$ were determined where $f_z(n)$ represents the fraction of fission events

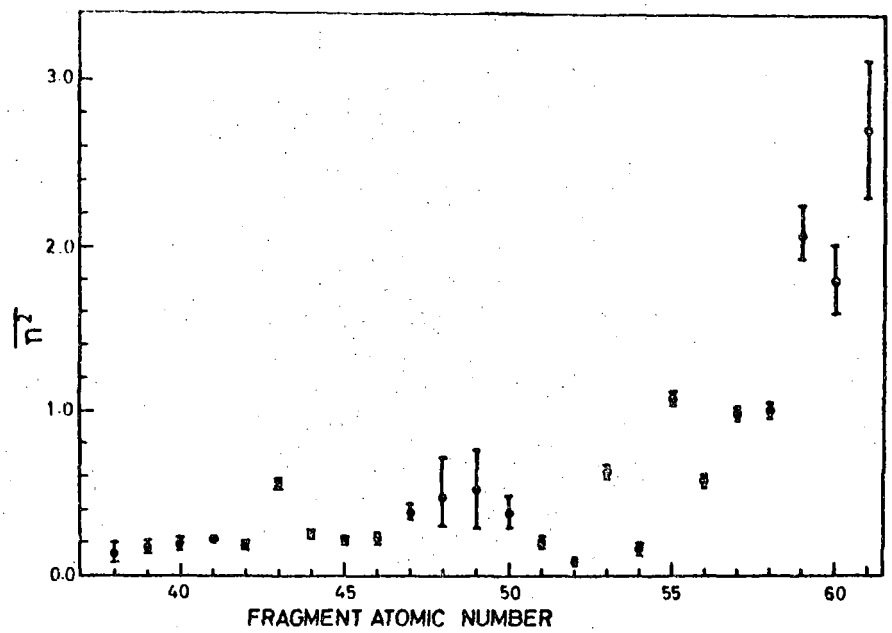

Fig. 20. The second moment $\bar{n}^2$ of the x-ray emission distribution function for fragments of different atomic numbers.

in which n x-rays are emitted in a cascade from fragments of atomic number Z. The results are as shown in Figs. 19 and 20. A noteworthy feature of these results is that the yield of the additional K x-rays per fragment in those cases where it is known to have already emitted one K x-ray is found to be in general, higher than the average unbiased K x-ray yield per fragment from the fragments of the same atomic number. This implies that there exists a significantly large probability for a cascade of x-ray emission in some cases. The values of $\bar{n}^2$ are found to smaller for the light group of fragments as compared to the heavy group. In the heavy group, similar to the behaviour of $\bar{n}$ the values of n^2 are also found to reflect a strong dependence on the odd-even nature of the fragment atomic number and also show a striking increase with the onset of the deformed region of $N \geq 88$. The effects on the normal average K x-ray yield per fragment, if only those events are selected in which the complementary fragment charge has emitted a K x-ray, were also determined.

+ Work performed under contract with IAEA, Vienna.

Probably

see also TOMANDL 2
INDC(SEC) - 48 45 NP
BARC-553 4

3. Emission of Long Range Charged Particles in the Fission of ^{235}U by Thermal to 4 MeV Neutrons

(D.M. Nadkarni and S.S. Kapoor)

The rate of emission of long range charged particles in fission has been determined in the case of fission of ^{235}U induced by thermal, 2 MeV and 4 MeV neutrons. The method used consisted in recording the energy spectrum of these charged particles, using a semiconductor detector, in coincidence with fission fragments detected in a 2 geometry with a parallel plate ionization counter. Together with earlier measurements of the emission probability of long range alpha particles in 3 MeV neutron-induced fission of ^{235}U[1], the present results indicate a rather weak dependence of the emission probability of charged particles in fission on the excitation energy of the fissioning nucleus. These results, obtained for the case of a single fissioning nucleus, are compared in Fig.21 with those obtained by other workers

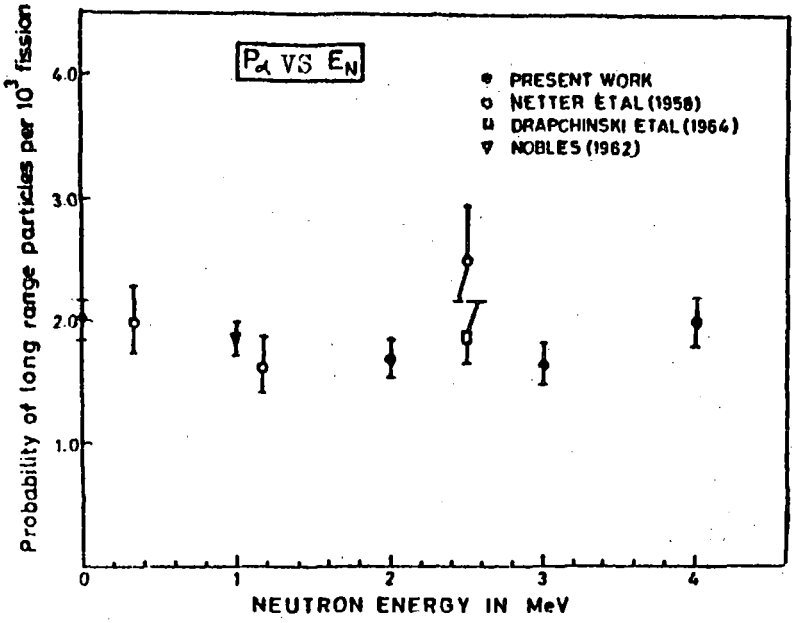

Fig. 21. Probability of α particle emission in the fission of ^{235}U as a function of neutron energy.

at much higher excitation energies where multiple chance fissions contribute.

---

1. V.A. Hattangadi, T. Methasiri, D.M. Nadkarni, R. Ramanna and P.N. Rama Rao, Physics and Chemistry of Fission, Vol.II, 397(1965)

Yes. Probably must request data. (See INDC(SEC)-18 46)

4. Excitation Functions for the Neutron Induced Fission of Heavy Nuclei

(K.N. Iyengar+, R.H. Iyer*, D.M. Nadkarni, M.L. Saghu*, and S.S. Kapoor)

The cross-section of ^{241}Am relative to that of ^{235}U has been measured in the neutron energy region of 0.32 to 2.1 MeV at energy intervals of about 100 keV. Fission events were recorded using Lexan Solid State Track detectors in a 2π geometry. Monoenergetic fast neutrons were generated with the $T(p,n)^3He$ reaction using the 5.5 MeV Van de Graaff Accelerator.

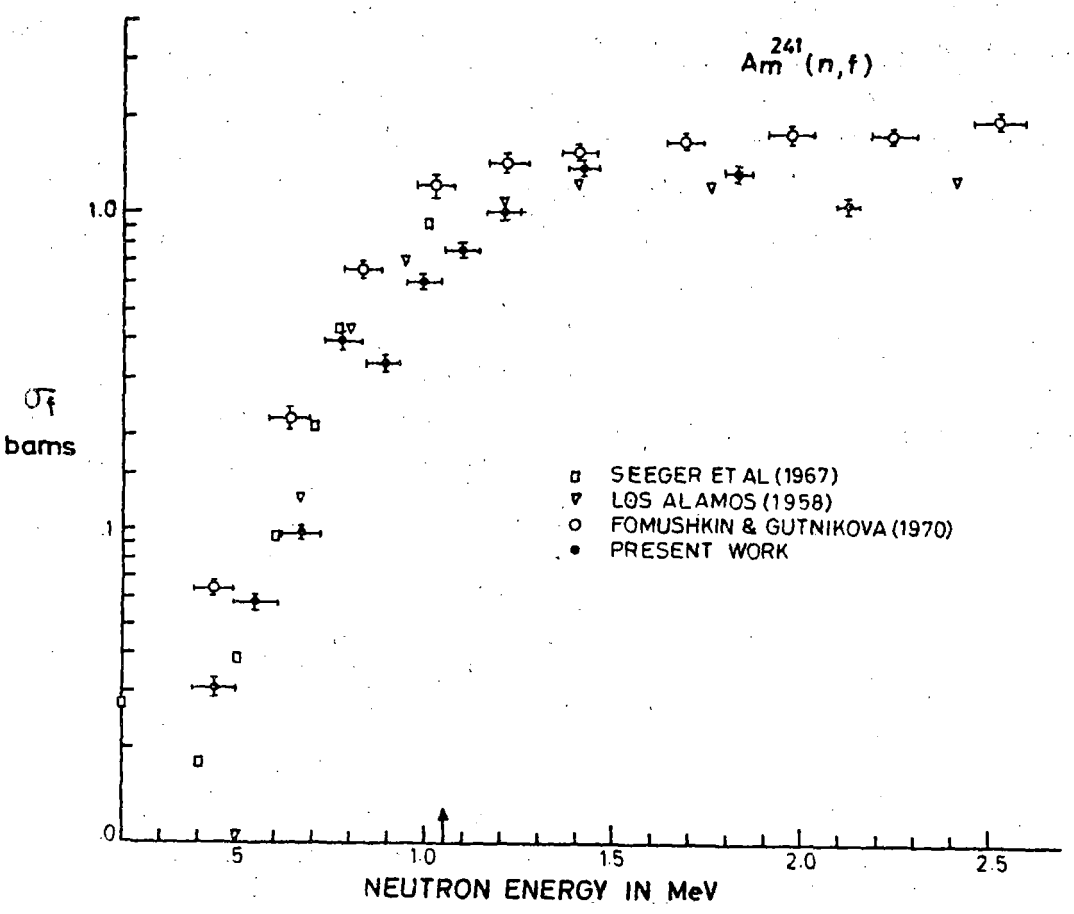

Fig. 22. Fission cross section of ^{241}Am for neutron energies upto 2.5 MeV.

The results of these measurements are shown in Fig. 22 alongwith those of other workers(1,2,3)

+ Member of TIFR

* Radiochemistry Division

1. P.A. Seeger, A. Hemmendinger and B.C. Diven
Nucl. Phys. A196,605(1967)

2. BNL-325 (Second Edition) 1958

3. E.F. Fomushkin and E.K. Gutnikora
Soviet Jour. Nucl. Phys. 10 No.5, 529(1970)

5. Semiconductor X-ray Spectrometer for non-destructive Element Analysis.

(Madan Lal and S.S. Kapoor)

A high resolution semiconductor X-ray spectrometer has been set up for a rapid non-destructive element analysis of any sample. The spectrometer will analyse the fluorescence x-rays excited in the sample by suitable radiations from a radioactive source. The setting up of the spectrometer, employing a cooled Si(Li) detector and FET preamplifier has been completed and efforts are being made to achieve the best possible resolution by a selection of low noise FET and feed back resistor, and optimizing other factors. The present resolution of the systems in terms of FWHM of 6.4 kev K x-rays of iron is about 400 eV.

6. Interfaces for the Four Parameter Data Acquisition System

(B.R. Ballal, S.K. Kataria, P.N. Rama Rao and S.L. Raote)

At present the data from the four parameter data acquisition system (FPDAS) used with the fission experiments can be recorded only on punched paper tape which restricts the use of the system to low counting-rate experiments only. Moreover, the analysis of data recorded on paper tape is cumbersome and consumes more computer time. Tof facilitate the data analysis, and to use FPDAS for high count rate experiments, the use of incremental magnetic tape recorder has been proposed. The interface unit for transcribing the data from the FPDAS to take recorder has been fabricated and is being tested.

For smooth running of the experiments it is essential to have preliminary on-line analysis of data. At present only off-line analysis with computer is possible, which introduces inordinate delays in taking corrective measures. A "Read" interface has been fabricated which

processes the data on-line, of one APC of FPDAS at a time with the help of a 512 channel analyser. Another interface is being made which will enable the analysis of the data recorded on the magnetic tape and thus eliminate any delay in applying feed back.

B. SOLID STATE PHYSICS

I. X-RAY CRYSTALLOGRAPHY

1. The Crystal Structure of Ammonium Sulphamate

(V.K. Wadhawan and V.M. Padmanabhan)

The X-ray crystal structure of ammonium sulphamate, $NH_4\ NH_2\ SO_3$, has been solved using visually estimated intensities of 553 independent reflections, recorded by the multiple-film Weissenberg technique. The space group is Pbca, with a = 7.558(6)Å, b = 7.835(9)Å, c = 14.48(2)Å, and Z = 8. The signs of structure factors were determined by symbolic addition method. The data, severely affected by extinction, were corrected by the Zachariasen method. Full-matrix, anisotropic, least-squares refinement gave a final R index of 0.085.

The structure is held together by a network of N^+-H.....O hydrogen bonds. The sulphamate ion is nearly tetrahedral, with angles varying between 106.4° and 113.0°. The N - S bond length is 1.636 (2) Å. As the hydrogen atom positions could not be determined from the X-ray study, neutron diffraction work on the structure has been undertaken to decide conclusively whether the configuration around the amide nitrogen is planar or tetrahedral.

2. The Crystal Structure of Potassium Dinitrodiglycinato Cobaltate (3^+)

(V.K. Wadhawan and V.M. Padmanabhan)

An investigation of the crystal structure of $K\left[Co(NH_2CH_2COO)_2(NO_2)_2\right]$ is in progress. Complete three-dimensional X-ray data have been obtained by the Weissenberg technique using Cu Kα radiation and the raw intensities are being processed. The compound crystallises in the space group Cc, with a = 23.14(2)Å, b = 15.39(2)Å, c = 8.153(5)Å, β = 121° 57'(6'), and Z = 8. The values for the cell parameters were obtained by least-squares refinement from the film data, using the computer programme CELPAR described below (See article 5)

3. X-ray Analysis of Peptide Crystals

(V.M. Padmanabhan and V.S. Yadava)

Glycyl-L-threonine dihydrate crystallises in the orthorhombic system with cell parameters a = 10.63Å, b = 10.02Å, and c = 9.61Å. The space group is $P2_12_12$ with four molecules per unit cell. Three dimensional intensity data were collected by Weissenberg method and the structure is being determined by the symbolic addition method.

4. Crystallisation of Pepsin

(V.M. Padmanabhan)

Systematic attempts to grow single crystals of pepsin have been started in order to study the structure of this protein. Several attempts to grow crystals from $2M(NH_4)_2SO_4$ solution buffered at different pH were not successful. A concentration of 2% of protein in 20% ethanol at pH 3.0 (with 5 N sulphuric acid) gave acicular crystals too thin for x-ray use. Crystallisation is being tried at different concentrations and pH values to get bigger crystals.

5. Computer Programme CELPAR

(V.K. Wadhawan)

This least-squares refinement programme has been developed for getting precise and accurate values for cell parameters in a simple way from routine, zero-layer,Weissenberg photographs. For a zero-layer photograph, a measurement of the ordinates of the various spots above the central base line gives directly their Bragg angles, θ_{obs}. These are compared with the calculated values, θ_{cal}, obtained from approximate starting values for the reciprocal lattice parameters. An allowance for practically all the systematic errors is made by expressing θ_{cal} as

$$\theta_{cal} = \theta_o + C_{-1}\theta_o^{-1} + C_o + C_1\theta_o + C_2\theta_o^2.$$

Here θ_o is the value of Bragg angle which would be obtained if all the systematic errors were absent. The extra parameters introduced: C_{-1}, C_o, C_1 and C_2, which are unknown to start with, are given a starting value of zero and are determined in the course of the least-squares refinement along with the reciprocal lattice parameters.

II. NEUTRON CRYSTALLOGRAPHY

1. Extinction Effects in Neutron Diffraction

(A. Sequeira and R. Chidambaram)

The validity of the recent general theory of secondary extinction due to Zachariasen[1] has been examined in the light of severely extinction-affected neutron diffraction data from two crystals, viz., RbH_2PO_4 and Glutamic acid.HCl. In both these cases, the conventional one-parameter empirical corrections of a linear or exponential type were found to overcorrect the strong reflections considerably and the data so corrected did not lead to reasonable structural parameters. Zachariasen's new method is found to be far superior to these old methods, although there is a general tendency to under-correct the most severely affected reflections.

According to Zachariasen's theory, the integrated intensity I is given by

$$I = I_k Y = \left[I_o V A(\mu) Q \right] Y$$

where y is the extinction factor and has the form

$$Y = \left[1 + 2x \right]^{-1/2}$$

where

$$X = r^* \lambda^{-1} Q \bar{T} \quad \text{for neutrons}$$

and

$$r^* = r \left[1 + \left(\frac{r}{\lambda g} \right)^2 \right]^{-1/2}$$

(r defines the average particle size and g defines the Gaussian mosaic spread)

If $r \gg \lambda g$, as in type I crystals,

$$r^* = \lambda g \; ; \; x = gQ\bar{T}$$

If $r \ll \lambda g$, as in type II crystals

$$r^* = r$$
$$x = r \lambda^{-1} Q \bar{T}$$

Neutron data from RbH_2PO_4 and Glutamic acid.HCl. have been corrected for extinction by the above method, using a modified version of Busing and Levy's crystallographic least-squares programme XFLS, the modification involving a provision for refining the isotropic extinction parameter, r*.

(a) RbH_2PO_4: In the least-squares refinement of the structure, 22 variable parameters including an extinction parameter were refined based on the intensities of 204 reflections recorded at a neutron wavelength of 1.402 Å. The final value of the conventional R-factor was 0.0393. The Fo^2/Fc^2 value for the worst-affected reflection was 0.12, and the final value of the extinction factor $g(= r^* \lambda^{-1})$ was 4.23×10^4. This corresponds to an equivalent mosaic spread of 1.2 seconds.

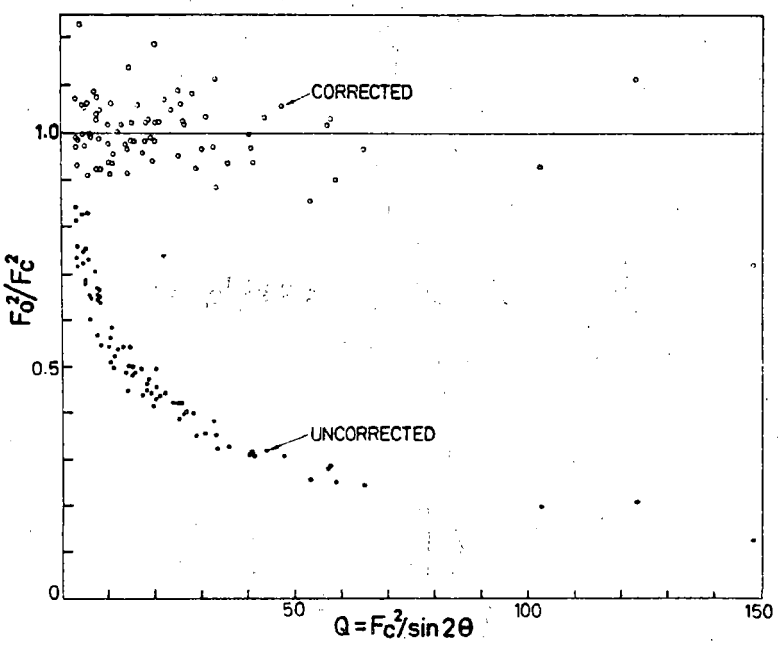

Fig. 23. Extinction Effects in RbH_2PO_4.

The variation of the extinction factor $y(=Fo^2/Fc^2)$ is shown in

Fig.23 as a function of the reflectivity Q, and in Fig.24 as a function of the parameter $x(= r^* \lambda^{-1} Q \bar{T})$. As can be seen from Fig.24 the agreement with the theory is quite good.

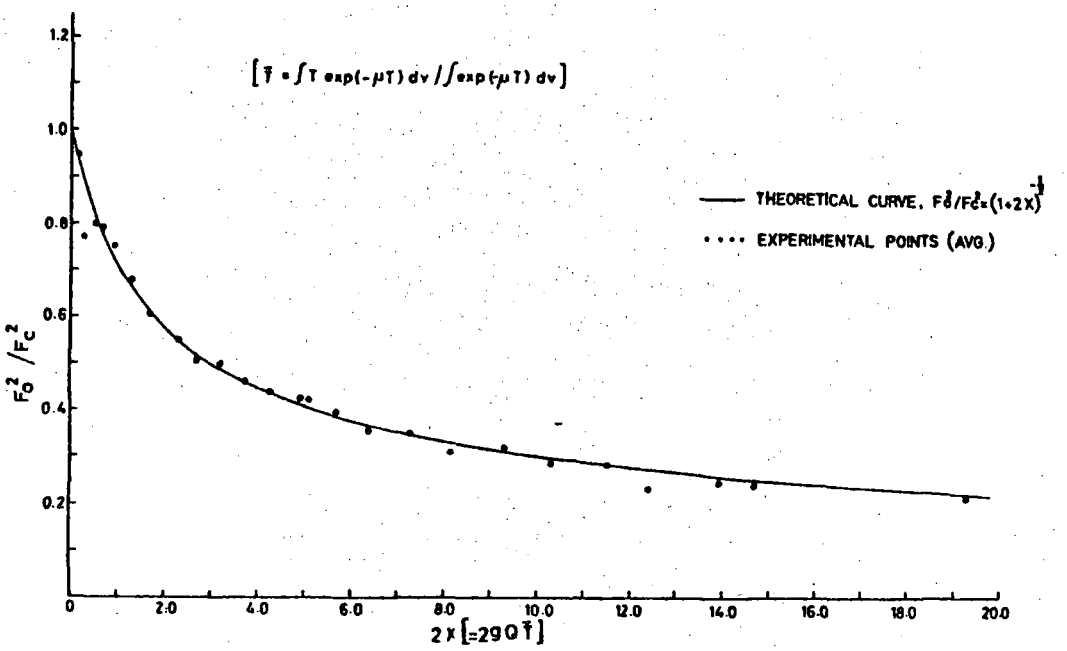

Fig. 24. Variation of Extinction with $x = gQ\bar{T}$ in RbH_2PO_4

(b) Glutamic acid.HCl : In this structure, neutron intensities of 639 independent reflections recorded at $\lambda = 1.406$ Å, were used to refine 191 parameters including an extinction parameter. The value of Fo^2/Fc^2 for the worst-affected reflection was 0.06. The final value of the conventional R-factor was 0.0427 and the value of the extinction parameter $g(= r^* \lambda^{-1})$ was 14.8×10^4.

The variation of $y(= Fo^2/Fc^2)$ with Q for this crystal is shown in Fig23 and with $x(= r^* \lambda^{-1} Q \bar{T})$ in Fig.26. About 20 reflections for which $x < 20$ are not included in Fig.26. For these reflections however, the observed values of Fo^2/Fc^2 were systematically lower than those predicted by Zachariasen's theory and hence were omitted from the least-squares refinement. As can be seen from Fig.26, reflections for which $x < 20$, are again well corrected for extinction.

These two studies show that Zachariasen's recent method of correcting for secondary extinction is satisfactory on the whole,

although it has a tendency to under-correct a few very strong reflections, for which Fo^2/Fc^2 is less than about 0.25.

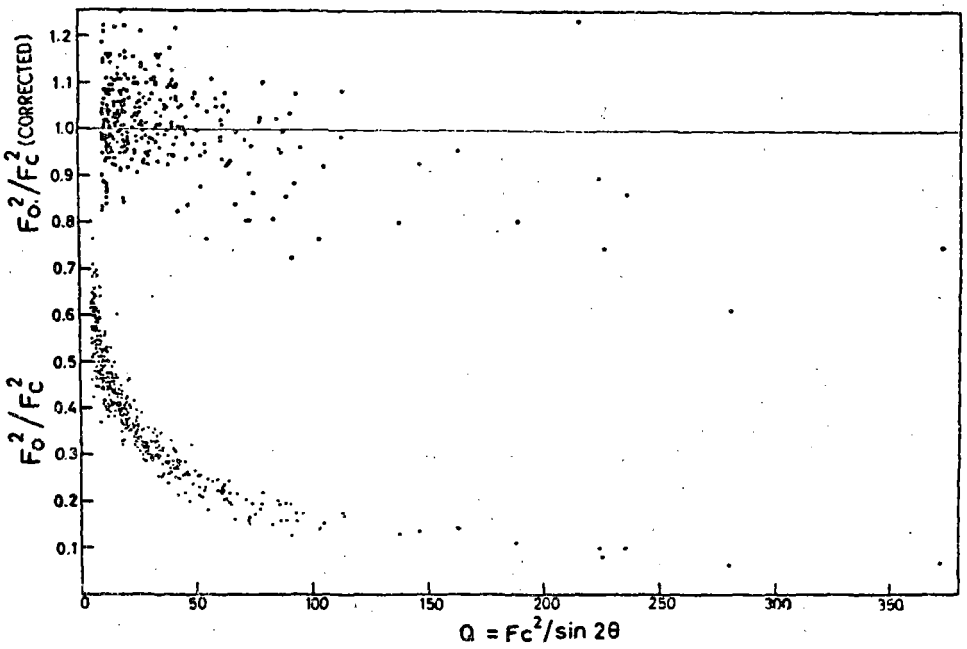

Fig. 25. Extinction Effects in Glutamic Acid HCl

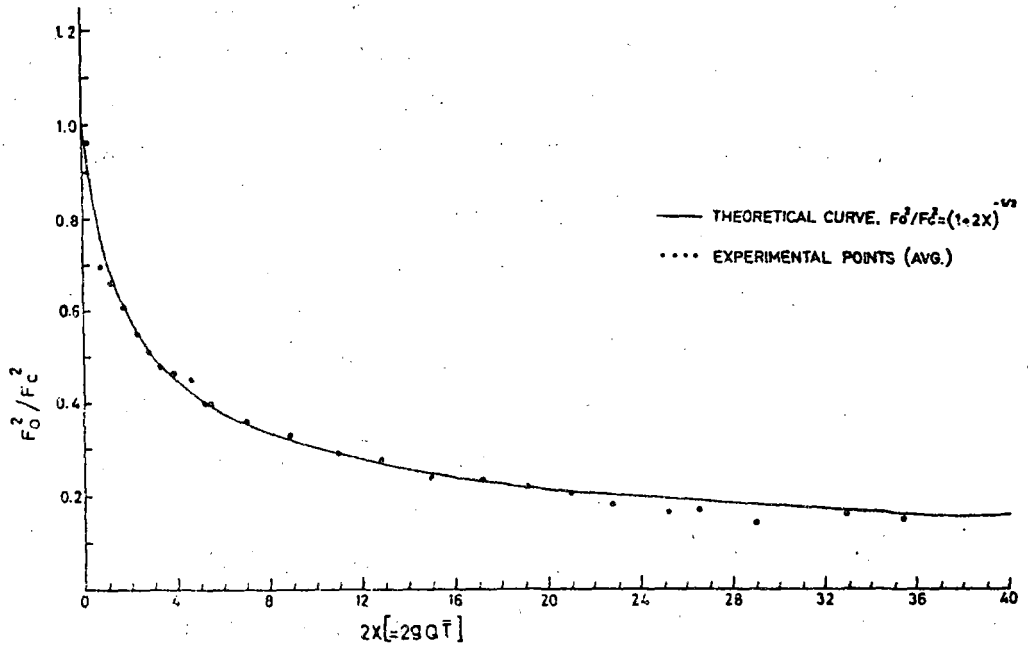

Fig. 26. Variation of Extinction with $x = gQ\bar{T}$ in Glutamic Acid HCl.

1. W.H. Zachariasen, Acta , Cryst. 23 558(1967)

2. Molecular Packing from Energy Considerations

(S.K. Sikka & R. Chidambaram)

Kitaigorodskii and Murskaya[1] and Williams[2] have shown that the structures of crystals containing rigid molecules bound together by Van der Walls forces can be predicted from energy calculations. An attempt has been made to extend this approach to crystals containing rigid molecules but held together by hydrogen bonds as well. For this the necessary computer programmes (PACKING and PACK) have been developed and tested on the structure of C_6H_6. The calculations for the structure of α-resorcinol, $C_6H_4(OH)_2$ are in progress. For hydrogen bonds, the Lippincott-Schroder potential function as modified by the authors[3] is being used.

---

1. I. Kitaigorodskii and K.V. Mursakaya , Kristallographia,6,408(1961)
2. D.E. Williams Science 147,605(1965)
3. R. Chidambaram and S.K. Sikka , Chem.Phys.Letters 2,162(1968

3. A Neutron Diffraction Refinement of the Structure of L - Asparagine Monohydrate

(M. Ramanadham, S.K. Sikka & R. Chidambaram)

A single crystal neutron diffraction refinement of the L - asparagine monohydrate structure (space group $P\,2_12_12_1$: a = 5.582, b = 9.812 and c = 11.796 Å) has been carried out. Three-dimensional intensity data were collected on the diffractometer 'SAND'[1] on the Θ-plate of which a full-circle Siemens crystal orienter was mounted. From a single crystal weighing 37 mgms, the integrated intensities of 890 reflections upto $\sin\theta/\lambda = 0.65$ Å^{-1} were measured. Out of these 749 were nonzero. These were corrected for absorption ($\mu = 2.74$ cm^{-1}) and reduced to $|Fo|^2$. The 10 hydrogen atoms in the asymmetric unit were located from a neutron scattering density Fourier map, computed with observed Fo's as amplitudes and phases from the known X-ray positions of non-hydrogen atoms[2]. The structural parameters were refined by the full matrix anisotropic least squares method. The extinction corrections to the observed data were applied by a method due to Zachariasen. For this, the programme XFLS[3] was modified.

Table 1. Final positional and thermal parameters for L-asparagine monohydrate Least squares standard deviations are shown in parentheses. All parameters are multiplied by 10^4 and the thermal parameters are in the form of $\exp\left[-(\beta_{11}h^2 + \beta_{22}k^2 + \beta_{33}l^2 + 2hk\,\beta_{12} + 2hl\,\beta_{13} + 2kl\,\beta_{23})\right]$.

Atom	x/a	y/a	z/a	β_{11}	β_{22}	β_{33}	β_{12}	β_{13}	β_{23}
C(1)	-1245(10)	- 580(5)	360(4)	192(18)	51(5)	37(3)	- 22(10)	4(8)	- 2(4)
C(2)	-3053(9)	- 291(5)	1296(4)	149(17)	48(5)	36(3)	29(8)	12(8)	2(3)
C(3)	-2104(9)	562(5)	2275(4)	161(17)	42(4)	40(4)	15(9)	-34(8)	2(4)
C(4)	165(10)	- 19(5)	2777(4)	163(17)	34(4)	40(4)	- 10(8)	10(9)	4(4)
N(1)	-4160(7)	-1560(3)	1718(3)	159(12)	49(3)	39(2)	- 3(7)	8(6)	- 1(2)
N(2)	1069(8)	640(4)	3686(3)	269(16)	63(4)	48(3)	25(8)	-32(7)	- 15(3)
O(1)	- 77(12)	435(6)	18(6)	240(23)	46(6)	75(5)	- 27(12)	31(11)	- 17(5)
O(2)	-1192(13)	-1738(6)	- 67(5)	237(22)	57(6)	51(4)	- 9(13)	31(11)	- 15(4)
O(3)	1145(13)	-1061(6)	2383(5)	185(21)	66(6)	55(5)	4(12)	29(10)	- 15(5)
O(4)	3082(14)	2301(7)	1133(5)	328(28)	80(7)	57(5)	- 69(14)	-14(12)	3(5)
H(1)	1820(24)	1739(11)	704(10)	377(51)	84(13)	104(11)	-102(25)	-27(23)	- 30(10)
H(2)	3474(24)	3040(11)	599(9)	346(47)	79(11)	88(10)	- 43(25)	-52(22)	- 3(9)
H(3)	-3107(22)	-2020(10)	2338(8)	333(47)	51(9)	62(8)	2(19)	-20(20)	17(8)
H(4)	-4435(23)	-2279(9)	1067(8)	360(46)	38(9)	63(7)	- 72(19)	36(20)	- 11(7)
H(5)	-5851(22)	-1370(9)	2053(10)	289(43)	46(9)	92(10)	- 61(19)	21(21)	- 9(9)
H(6)	2506(19)	276(11)	4073(9)	198(31)	102(14)	62(8)	- 16(20)	6(16)	- 9(9)
H(7)	285(23)	1502(12)	3948(9)	400(53)	84(12)	70(9)	- 7(25)	57(21)	- 18(9)
H(8)	-4494(20)	347(10)	922(9)	223(35)	70(11)	91(9)	71(19)	- 6(18)	23(9)
H(9)	-1675(22)	1596(9)	1941(10)	289(42)	38(8)	104(10)	12(19)	3(20)	15(8)
H(10)	-3385(22)	750(13)	2933(10)	221(38)	144(16)	89(10)	52(24)	33(19)	- 33(12)

The final R-factor ($= \frac{\Sigma ||F_o| - |F_c||}{\Sigma |F_o|}$) attained was 0.096. The final nuclear parameters are given in Table I. A projection view of the structure on the (100) plane is shown in Fig.27.

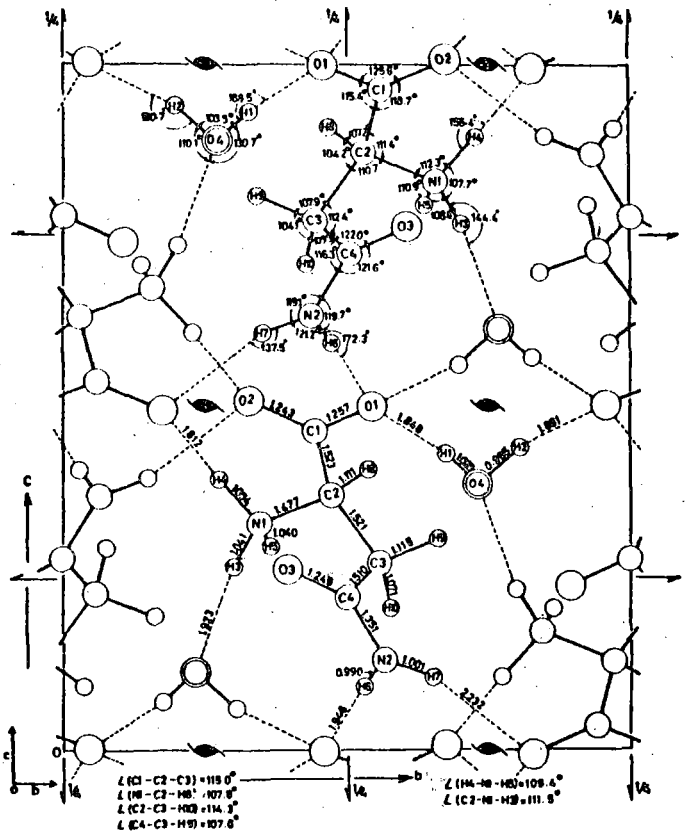

Fig. 27. Projection of the structure of L-Asparagine monohydrate on the (100) plane.

The dimensions of the amino acid group for the asparagine molecule are in good agreement with the average values for other amino acids reported by Marsh and Donohue[4]. The hydrogen bond scheme has been elucidated and the X-ray result that the structure of the asparagine molecule is an open chain, is confirmed.

---

1. R. Chidambaram, A. Sequeira and S.N. Momin, Ind. J. Pure Appl. Phys. 6,550(1968)
2. G. Kartha and A. DeVries, Nature, 192,862(1961)
3. W.R. Busing, K.O. Martin and H.A. Leoy, ORFLS, A Fortran Crystallographic Least Squares Program, Oak Ridge National Laboratory Report ORNL-TM-305. The version incorporates modifications by W.C. Hamilton, J.A. Ibers and C.K. Johnson.
4. R.E. Marsh and J. Donohue, Adv. Protein Chem. 22,235(1967)

4. A Neutron Diffraction Refinement of the Structure of D, L-Glutamic Acid. HCl.

(A. Sequeira, H. Rajagopal and R. Chidambaram)

A single crystal neutron diffraction refinement of the structure of D, L-Glutamic acid. HCl has been carried out as a part of a series of investigations of the crystal structures of amino acids.

α -Glutamic acid. HCl, $NH_3^+CH(CH_2CH_2COOH)COOH.Cl^-$, crystallises in the orthorhombic space group $P2_12_12_1$ with 4 molecules per unit cell of dimensions: a = 5.138A, b = 11.78Å and c = 13.34Å. A two dimensional x-ray study was carried out by Dawson[1] but the positions of the hydrogen atoms were not determined.

In the present investigation neutron intensities of 639 independent reflections, within the limit $\sin\theta/\lambda \leq 0.57$ ($\lambda = 1.406$Å), from a single crystal (weight 35 mgm) were measured using the Trombay automatic diffractometer,3D FAD[2]. These were corrected for absorption ($\mu = 2.75\ cm^{-1}$) and reduced to Fo^2 values in the usual way. The positions of the hydrogen atoms were located from a Fourier synthesis of the neutron scattering density based on the phases given by the heavy atom positions. All the structural parameters including an isotropic extinction parameter were refined by the method of least squares. The data were severely affected by extinction and were corrected by the Zachariasen's method (see article 1 of this section). The correction was quite satisfactory except for a few very severely affected reflections which had a tendency to be undercorrected. Out of the 639 reflections recorded only 579 for which $Fo^2/Fc^2 > 0.22$ and $Fo^2 > \sigma(Fo^2)$ were used in the refinement. Corresponding to these, the final value of the conventional R-factor was 0.0427. The resulting parameters are given in Table I, and a stereoplot of the molecule is shown in Fig.28. The molecules in the structure are held together by a three dimensional net work of O—H.....O, O—H.....Cl, N—H.....O and N—H.....Cl hydrogen bonds. The bond distances and bond angles are listed in Table II.

---

1. Dawson, Acta Cryst. 6,81(1953)

2. Momin, S.N., Sequeira, A and Chidambaram, R. Seminar on Crystallography, Centre of Advanced Study in Crystallography, Madras, Feb. (1969).

Table I Positional and thermal parameters for Glutamic Acid HCl. All the parameters have been multiplied by 10^4 and the standard deviations are given in parentheses. Temperature factor used is of the form

$$\exp -(\beta_{11}h^2 + \beta_{22}k^2 + \beta_{33}l^2 + 2\beta_{12}hk + 2\beta_{13}hl + 2\beta_{23}kl)$$

Atom description	x/a	y/b	z/c	β_{11}	β_{22}	β_{33}	β_{12}	β_{13}	β_{23}
C(1)	3867(10)	1434(5)	4105(3)	146(19)	35(4)	20(2)	15(7)	31(5)	-6(3)
C(2)	5688(9)	1963(4)	3324(3)	56(14)	34(3)	11(2)	2(7)	3(5)	-2(2)
C(3)	4806(8)	1550(4)	2286(3)	104(14)	21(3)	19(2)	-26(6)	11(5)	7(2)
C(4)	6616(10)	1835(4)	1417(3)	153(17)	25(3)	18(2)	-18(7)	-7(6)	-4(3)
C(5)	5785(10)	1292(4)	473(4)	176(17)	19(3)	24(3)	-9(8)	-5(7)	-6(2)
O(1)	4367(14)	374(5)	4270(5)	234(23)	37(5)	54(4)	10(10)	74(10)	14(4)
O(2)	2091(15)	1973(5)	4489(4)	295(26)	46(5)	26(3)	-28(10)	27(9)	-0(3)
O(3)	4196(16)	519(6)	449(4)	405(29)	54(5)	17(3)	-29(12)	-6(9)	-9(3)
O(4)	6932(14)	1672(6)	-341(4)	296(25)	50(5)	22(3)	-32(11)	6(8)	4(3)
N	5598(7)	3213(3)	3423(2)	117(11)	30(3)	24(2)	-18(5)	-19(5)	-4(2)
CL	542(7)	4281(3)	2384(3)	152(11)	42(2)	35(2)	-24(5)	15(5)	-6(2)
H(1)	2916(22)	25(9)	4687(8)	306(45)	47(8)	54(6)	-66(16)	73(15)	1(6)
H(2)	6461(25)	1283(9)	-954(7)	376(45)	62(8)	27(4)	4(17)	41(13)	-6(5)
H(3)	5803(25)	3441(10)	4174(6)	420(45)	75(9)	22(4)	-121(20)	59(13)	-16(5)
H(4)	7188(21)	3567(8)	3031(8)	244(37)	28(7)	45(6)	-46(14)	48(13)	-2(5)
H(5)	3798(21)	3547(12)	3136(9)	176(37)	78(11)	61(7)	25(17)	22(13)	-24(8)
H(6)	7653(15)	1682(10)	3485(8)	36(26)	71(9)	55(6)	19(13)	9(11)	-9(7)
H(7)	4574(32)	638(8)	2314(8)	706(70)	31(6)	45(5)	41(20)	56(21)	-14(6)
H(8)	2943(24)	1893(13)	2143(9)	261(39)	109(12)	48(6)	-53(22)	13(16)	-7(8)
H(9)	8585(19)	1541(14)	1606(8)	71(29)	140(14)	45(6)	-10(17)	8(12)	-20(8)
H(10)	6819(35)	2764(9)	1292(8)	922(93)	34(7)	39(5)	-165(24)	76(21)	-7(5)

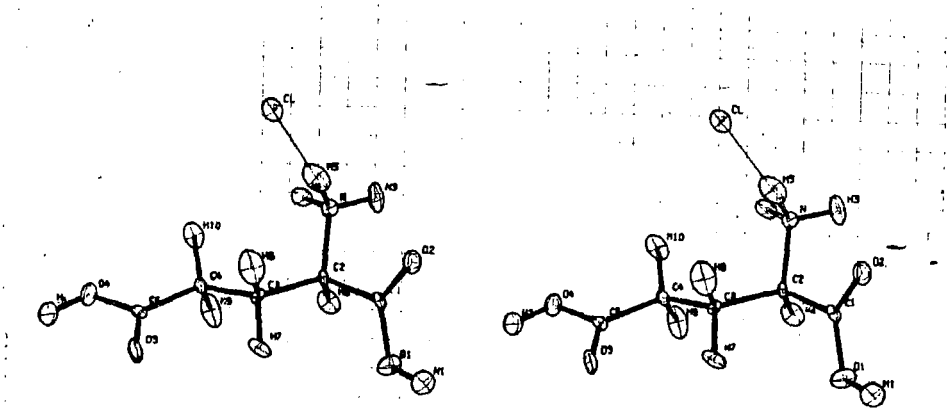

Fig. 28. Stereo view of D-L Glutamic Acid Hcl.

Table II

Bond distance in bond angles in Glutamic Acid HCl. (Labelling of the atoms is as in the figure; standard deviations are given in parentheses).

a. Intramolecular

$C_1 - C_2$ = 1.533(7)Å	;	$O_1 - H_1$ = 1.017(13)Å	
$C_2 - C_3$ = 1.536(6)	;	$O_4 - H_2$ = 0.968(11)	
$C_3 - C_4$ = 1.524(6)	;	$N - H_3$ = 1.043(9)	
$C_4 - C_5$ = 1.475(7)	;	$N - H_4$ = 1.056(11)	
$C_1 - O_1$ = 1.294(8)	;	$N - H_5$ = 1.075(12)	
$C_1 - O_2$ = 1.224(9)	;	$C_2 - H_6$ = 1.084(10)	
$C_5 - O_3$ = 1.224(9)	;	$C_3 - H_7$ = 1.081(11)	
$C_5 - O_4$ = 1.314(8)	;	$C_3 - H_8$ = 1.056(13)	
$C_2 - N$ = 1.479(6)	;	$C_4 - H_9$ = 1.099(11)	
		$C_4 - H_{10}$ = 1.112(12)	

b. Intermolecular

$H_1 \ldots\ldots O_3$ = 1.619(13)Å	;	$\angle O_1 - H_1 \ldots\ldots O_3$ = 174.1°(1°)	
$H_2 \ldots\ldots Cl$ = 2.075(10)	;	$\angle O_4 - H_2 \ldots\ldots Cl$ = 170.2°	
$H_3 \ldots\ldots O_2$ = 1.965(11)	;	$\angle N - H_3 \ldots\ldots O_2$ = 147.5°	
$H_4 \ldots\ldots Cl$ = 2.103(11)	;	$\angle N - H_4 \ldots\ldots Cl$ = 174.5°	
$H_5 \ldots\ldots Cl$ = 2.134(12)	;	$\angle N - H_5 \ldots\ldots Cl$ = 171.9°	

III. NEUTRON DIFFRACTION STUDIES OF MAGNETIC MATERIALS

1. Exchange Integrals in $Mg_xMn_{1-x}Fe_2O_4$ Ferrite System

(N.S. Satya Murthy, L. Madhav Rao, R.J. Begum, S.K. Paranjpe, V.C. Rakhecha and M.R.L.N. Murthy)

In a ferrite such as $ZnFe_2O_4$ where only one type of exchange interaction i.e. J_{BB} $(Fe^{3+} - Fe^{3+})$ exists, the most suitable method for measuring this quantity is by the paramagnetic neutron scattering technique. But in a mixed ferrite system such as $Mg_xMn_{1-x}Fe_2O_4$ where several types of exchange interactions are operative this procedure alone is not applicable. On the other hand, the molecular field theory yields unrealistically high values for the intrasublattice exchange integrals, as pointed out by Smart[1]. Therefore, a combination of the paramagnetic neutron scattering technique and the molecular field analysis has been applied, to evaluate the relevant exchange integrals in the mixed ferrite system, $Mg_xMn_{1-x}Fe_2O_4$. Neutron diffraction measurements were made to determine the temperature dependence of the sublattice magnetisations in this system. The data were analysed in the molecular field framework, fixing J_{BB} to be 1°K as obtained in an earlier paramagnetic neutron scattering experiment[2].

In $MgFe_2O_4$ the exchange constants J_{AB} and J_{AA} have been determined to be -22°K and -4°K respectively, (see following article) while for $MnFe_2O_4$ the corresponding values are -8.6°K and -0.5°K. The J_{AB} in $MnFe_2O_4$ can be thought of as consisting of two parts, $J_{AB}(Fe^{3+} - Fe^{3+})$ and $J_{AB}(Mn^{2+} - Fe^{3+})$. Taking into account the cation distribution of $MnFe_2O_4$ and using the value of $J_{AB}(Fe^{3+} - Fe^{3+})$ obtained from the $MgFe_2O_4$ data, $J_{AB}(Mn^{2+} - Fe^{3+})$ comes out to be -7.7°K. Table I lists the exchange integrals for all the members of the series. The calculated values for J_{AB} have been obtained from the measured values of $J_{AB}(Mn^{2+} - Fe^{3+})$ and $J_{AB}(Fe^{3+} - Fe^{3+})$ weighting them properly according to the cation distribution.

Table I

Exchange Integrals in $Mg_x Mn_{1-x} Fe_2O_4$ system.

X	Cation Distribution	J_{AA} (°K)	J_{AB} (°K) Obs.	Calc.
0.0	$(Mg_{0.13} Fe_{.87})\ M_{.87} Fe_{1.13}$	-4.0	-22.0	..
1.0	$(Mn_{.93} Fe_{.07})\ Mn_{.07} Fe_{1.93}$	-0.5	- 8.6	..
0.25	$(Mg_{.03} Mn_{.29} Fe_{.68})\ Mg_{.22} Mn_{.46} Fe_{1.32}$	-3.0	-13.5	-17.3
0.50	$(Mg_{.09} Mn_{.39} Fe_{.52})\ Mg_{.41} Mn_{.11} Fe_{1.48}$	-2.6	-14.5	-14.1
0.75	$(Mg_{.11} Mn_{.10} Fe_{.79})\ Mg_{.64} Mn_{.15} Fe_{1.21}$	-3.3	-17.5	-18.4

It is seen that the agreement between the observed and the calculated values is good except for x = 0.25. This discrepancy in the latter case is due to the fact that appreciable amounts of Mn^{2+} ions exist on both the sublattices and for a proper evaluation of the effictive J_{AB}, $J_{AB}(Mn^{2+} - Mn^{2+})$ should be known.

---

1. J.S. Smart Magnetism Vol. III, Edited by G.T. Rado and H. Suhl, (Academic Press, N.Y.) 1963.

2. N.S. Satya Murthy, L. Madhav Rao, R.J. Begum, M.G. Natera and S.I. Youssef, International Conference on Magnetism, Grenoble, 1970 Paper No. (Me A8)

2. *Evaluation of Exchange Integrals in $MgFe_2O_4$:*

(V.C. Rakhecha, R.J. Begum and N.S. Satya Murthy)

The prominent exchange integrals in $MgFe_2O_4$ were evaluated using molecular field expressions to fit the temperature dependence of the A and B sublattice magnetisations, $M_A(T)$ and $M_B(T)$ obtained from neutron diffraction data[1]. The expressions used were,

$$M_A(T) = M_0 \; B_{S_A}\left[\frac{2M_{S_A}}{g^2T}\left\{-J_{AA}\,Z_{AA}\,M_A + J_{AB}\,Z_{AB}\,M_B\right\}\right]$$

$$M_B(T) = M_B^\circ \quad B_{S_A}\left[\frac{2M_{S_B}}{g^2T}\left\{-J_{AB}\,Z_{BA}\,M_A + J_{BB}Z_{BB}\,M_B\right\}\right]$$

Here M_A, M_B are the average moments on the A and B sites and M_A°, M_B° are the corresponding values extrapolated to 0°K. $S_A = S_B = 5/2$ for the Fe^{3+} ions on the A and B sites. M_{S_A} and M_{S_B} are the magnetic moments for the full spin values. B_S is the Brillouin function with $S = S_A$ or S_B. Z_{AA}, Z_{AB}, Z_{BA} and Z_{BB} correspond to the number of neighbours of the appropriate atoms (Z_{AA}, for example, is the number of A site nearest neighbours of an A site ion etc.) and are known from the spinel structure.

The exchange integrals were extracted using a computer programme in which the sum

$$d = \sum_T \left[M_A(T) - M_A^{Cal}(T)\right]^2 + \left[M_B(T) - M_B^{Cal}(T)\right]^2$$

was minimised using the exchange integrals as parameters. The procedure was rather insensitive to the variation of J_{AA} and J_{BB} (because of the relatively small coefficients they have) and they were therefore fixed from other considerations (paramagnetic neutron scattering[2] and Moglestue's evaluation of J_{AA} in Fe_3O_4[3]. The final values thus obtained for $MgFe_2O_4$ (which is 87% inverted) are: $J_{AA} = -4$°K, $J_{BB} = 1$°K and $J_{AB} = -22$°K.

---

1. BARC-501 Annual Report of the Nuclear Physics Division 1969-70, p.44
2. BARC-501 Annual Report of the Nuclear Physics Division 1969-70, p.50
3. K.T. Moglestue, Inelastic Scattering of Neutrons, IAEA, Vienna, Vol.II, p.117(1968)

3. Magnetic Structure of Co_2TiO_4

(R.J. Begum, L. Madhav Rao, C.S. Somanathan, B.S. Srinivasan and M.R.L.N. Murthy)

Figure 29 shows a high resolution diffraction pattern of Co_2TiO_4 taken at 4.2°K with the pattern at 300°K also included for comparison. The interesting feature of the low temperature pattern is the presence of satellite reflections associated with the fundamental reflection (111) which is essentially magnetic in origin. The simplest magnetic

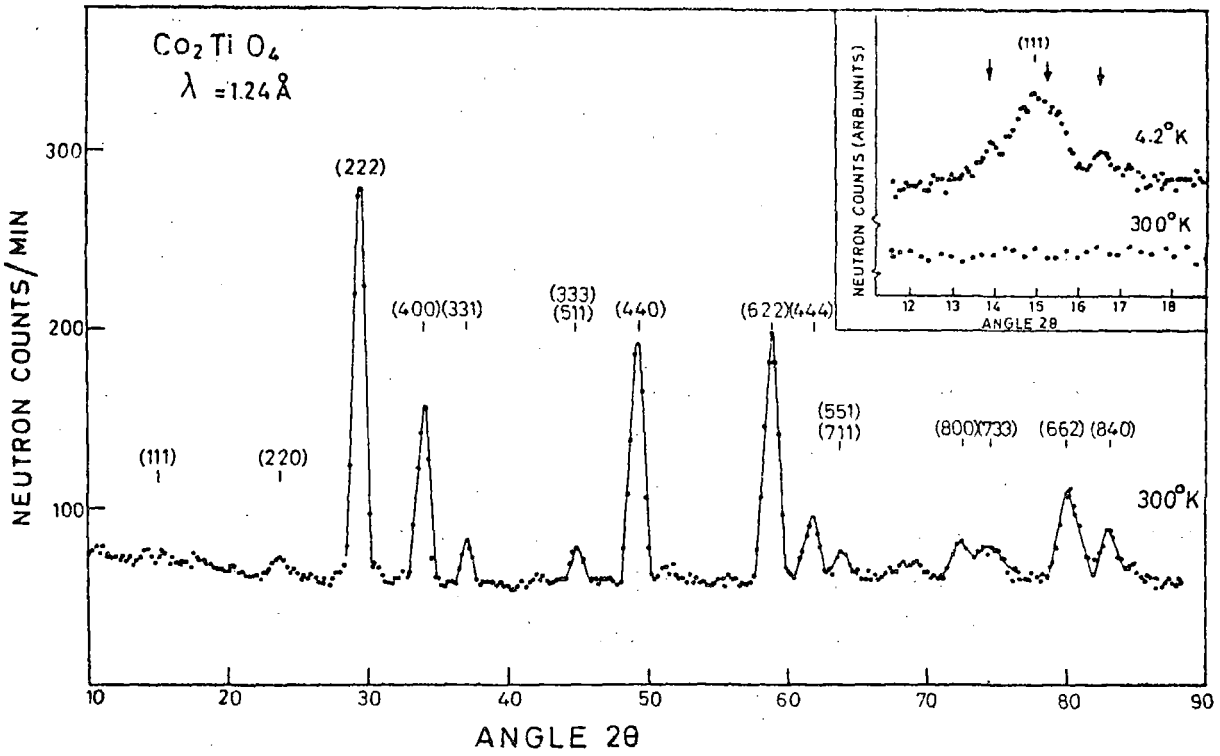

Fig. 29. Neutron Diffraction Pattern of Co_2TiO_4 at 4.2°K

structure constructed from these observations is a conical spiral arrangement of the Co^{2+} magnetic moments on the B-sublattice as shown in Fig. 30

The satellite reflections are associated with reciprocal lattice vectors $\underline{G} = \underline{G}_0 + \underline{\tau}$ where $\underline{G}_0$ is the reciprocal lattice vector corresponding to the fundamental reflection and $\underline{\tau}$ is the propagation vector for the transverse component of the atomic magnetic moment. Using a computer programme specially written for this purpose, various possible

satellites for different $\underline{\tau}$ have been calculated. A direction of propagation along [110] gives rise to the satellites observed, for the

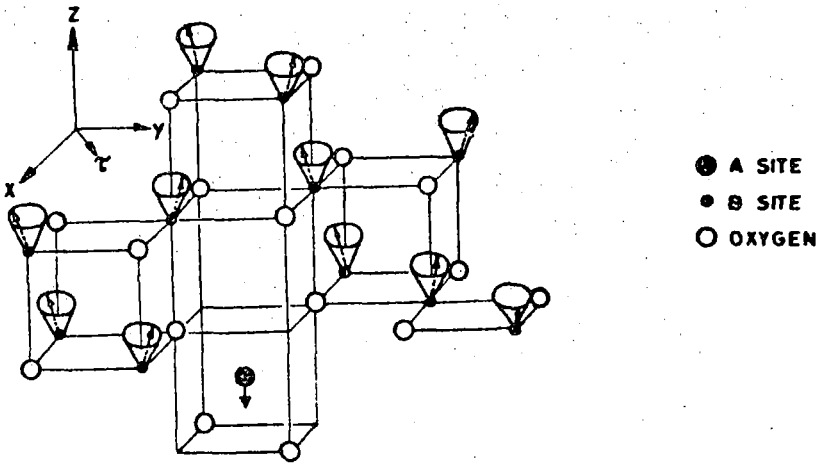

Fig. 30. Probable Magnetic Structure of Co_2TiO_4

positions are then given by

$$\frac{1}{d'^2} = \frac{1}{d^2} + \tau^2 + \frac{\sqrt{2}\,|\tau|}{a_0}(h+k)$$

and the possible values of $(h+k)$ for $\{111\}$ reflections are 0 and ± 2. The arrows in Fig. 30 indicate the satellites

$$(111)^0,\quad (111)^{+2} \text{ and } (111)^{-2}$$

A comparison of the (222) and the (440) reflections seem to show evidence of orbital contribution to Co^{2+} magnetic moments on the B-sites.

4. Neutron Diffraction Studies of some Manganites

(N.K. Radhakrishnan)+

The cation distributions in certain oxidic spinels containing manganese, which are not yet unequivocally known, have been investigated. The individual manganites were prepared, starting from the pure oxides, by the usual ceramic technique. Some of the more important results are:

i) Copper manganite has a cubic symmetry with cell edge $a_0 = 8.32$Å. It is partially inverted the degree of inversion being 25%. The value of the oxygen parameter is 0.2627. The experimental results indicate a distribution $(Cu_{.75}\,Mn_{.25})\,[Cu_{.25}\,Mn_{1.75}]\,O_4$, which is fairly in good agreement with the work of Zsalvaskii et al[1].

ii) Zinc manganite is tetragonal with lattice parameters a = 8.09Å and c = 9.21Å. Samples, subjected to different thermal treatment, gave identical patterns corresponding to a completely normal arrangement.

iii) A modification of the cation distribution of $MgMn_2O_4$ has been found with temperature, thereby confirming[2] the migration of Mg^{2+} ions from the tetrahedral to the octahedral sites at elevated temperatures. The degree of inversion is found to vary from 20% for the annealed sample to 40% for the sample quenched from 450°C.

+ Research Student from the Indian Institute of Technology, Bombay.

1. A.I. Zsalvskii and V.P. Plakhtii, Sov. Phys-Solid State, 11,672(1969)

2. K.S. Irani, A.P.B. Sinha and A.B. Biswas, J. Phys. Chem. Solids, 23,711(1962)

5. Paramagnetic Neutron Scattering From $ZnCr_2O_4$

(R.J. Begum, L. Madhav Rao and N.S. Satya Murthy)

The technique of cold neutron inelastic scattering in the paramagnetic state has been used to extract the $Cr^{3+} - Cr^{3+}$ B site exchange integral in $ZnCr_2O_4$ by the de Gennes method of moments. The cation distribution in the sample was found to be completely normal from the neutron diffraction study at 300°K and hence the only dominant exchange integrals operating is that between the B-site ions. It is known that the complicated spin ordering that appears at extremely low temperature in normal spinels like $ZnCr_2O_4$ and $ZnFe_2O_4$ is due to distant neighbour B-B interactions. However, they are much smaller in magnitude than the nearest neighbour B-B interaction and can be ignored to a first approximation at high temperatures. In the paramagnetic scattering experiment, the energy exchange with the neutrons can be reasonably assumed to arise mainly from this dominant interaction, especially as the

second moment involves the squares of the J's. The value evaluated on this assumption is

$$J_{BB}\ (Cr^{3+} - Cr^{3+}) = 2.38°K$$

using a S value of 1.314[1].

---

1. R. Plumier, Ph.D. Thesis, University of Paris, (1968)

6. Neutron Scattering from Short Range Ordered Paramagnets - the Modified Convolution Approximation Model

(L. Madhav Rao)

The modified convolution approximation (MCA) model recently proposed[1] to explain neutron scattering from short range ordered paramagnets like MnO has been further applied to explain other available experimental data on MnO. The MCA model successfully explains[2] the oscillatory nature of the width of the neutron spectra scattered from powder MnO at 295°K observed by Iyengar and Brockhouse[3] on a triple axis spectrometer. Based on this model, theoretical neutron spectra have been computed and compared with the time-of-flight spectra of Kroo and Bata[4] at 124°K and 143°K. The MCA model is able to explain qualitatively the observed energy shifts in the spectra scattered from

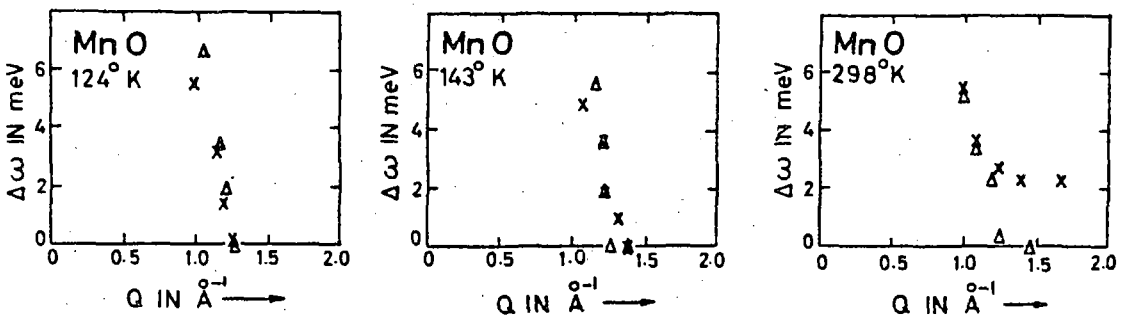

Fig. 31. Energy distribution of scattered neutrons from paramagnetic MnO. X are the result of the present calculation while Δ represent the data points of Kroo and Bata.

paramagnetic MnO over a wide range of temperatures, without assuming the existence of spinwave like excitations[2] (see Fig. 31). The MCA

model points out that these observed energy shifts arise essentially due to the non-constant-Q nature of the experiments. The principal conclusion of these model calculations is that existing time-of-flight experiments have not provided an unambiguous answer to the question whether collective spin-wave-like excitations exist or not in paramagnetic MnO. To verify this point, a constant-Q experiment using a single crystal of MnO is clearly essential.

---

1. L. Madhav Rao, B.A. Dasannacharya, N.S. Satya Murthy and P.K. Iyengar, Solid State Communications, 7,123(1969).

2. L. Madhav Rao, Ph.D. Thesis, University of Bombay, 1970.

3. P.K. Iyengar and B.N. Brockhouse, Bull. Am. Phys. Soc. 3,195(1958)

4. N. Kroo and L. Bata, Symposium on Neutron Inelastic Scattering (I.A.E.A. Vienna, 1968) Vol. 2, page 111.

7. Helical Guide field for Polarised Neutron Spectrometer

(N.S. Satya Murthy, L. Madhav Rao, C.S. Somanathan, B.S. Srinivasan, M.R.L.N. Murthy and S.K. Paranjpe)

The polarised neutron spectrometer has been made more versatile by installing a new magnetic guide field between the polarising crystal and the sample table. This enables measurement on the spectrometer of both spin-density distributions and magnon dispersion curves, by the diffraction technique. Small ceramic magnets have been used in the construction of the guide field. The guide field consists of two parts. The first part, nearer to the polarising crystal is 41 cm. long and provides a constant vertical magnetic field of 100 Oersted parallel to the polarising field. It also houses the resonant flipper coil. The second part, 35 cm long, consists of ten rotatable sections. These sections can either be fixed in the vertial mode to provide a constant vertical magnetic field parallel and equal to the field in the first section or rotated to get a helical magnetic field which enables the neutron polarisation to turn from the vertical to the horizontal. This is achieved by turning each section by 9° with respect to the previous section thus starting from a vertically aligned field at one end to a

horizontal field at the exit end of the collimator.

A counter arm with a traverse in the vertical plane has been installed to measure the polarisation of the beam after the neutron polarisation is turned through a right angle. The polarisation of the beam with horizontal spin alignment was has been measured to be 97% as compared to the 95% vertical polarisation of the original beam. Fig.32 shows a schematic diagram of the helical guide hield and vertical traverse counter.

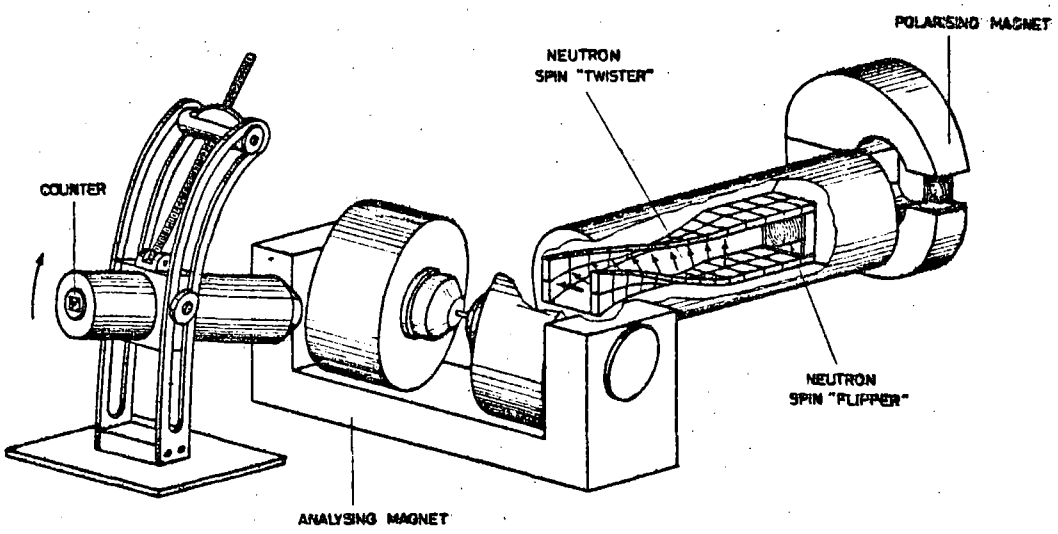

Fig. 32. Set-up for turning the neutron spin polarisation through 90° using a helical guide field.

The field on the sample is in the horizontal plane for the measurement of the polarisation after the 90° turn as well as for magnon measurements of the Bragg-misset technique. Preliminary measurements on magnons in Fe_3O_4 are underway to check the performance of the system.

8. Propagating Modes in Paramagnetic $KMnF_3$

(K. Usha Deniz and P.S. Goyal)

Neutron inelastic scattering studies have been carried out so as to observe propagating modes in paramagnetic $KMnF_3$. In the ordered state ($T < T_N \approx 88°K$), $KMnF_3$ is an antiferromagnet. It has a perovskite structure and its magnetic anisotropy is negligible for temperatures above the Neel temperature, T_N. The scattering measurements were made with a polycrystalline sample of $KMnF_3$ at three temperatures, 300°K, 170°K and 135°K, using incident neutrons of energy 4.7 meV(λ = 4.18 Å). At the two lower temperatures, the neutron energy spectra were observed at four scattering angles, θ, corresponding to values of Q_o ($= \frac{4\pi}{\lambda}$ in $\theta/2$) of 0.39, 0.65, 1.30 and 1.84 $Å^{-1}$. At 300°K, the spectra were only obtained for Q_o equal to 0.65 and 1.30 $Å^{-1}$. A fair degree of short range order is indicated at 135°K and 170°K by the magnetic structure factor, S(Q) (where Q is the neutron momentum transfer), which is peaked at Q 1.2 to 1.3 $Å^{-1}$.

The experimental data has been analysed to obtain the relaxation function, $R(Q,\omega)$, which is an even function of ω ($\hbar\omega = -\epsilon$ = the neutron energy loss). This function is related to S(Q,), the Fourier transform of the pair correlation function between spins, by the following relation: $$R(Q,\omega) = S(Q,\omega)\left\{\frac{\hbar\omega}{1-\exp\left(-\frac{\hbar\omega}{K_B T}\right)}\right\}^{-1}$$

At 300°K, $R(Q,\omega)$ obtained from both experimental distributions is well approximated by Gaussians in ω . Using de Gennes' theory, the values of the nearest neighbour exchange integral have been obtained from these distributions and are 0.321 ± 0.016 meV and 0.301 ± 0.029 meV for Q_o equal to 0.65 $Å^{-1}$ and 1.30 $Å^{-1}$ respectively. The two values are seen to be in fairly good agreement.

The relaxation function, $R(Q, \omega)_{exp}$, obtained from the experi-

mental data at 135°K and 170°K is plotted (open circles) as a function of ϵ in Fig.33.

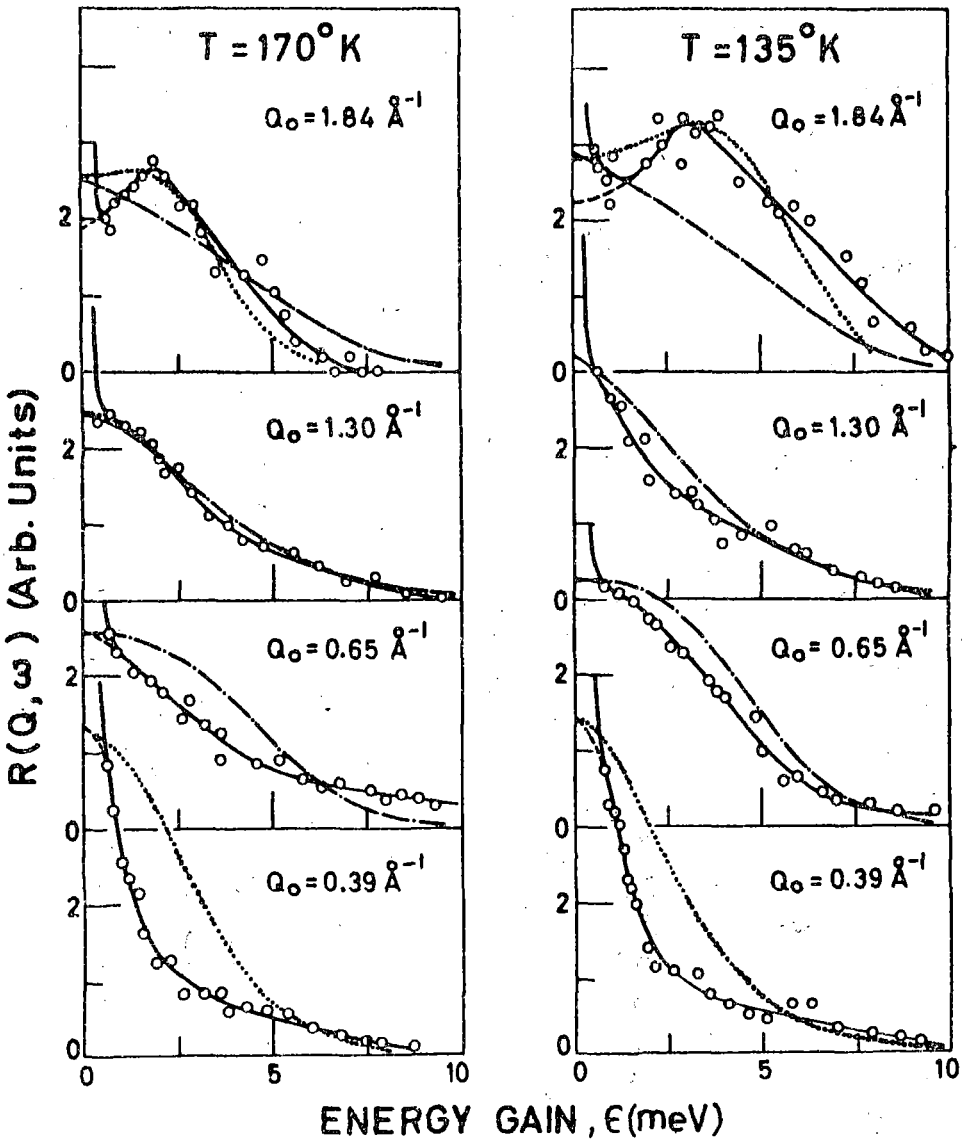

Fig. 33. $R(Q,\omega)$ as a function of ϵ . The full and dashed line curves are guides to the eye.

Quasi-elastic peaks are observed for Q_o equal to 0.39, 0.65 and 1.30 $Å^{-1}$, at both temperatures. The width of the quasi-elastic peak (width

at half-height) increases when Q_o increases from 0.39 to 0.65 $\AA^{-1}$ but decreases again for Q_o equal to 1.30 $\AA^{-1}$ (corresponding to the maximum of the short range order peak), thus exhibiting the 'de Gannes narrowing' effect. The distributions at $Q_o = 0.39$ $\AA^{-1}$ can be fitted well by Lorentzians, signifying that a diffusive type of behaviour characterises the spin dynamics at this value of Q_o. Both the distributions for $Q_o = 1.84$ $\AA^{-1}$ are peaked at non-zero values of ϵ (say ϵ_p) with $\epsilon_{p_{135°K}} > \epsilon_{p_{170°K}}$, indicating the presence of propagating modes.

The distributions of $R(Q, \omega)_{exp}$ have been compared to calculations based on two theories - (i) the Bennett theory[1], and (ii) the Modified Gaussian Approximation[2]. The Bennett Model (BM) predicts that there is a critical value, Q_c, of Q, which separates the domain where propagating modes are predominant ($Q >> Q_c$) from that where diffusive modes are predominant ($Q << Q_c$). For Q_o equal to 0.39 and 1.84 $\AA^{-1}$, $R(Q, \omega)$ has been calculated from BM, using the values of the moments $\langle\omega^2\rangle_Q$ and $\langle\omega^4\rangle_Q$ of $R(Q,\omega)$, obtained from the present results by assuming $Q = Q_o$, and is shown as dotted curves in Fig.33. It is seen that BM predicts well the trend of $R(Q,\omega)_{exp}$, though qualitatively. The lack of quantitative agreement is probably due to the errors in the determination of $\langle\omega^2\rangle_Q$ and $\langle\omega^4\rangle_Q$. The modified Gaussian approximation (MGA) is expected to describe the spin dynamics only for the appropriate range of ($Qb > 1$, where b is a lattice constant). This model predicts

$$R(Q,\omega)_{MGA} \propto S Q^{3/2} \left\{ \exp\left(-\epsilon^2 S(Q)/2\langle\epsilon^2\rangle\right) \right\} \qquad (1)$$

where $\langle\epsilon^2\rangle$ is the second moment of $R(Q,\omega)$ for large values of Q ($S(Q) \to 1$, as $Q \to \infty$). It is found that for constant Q_o, $R(Q, \omega)_{MGA}$ is peaked at finite value, ϵ_p, of ϵ, and that ϵ_p tends to zero for large values of Q_o. The dot dashed curves in Fig.33 for the three larger values of Q_o are calculated, using MGA with $\langle\epsilon^2\rangle = 12.7$ meV^2. The trend shown by these curves is exactly opposed to that shown by $R(Q,\omega)_{exp}$, the disagreement between $R(Q,\omega)_{MGA}$ and $R(Q,\omega)_{exp}$ being most pronounced for $Q_o = 1.84$ $\AA^{-1}$, where MGA fails to predict the inelastic peak. This failure can only be due to the fact that in MGA

the presence of collective excitations in the spin system is not considered.

It has thus been shown that propagating modes are present in paramagnetic short range ordered $KMnF_3$. It is hoped to examine the manner in which these modes are related to the magnons in the ordered state, by making measurements at constant Q with a single crystal.

---

1. H.S. Bennett, Phys. Rev. 176,650(1968)

2. L. Madhav Rao, B.A. Dasannacharya, N.S. Satya Murthy and P.K. Iyengar, Solid State Commn. 7, 123(1969)

IV. NEUTRON INELASTIC SCATTERING

1. Lattice Dynamics of Calcium Oxide

(P.R. Vijayaraghavan and P.K. Iyengar)

Inelastic scattering of thermal neutrons provides an extremely powerful tool for the direct determination of the phonon dispersion curves in crystalline solids. Amongst the several techniques that could be used on a triple axis spectrometer, the constant Q mode of operation has the added advantage that the phonon wave vector is kept unchanged during the course of the experiment. However, in medium flux reactors, when the sample sizes are small and the phonon frequencies high, the problem of very low counting rates arises and it has become necessary to find out whether other instruments (like the filter detector spectrometer) which give much higher counting rates could effectively utilized in the above studies. Measurements have been made, at room temperature, on calcium oxide which has the sodium chloride structure. Whereas the acoustic branches have been observed on a conventional triple axis spectrometer, the optic branches have been observed using a filter detector spectrometer (FDS) using beryllium oxide as the filter. The data on optical branches have not been used in the least squares analysis for a three parameter (point ion) model for which the input data consisted of the acoustic branches, elastic constants[1] and optical measurements[2].

A single crystal of calcium oxide, weighing approximately 13.6 gms, was aligned with the $[1\bar{1}0]$ axis vertical. The sample, being hygroscopic, was kept sealed in an airtight aluminium container. The measured dispersion curves for phonons propagating along the $[100]$, $[110]$, and $[111]$ directions are shown in Fig. 34. The lower open square at q = 0, corresponds to the infrared absorption frequency while the upper open square also at q = 0, corresponds to the infrared absorption frequency while the upper open square also at q = 0, corresponds to the frequency of the longitudinal optic mode calculated using the dielectric constants[3] and the Lyddane-Sachs-Teller relation. Optical measurements at q = 0 of Jacobson and Nixon[5] are also shown in Fig. 34. The continuous lines are a three parameter fit to the data. Some measurements were done in the 100 orientation also.

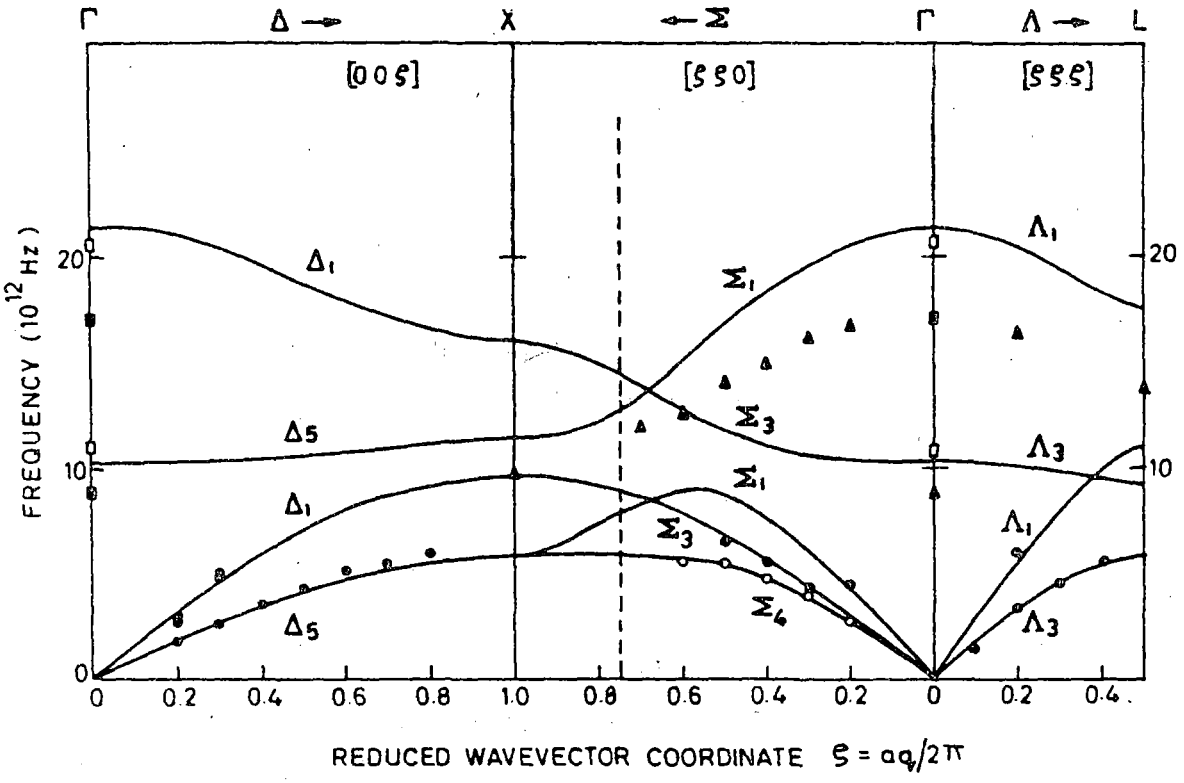

Fig. 34. Phonon Dispersion curves for Calcium Oxide at Room Temperature.

The values of the various parameters, obtained by a least square analysis of the data are given in Table I. The three parameter model itself gives a good fit to the acoustic branches.

Table I

Parameter of the three parameter model
($\mathcal{V}$ is the volume of the primitive unit cell)

Parameter	Unit	Value	Definition
A	$(e^2/2v)$	25.52	near neighbour short range radial force constant
B	$(e^2/2v)$	-2.62	near neighbour short range tangential force constant
Z	(e)	1.60	ionic charge

It has been shown by Thaper et al[4] that the BeO filter detector spectrometer gives the correct frequencies if they assume a value of 0.0025 ev for the mean energy of the scattered neutrons. The present measurements are also based on this value for the energy of the scattered neutron. It is observed that the frequency of the transverse optic mode at q = 0 as seen on the FDS and the frequency of the LO mode at q = 0 (as derived from the trend of the Σ_1 branch) are in disagreement with earlier measurements[2]. However, they are consistant with the more recent measurements on these frequencies by Jacobson[5].

Measurements are being continued on the FDS for additonal data on the optic branches as these are necessary for a complete analysis.

1. H.E. Hite and R.J. Kearney, J. Appl. Phys. 38,5424(1967).
2. B. Szigeti, Trans. Faraday. Soc. 45,155(1949)
3. K. Hojendahl, K. Danske Vidensk Selskab, 16, No.2 (1938)
4. See article 3 of this Section.
5. J.L. Jacobson and E.R. Nixon, J. Phys. Chem. Solids, 29,967(1968)

2. Phonons in Calcium Fluoride at 85°K

(P.R. Vijayaraghavan and P.K. Iyengar)

The frequency wavevector relation for phonons propagating along the [100] direction of calcium flouride has been measured at 85°K using the technique of inelastic scattering of thermal neutrons. The measurements were done on a triple axis spectrometer in the constant-Q mode keeping the energy of the incident neutron constant. The sample was mounted in an all-metal cryostat which is shown in Fig.35. The construction of the cryostat is such that it enables the introduction of an exchange gas around the sample.

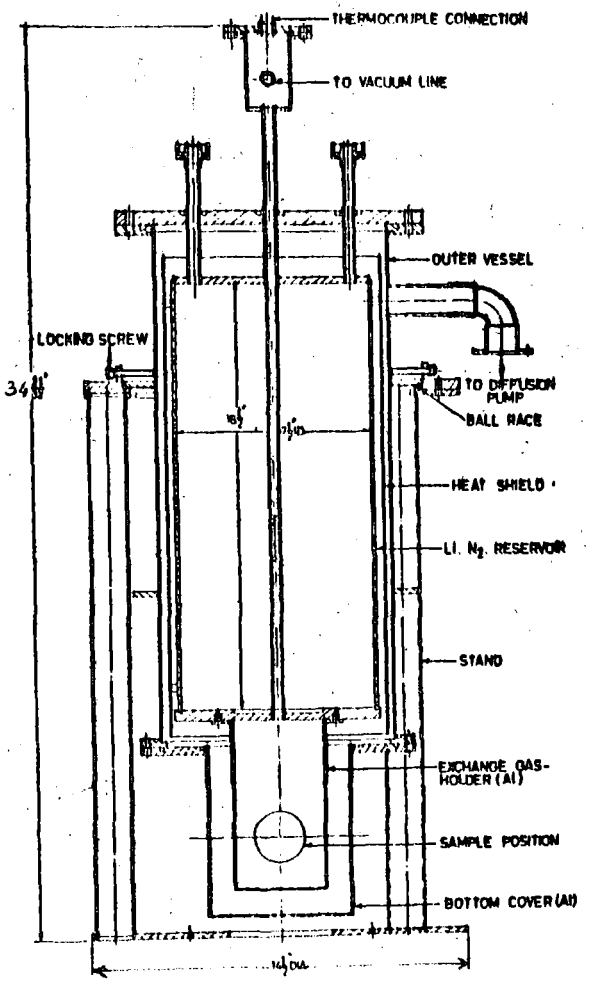

Fig. 35. Liquid Nitrogen Cryostat for phonon measurements

The results of measurements done are shown in Fig.36. They are

being continued along the [110] and [111] directions for a shell model analysis.

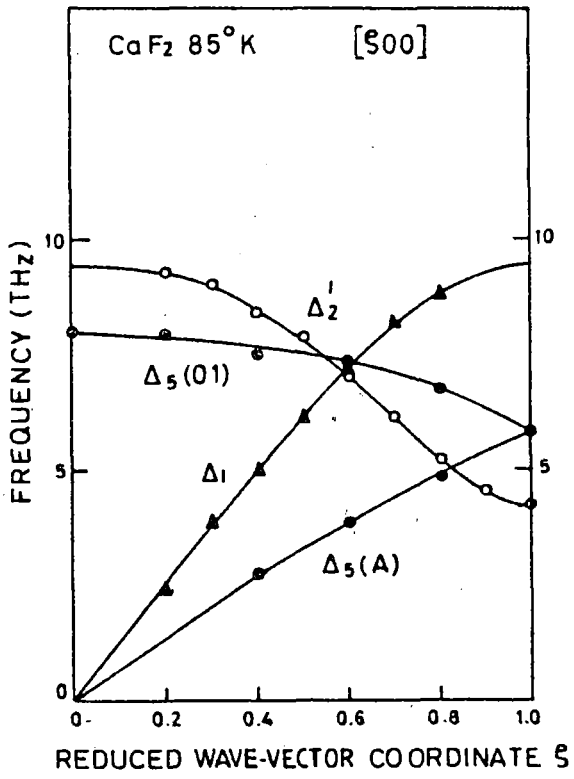

Fig. 36. Phonon dispersion curves for CaF_2 along [100] direction at 85°K

3. Phonon Measurements on the Filter Detector Spectrometer

(C.L. Thaper, B.A. Dasannacharya, T. Srinivasan I.Y. Mithani and P.K. Iyengar)

The measurement of high frequency phonons on a conventional triple axis spectrometer is usually a difficult task with medium flux reactors. A filter detector spectrometer affords a promising possibility, but the uncertainity in the outgoing neutron wave vector, $\underline{k}'$ (arising from the analyser function of the filter material) makes it difficult to fix uniquely the magnitude and direction of the phonon

wave vector q. At first sight, therefore, the method does not look promising for the measurement of phonon dispersion curves unless they have almost zero slope. However, if a proper choice of an effective k' can be made the technique becomes viable. Phonon measurements carried out on the filter detector spectrometer using BeO filter, reveal that the use of k' which corresponds to the mean energy (E' = 2.5 meV) of the filter cut-off spectrum gives accurate phonon dispersion curves even when their slopes are large.

The measurements have been made along the $[00\xi]$ and $[\xi\xi\xi]$ directions in silicon which has been well studied on a triple axis instrument and also through optical methods.

The experiments have been performed in the "constant - Q" and "constant - E" modes of operation. Some typical phonon groups obtained in the "constant - Q" mode along the $[00\xi]$ direction are shown as (a), (b), (c) and (d) in Fig. 37. The vertical lines in the figure

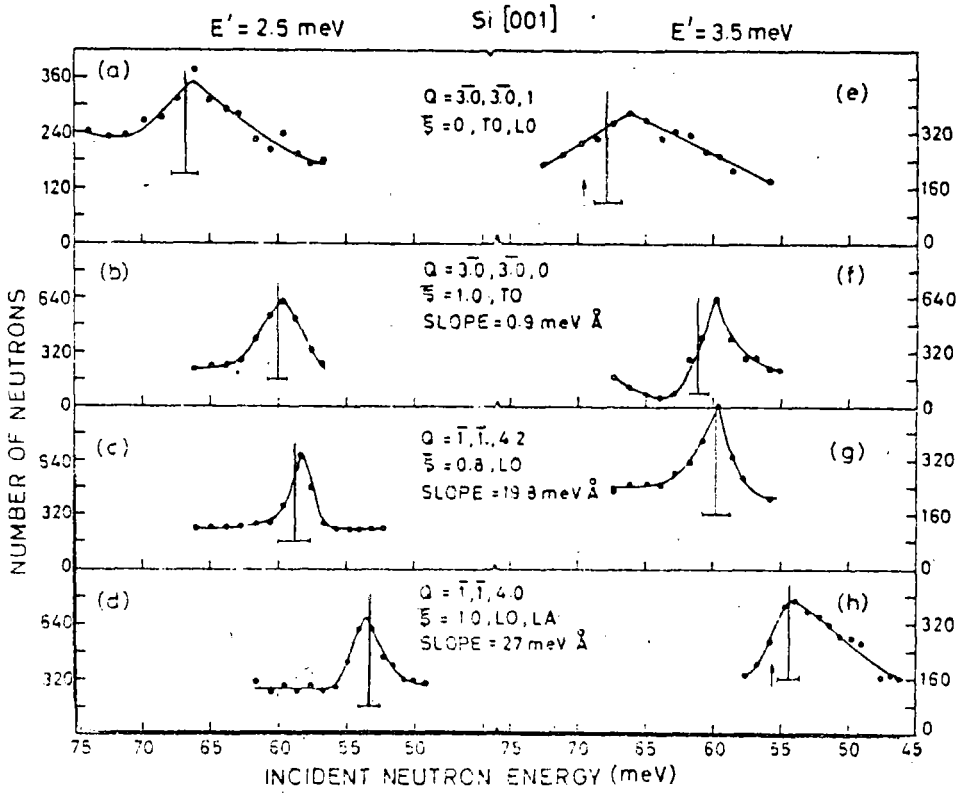

Fig. 37. Constant-Q Phonons in Silicon using the BeO filter detector spectrometer.

show the phonon energies as measured by Dolling on a triple axis

spectrometer[1]. It is seen that the agreement between the peak positions observed here and those obtained by Dolling is good. Table I gives a more detailed comparison.

Table I

Comparison of phonon frequencies [in units of 10^{12} cps] observed by Filter detector spectrometer (FDS) and Triple axis spectrometer (TAS)

Direction and mode	Instrument	q/q_{max} 0	0.2	0.4	0.6	0.8	1.0
$[00\xi]$ LO	FDS	15.41	15.26	15.12	14.2	13.58	12.36
	TAS	15.53	15.55	15.15	14.6	13.6	12.32
$[00\xi]$ TO	FDS	15.41	15.41	14.71	14.19	13.94	13.82
	TAS	15.53	15.40	14.65	14.18	13.95	13.90
$[\xi\xi\xi]$ LO	FDS	15.41	15.47			13.35	12.55
	TAS	15.53	15.45			13.30	12.60

An interesting feature observed in this instrument is the focussing which is quite similar to the one seen in a triple axis spectrometer. This is illustrated in Fig. 38 for the longitudinal optic phonon at $q/q_{max} = 0.8$ along the $[0\,0\,\xi]$ direction observed at the positions shown in the reciprocal lattice diagram (Fig.38). Fig.38(a) and (b) show the focussed phonon groups respectively seen in the "constant-Q" scan. The phonon

at $\mathcal{J} = 13.6 \times 10^{12}$ cps observed in the "constant-E" scan along $[\bar{1}\bar{1}\xi]$ is shown in Fig.38(c).

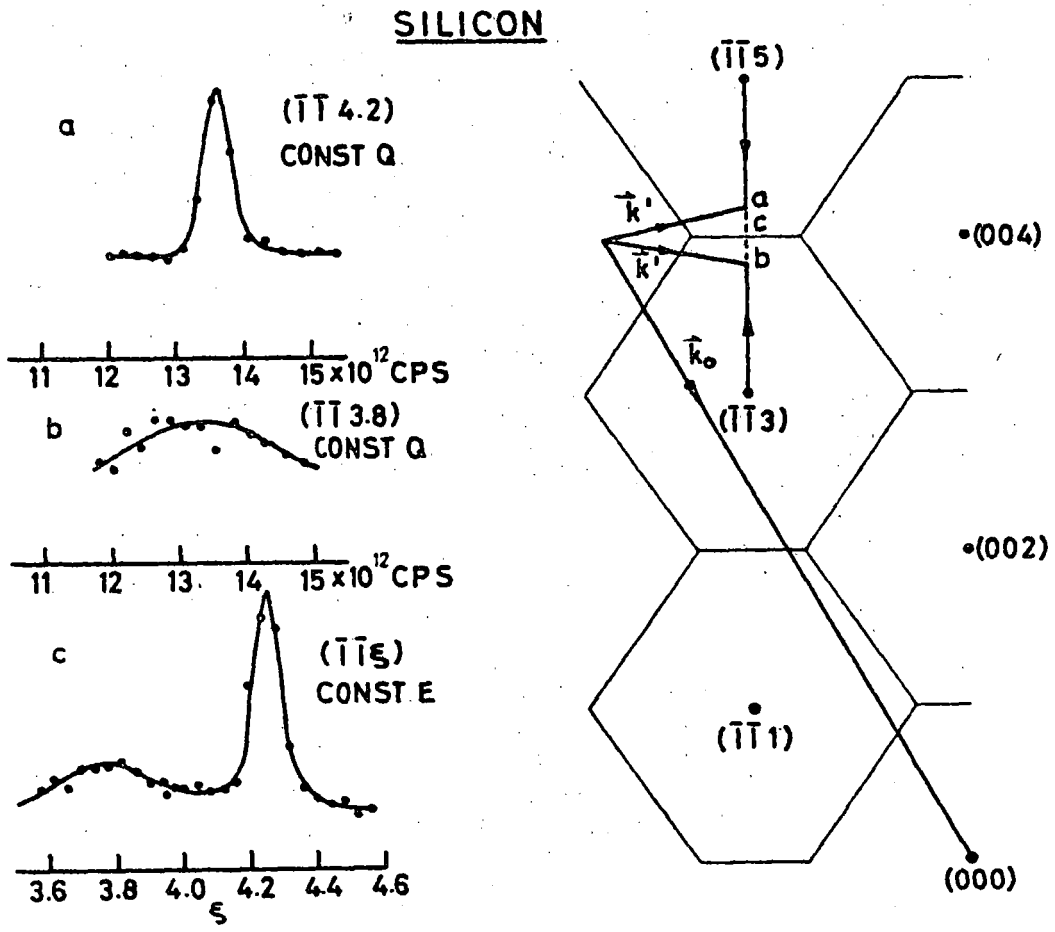

Fig. 38. Focussing effects in Phonon measurements in the filter detector spectrometer.

To see the effect of a different effective $\underline{k}'$ on the neutron groups, experiments have also been carried out in the "constant - $\underline{Q}$" mode for a k' appropriate to $E' = 3.5$ meV. The observed neutron groups, shown as (e), (f), (g) and (h) in Fig.37 reveal that the peaks do not always agree with Dolling's quoted values (vertical lines). Another possibility, for this choice of k' is to look for the cut-off in the neutron groups[2]. However, the present observations show that the cutoff cannot always be located (Fig.37(g)). The cases in which it can be located (arrows in

Fig. 37(e), (f), (h)) the agreement with Dolling's measurement is not uniform. Similarly an E' = 1.5 meV was also not found to be suitable.

The filter detector spectrometer with BeO, therefore affords a viable method for measuring accurate phonon dispersion curves if a k' = 1.1 $\AA^{-1}$ is utilised for "constant-Q" or "constant - E" calculations. The instrument is useful even when the slopes of the dispersion curves are large. The intensities observed in this method are much higher than those obtained on a triple axis spectrometer. However, the method suffers from the well known restriction in the choice of the available reciprocal lattice points.

The instrument has been used to obtain dispersion curves in CaO[3] and in beryllium along $[0\,0\,0\,\xi]$ and $[0\,\xi\,\bar{\xi}\,0]$ directions. The computation of phonon shapes through detailed resolution function calculations is in progress.

---

1. G. Dolling in Inelastic Scattering of Neutron in Solids and Liquids, II, IAEA, Vienna (1963)37-47
2. The cut-off method with beryllium filter is used by Bergsma (Petten report RCN-121, 1970) and also by B. Haywood and M. Collins (Harwell report, AERE-P.R./-PMD2, 1970). Their work came to the notice of the authors after these measurements were completed.
3. See article 1 above.

4. Frequency Spectrum of Solid Ammonia

(P.S. Goyal, B.A. Dasannacharya, C.L. Thaper and P.K. Iyengar)

Neutron energy gain and energy loss experiments have been performed on solid ammonia at 106°K on the rotating crystal spectrometer and the filter detector spectrometer. The positions of the peaks observed in the scattered neutron distributions have been compared with optical data earlier[1].

The data taken using the energy gain and energy loss methods have been combined to obtain the effective frequency distribution function, $g_{eff}(\omega)$, following the method of Prask and coworkers[2]. Fig. 39 shows the $g_{eff}(\omega)$. The translational and rotational regions seem to be

well separated, as indicated by the dashed lines. This kind of separation

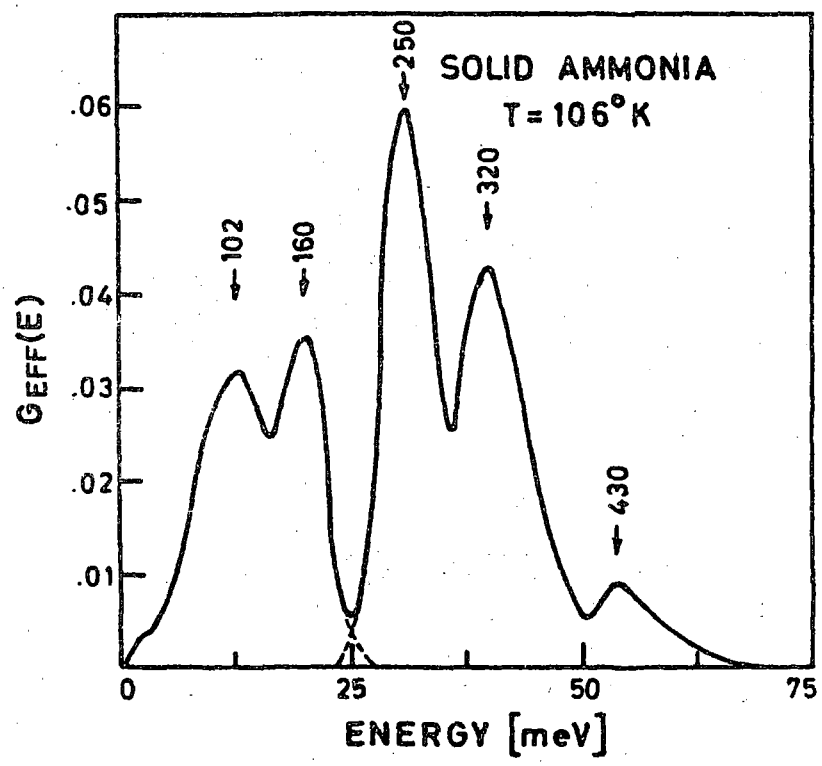

Fig. 39. Frequency Spectrum of Solid Ammonia measured on the rotating crystal spectrometer with incident neutron energy of 4·87 MeV.

is supported by optical data and also by an analysis of the $g(\omega)$ and the specific heat.

The specific heat, C_v, calculated using the $g(\omega)$ agrees with the measured value to within 2% upto 110°K; at higher temperatures, the anharmonic contributions become larger. The specific heat data have also been used to calculate the translational and rotational moments, following the method of Leadbetter[3]. These moments are given in Table I along with the moments calculated from the observed $g(\omega)$. The agreement is found to be reasonable.

Table I

Comparison of moments of frequency spectrum of Solid ammonia

Moments	Neutron cm^{-1}	Sp. heat cm^{-1}
$(\mu_2)_T^{112}$	129	120
$(\mu_4)_T^{114}$	140	127
$(\mu_4)_T^{116}$	148	131
$(\mu_2)_R^{112}$	280	300
$(\mu_4)_R^{114}$	296	298
$(\mu_6)_R^{116}$	312	300

1. BARC-501, Annual Report of the Nuclear Physics Division,1970.p.61
2. H. Prask, H. Boutin and S. Yip, J. Chem. Phys. 48,3367(1968)
3. A.J. Leadbetter, Proc. Roy. Soc. 287A,403(1965)

5. Symmetry Properties of External Modes of Potassium Azide+

(K.R. Rao and S.F. Trevino*)

Group theoretic methods are extensively used to study lattice dynamics of complex crystals. Particularly since the publication of a paper by Maradudin and Vosko(1), a great spurt of activity is seen in this field. The lattice dynamics of potassium azide have been investigated by group theoretic methodsas a part of a programme to study aspects of stability of inorganic azides. There is a great deal of interest to study the structure and dynamics of these compounds as some of them are quite stable compared to others which are explosive. The infrared and Raman spectra of some of the axides have recently been reinvestigated(2,3).

Neutron scattering experiments have also been carried out to study the dynamical properties of potassium azide[4].

Potassium azide crystallises with tetragonal symmetry having the space group D_{4h}^{18}. The primitive unit cell has two formula units (KN_3). The azide ion is a linear ion. However, the ion is treated here as a non-linear unit possessing three degrees of freedom associated with translations and three with rotations. The dynamical problem associated with the external modes of vibrations of the lattice[5] can therefore be analysed in a 18 x 18 'dynamical space' using the Born-von Karman theory of lattice dynamics.

Making use of the formalism of Maradudin and Vosko, the symmetry properties of vibrations have been investigated corresponding to several wave vectors of high and low symmetry. At each of these points and lines of high symmetry, the group-theoretic methods have been employed to get

a) classification of external modes in terms of the irreducible multiplier representations

b) symmetry vectors using projection operator technique

c) the structure of the dynamical matrix and

d) the block diagonalisation of the dynamical matrix.

A detailed account of the work has been published[6]. The experimental work of measuring the dispersion relations concerns the high symmetry directions [001] and [110] .

+ Part of this work was performed at Army Material & Mechanical Research Centre, Watertown, U.S.A.

* Explosives Laboratory, Picatiny Arsenal, Dover, New Jersey, U.S.A.

1. A.A. Maradudin and S.H. Vosko, Rev.Mod. Phys.40,1(1968)

2. Z. Iqbal, M.L. Malhotra and K.D. Moller, Phys. Letters 31A, 73(1970)

3. Z. Iqbal, S.S. Mitra and C. Brown, J.Chem. Phys. (1970)

4. K.R. Rao, H. Prask, S.F. Trevino and R. Mical, Paper presented at the Nuclear Physics and Solid State Physics Symposium, Madurai (1970)

5. G. Venkataraman and V.C. Sahni, Rev. Mod. Phys. 42,409(1970)

6. K.R. Rao and S.F. Trevino, J. Chem. Phys. 53,4661(1970)

6. Symmetry Properties of External Modes of Sodium Nitrate+

(K.R. Rao, S.F. Trevino* and K.W. Logan*)

Sodium Nitrate crystallises with the rhombohedral symmetry having the space group D_{3d}^{6}. The crystal is isostructural with Calcite, KNO_3 etc. The primitive cell contains two molecules of $NaNO_3$. The symmetry properties of the external modes of the lattice have been studied at several points and lines of the Brillouin zone using the formalism of Maradudin and Vosko[1]. Details of this study are published elsewhere[2] Experimental studies of dispersion relations are currently under way[3] and the theoretical analysis of the data will be made using the information derived in this study.

+ Part of this work was performed at Army Material & Mechanical Research Centre, Watertown, U.S.A.

* Explosives Laboratory, Picatiny Arsenal, Dover, New Jersey, U.S.A.

1. A.A. Maradudin and S.H. Vosko, Revs. Mod. Phys. 40,1,(1968)

2. K.R. Rao, S.F. Trevino and K.W. Logan, J. Chem. Phys. 53,4645(1970)

3. S.F. Trevino and K.W. Logan (Unpublished).

7. Multiple Scattering of Neutrons in Liquid Methane

(K.R. Rao, B.A. Dasannacharya and S. Yip*)

Inelastic scattering of thermal and cold neutrons is recognised to be a powerful tool for probing atomic motions in liquids. In an analysis of such experiments, it is necessary to take into account corrections due to multiple scattering. The calculation of the correction requires a knowledge of fairly reasonable scattering law. The calculations are time-consuming and results appropriate to a specific measurement are usually not directly applicable to other experimental conditions. Hence there exist every few quantitative evaluations of multiple scattering corrections.

In this study an expression for second order scattering has been evaluated generalising the approach of Vineyard[1] for a flat specimen to include effects of anisotropy and inelasticity. It is believed that the scattering law given by a hindered rotation model[2], which was used earlier in the analysis of experimental data[3], is a reasonable one for quantitative estimates of corrections due to multiple scattering. Calculations are underway to estimate the corrections and obtain data which can be subjected to further theoretical studies.

---

* Department of Nuclear Engineering, Massachusetts Institute of Technology, Cambridge, U.S.A.

1. G.H. Vineyard, Phys. Rev. 96, 93(1954)

2. G. Venkataraman, B.A. Dasannacharya and K.R. Rao, Phys. Rev. 161,133(1967)

3. B.A. Dasannacharya and G. Venkataraman, Phys. Rev. 156,196(1967)

8. Development of a Computer Code to Study Symmetry Properties of Complex Crystals:

(K.R. Rao)

Study of symmetry properties of complex crystals containing several atoms in the primitive unit cell involves matrices of dimensions fairly large to be handled conveniently on desk. Particularly in dealing with crystals say of hexagonal or cubic symmetry, the point group of the lattice contains a fairly large number of symmetry operations. In addition there may be several wave vectors of fairly high symmetry. Hence to obtain information concerning

(a) transformation matrices of eigenvectors

(b) symmetry vectors

(c) the dynamical matrix elements and the like,

considerable effort is needed to work out the details by hand. The studies on KN_3 (described earlier in this report) prompted development of computer methods to investigate symmetry properties. In these two cases, specific programmes have been developed to (a) define the transformation matrices $T(q,R)^1$ (b) construct symmetry vectors using projection operator technique and most importantly (c) to get the algebraic relations between dynamical matrix elements for a given wavevector using

all the operations of the group of the wave vector. But for this programme, the extensive studies made in KN_3 and $NaNO_3$ would not have been possible. Efforts are underway to develop a more generalized computer code which can be used in a variety of crystals.

---

1. K.R. Rao and S.F. Trevino, J. Chem. Phys. 53,4624(1970)

9. Group Theoretic Classification of Long-Wavelength Modes in Ionic Crystals

(V.C. Sahni and G. Venkataraman)

The normal modes of oscillations of a crystal corresponding to a given wavevector $\underset{\sim}{q}$, are usually classified according to the irreducible multiplier representations of the point group $G_o(\underset{\sim}{q})$ underlying the group of the wavevector $G(\underset{\sim}{q})$[1]. In ionic crystals this scheme requires modifications due to retardation effects as a consequence of which one gets $(3n + 2)$ modes for every $\underset{\sim}{q}$ instead of the usual $3n$, some of these having a mixed photon-phonon character. (n is number of atoms in the primitive cell). A scheme is proposed wherein to classify these $(3n+2)$ modes, a $(3n + 2)$-dimensional space must be considered comprising of the usual $3n$-dimensional space associated with atomic displacements, and a two-dimensional space associated with the macroscopic transverse electric field. The latter space is spanned by two vectors chosen at right angles to $\underset{\sim}{q}$. By setting up the representations of $G_o(\underset{\sim}{q})$ in this composite space and then decomposing, one may systematically classify the long-wavelength modes in ionic crystals. As an illustration, the method has been applied to crystalline quartz in the phase D_3^6.

---

1. A.A. Maradudin and S.H. Vosko, Rev. Mod. Phys. 40,1 (1968).

10. Polariton Dispersion Relations in $CaWO_4$

(V.C. Sahni and G. Venkataraman)

Dispersion relations for polaritons propagating along a and c directions in calcium tungstate (space group C_{4h}^6) have been calculated using the dispersion parameters obtained by Baker[1] from his infrared-reflection studies. One result of the calculation is that even the modes associated with the so-called internal vibrations of the WO_4^{--} ion show considerable dispersion effects. Since the modes that participate in the polariton formation are Raman inactive in $CaWO_4$, it is suggested that it should be experimentally possible to study these dispersion curves using electric field induced Raman scattering, as has been done successfully in other inversion-symmetric substances.

---

1. A.S. Barker, Jr. Phys. Rev. 135, A742, (1964)

11. On the Validity of Saxon-Hutner Conjecture for Three-Dimensional Crystals

(R. Subramanian and K.V. Bhagwat)

The zero-range potential model was used to study the validity of Saxon-Hutner conjecture for three-dimensional lattices. Most of the existing work connected with this problem has been done for idealized one-dimensional lattices, and qualitative results obtained on the basis of such one-dimensional calculations were assumed to hold also in higher dimensions.

In this work, three-dimensional delta-function type potentials have been used in an attempt to generalize the one-dimensional calculations to three dimensions. For a linear periodic array of such three-dimensional potentials it has been provided that indeed the electronic energies forbidden in both pure A and pure B type lattices are forbidden also for an alloy of A and B of the type ABAB..... Thus a special case of Saxon-Hutner conjecture is proved for a three-dimensional system.

12. Surface States in Three-Dimensional Crystals

(R. Subramanian and K.V. Bhagwat)

The problem of the existence of surface states, which arise because of the finite dimensions of a real crystal, has been the subject of a number of investigations for several years. Here again, as in the case of the previous problem, most of the existing work is confined to one-dimensional models. In view of the not infrequent divergences in the qualitative features of one-dimensional and three-dimensional systems, it is necessary to do some three-dimensional calculations, at least for some idealized cases. So a finite chain of three-dimensional zero-range potentials was considered and how the energy levels vary with increase in the length of the chain was studied. As expected, in this case no surface states appeared. This work is preliminary to the study of a finite three-dimensional lattice of the same type of potentials.

V. MOSSBAUER EFFECT STUDIES

1. Relaxation Effects in Ferrites Using Mossbauer Effect

(P.K. Iyengar and S.C. Bhargava)

Mossbauer spectra of the mixed ferrites $(Zn,Co)Fe_2O_4$ have shown features characteristic of relaxation effects upto temperatures near the Neel temperature, the compositions $Zn_x\ Co_{1-x}\ Fe_2O_4$ for $x = 0.7$ and 0.5 have been systematically investigated over a wide temperature region. In both cases, the spectrum is a six finger spectrum, with insignificant relaxation effects, at low temperature. As the temperatures is increased, the central lines become intense compared to outer lines.

The theory of the line shape, in presence of electron spin relaxation, has been discussed by several authors. Using a stochastic model, the line shape has been calculated for Fe^{3+} ions in S-state. In a simple substance the calculated shapes depend only on two parameters. However, in systems like ferrites, the molecular field at the ion can not be calculated from the knowledge of Neel temperatures alone. A crude estimate can be made using values of exchange constants and taking into account nearest-neighbour interactions only. This value is then varied slightly to get

best fit to the experimental data. The comparison of the theoretical shapes with experimental data for $Co_{0.5}Zn_{0.5}Fe_2O_4$, gave values of parameters as shown in Table I.

Table I

Temperature (°K)	$S\left(=e^{-\frac{2\beta Ha}{KT}}\right)$	δ (rad.sec^{-1})	Relaxation time (sec.)
90	0.033	1.89×10^7	--
190	0.222	1.66×10^7	2.33×10^{-7}
222	0.293	1.61×10^7	1.00×10^{-7}
292	0.44	1.48×10^7	1.00×10^{-7}
313	0.484	1.39×10^7	2.00×10^{-7}
340	0.585	1.27×10^7	1.00×10^{-7}
359	0.65	1.27×10^7	1.20×10^{-7}
367	0.77	1.24×10^7	4.00×10^{-7}
397	0.93	1.11×10^7	5.50×10^{-7}
413	1.00	1.11×10^7	7.00×10^{-9}
433	1.00	1.11×10^7	2.00×10^{-9}
455	1.00	--	--

It is seen that S approaches the value of unity long before the split spectrum collapses to a sharp line. To confirm the conclusions, the sample was investigated by neutron diffraction and the Neel temperature (400 ± 5°K) thus found was consistent with the value of estimated from Mossbauer Effect.

The composition $Co_{0.3}Zn_{0.7}Fe_2O_4$ has also shown relaxation effects. Preliminary estimates indicate that replacement of Co with Zn changes the relaxation time. The other composition $Co_{0.75}Zn_{0.25}Fe_2O_4$ is being investigated to understand better the role of Zn ions in causing the relaxation effects.

2. Loud Speaker type Mossbauer Spectrometer (Instrumentation)

(P.K. Iyengar and P.S.P. Nathan)

Some improvements have been introduced in the constant velocity electromechanical speaker type Mossbauer spectrometer, resulting in spectra with better linearity and resolution. Only the linear portion of the symmetric saw-tooth driving signal is utilized (see section E-III for details). The typical standard spectra obtained with the system are shown in Fig.40 and Fig.41.

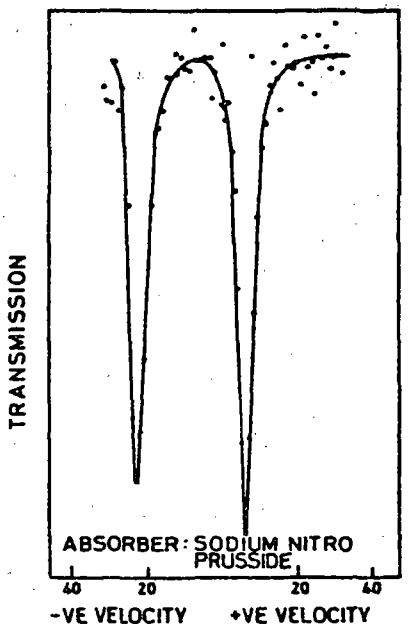

Fig. 40. Sodium Nitroprusside spectrum with improved drive.

Efforts are being made to introduce feedback in the drive system in order to improve further the linearity, resolution and efficiency characteristics.

Preliminary investigations have been started in the ternary alloys Fe_2TiAl and CoFeGe. From neutron diffraction studies, CoFeGe has been found to be of single phase, F.C.C. with a_o = 5.72 Å.

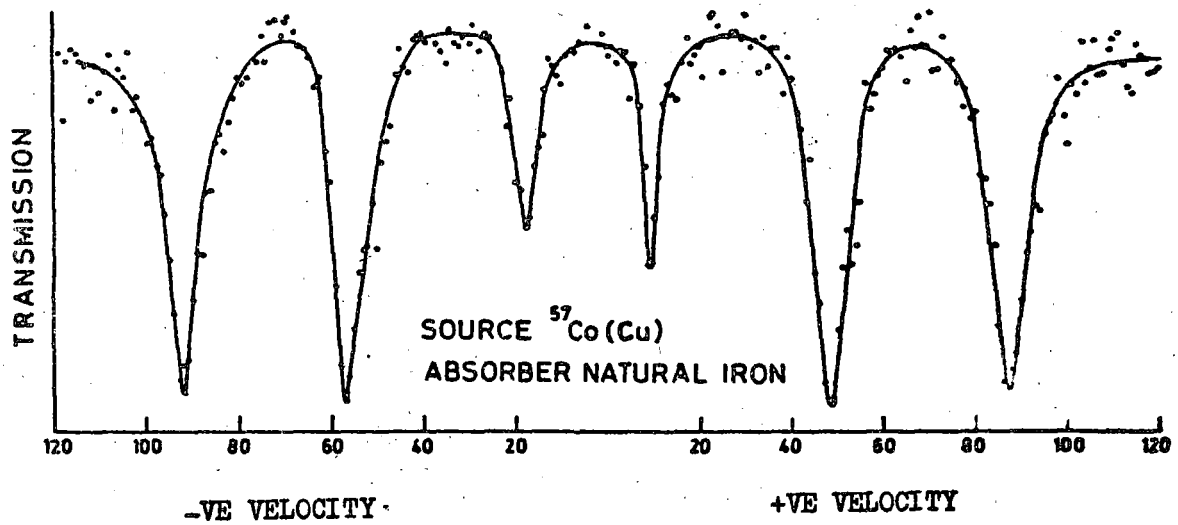

Fig. 41. $^{57}Co(Cu)$ Hyperfine Spectrum taken with the improved drive.

Fe_2TiAl showed only a quadrupole splitting of about 0.44 mm/sec at room temperature; CoFeGe shows an unresolved hyperfine splitting in addition to the symmetrically split lines close to zero velocity. Investigation in the liquid nitrogen temperature range is underway.

C. REACTOR NEUTRON PHYSICS

1. Measurement of Parameters of Interest in Reactor Physics

(M.P. Navalkar, O.P. Joneja, S.B.D. Iyengar, D.V.S. Ramakrishna, K. Subbukutty and J.S. Coachman)

The following calculations and preliminary experiments have been performed for the core reflector geometry of the proposed Pulsed Fast Reactor.

It is necessary to employ a three-dimensional, multi-group calculational method for a complicated geometry like that of the core and reflector of the proposed Pulsed Fast Reactor. With this purpose, a Monte Carlo method is being developed. The method has been verified by calculations with conventional methods in these cases:

1) K_{eff} as a function of radius for one zone spherical system,
2) K_{eff} as a function of radius for two zone spherical system,
3) K_{eff} as a function of radius for three zone spherical system,
4) K_{eff} as a function of radius and height for a bare cylindrical system,
5) K_{eff} as a function of radius and height for two zone cylindrical system and
6) K_{eff} as a function of radius and height for six zone cylindrical system.

Calculations have also been made using this method with regard to

1) the critical mass for the proposed core in six zone system,
2) the validity of using one and two dimensional calculational method with a few groups of energy for the proposed core.

Using the above method of calculation, the following parameters are being calculated for the present core geometry:

a) critical mass by static method,
b) critical mass by Kinetic method,
c) K_{eff} as a function of loading,
d) approach to criticality
e) Rossi-α as a function of K_{eff},
f) life time as a function of K_{eff},
g) leakage neutron spectrum as a function of loading and
h) kinetics of the Critical Facility.

An experiment was conducted at the thermal column of APSARA with a solid state track recorder to find its suitability for the measurement of fission rates or fluxes*. Absolute values of thermal neutron fluxes have been obtained within 10-15% using ^{239}Pu, ^{235}U, ^{233}U. A feasibility study for the measurement of neutron spectrum using threshold detectors of the fission and non-fission type has been made.

A He^3 sandwiched surface barrier spectrometer is being constructed. The design for the spectrometer head has been finalised and the electronic circuits are being designed and built. Preliminary results for the spectrum in a beam hole at the CIRUS reactor have been obtained.

The complete β-γ set-up for measuring absolute disintegration rates described in the last report has been transistorised.

About six threshold detectors were irradiated in the MELUSINE reactor in France and the data for the fast spectrum is being analysed by six different methods.

---

* This experiment was performed by Shri K.N. Iyengar (TIFR)

II. PULSED FAST REACTOR PROJECT

(P.K. Iyengar, M. Srinivasan, V.R. Nargundkar, K. Subba Rao
K. Chandramoleshwar, S. Das and T.K. Basu)

(i) Critical Facility

Work on the 2.5 litre core, PuO_2 fuelled Zero Energy Fast Reactor showed considerable progress during the year. The building to house the critical facility has been completed, and tests on the air handling system are under way. A 2.1 meter high steel platform to mount the critical assembly has been erected in the reactor vault. The stainless steel core vessel, grid plates and copper reflectors are ready while the steel reflectors are being machined. Over two dozen PuO_2 fuel pins have been fabricated at the Metallurgy Division. Prototype safety and control mechanisms have been assembled and tested by the Electronics Division. Most of the nuclear instrumentation is also ready. The reactor is expected to be made critical by August, 1971.

The operation of the critical facility and the planning and execution of the experimental programme are the responsibility of the Division. A detailed safety analysis report including a description of the facility, an assessment of the safety and control system and the start up and operational procedures, proposed to be adopted is under preparation.

The experimental programme is to be carried in three phases, as follows:

Phase 0 : Facility acceptance tests
Phase A : Good geometry experiments
Phase B : PFR geometry experiments.

Facility acceptance tests will include the first approach to critical of this reactor. Initially the K_{eff} of the assembly will be taken up through controlled fuel loading steps to a value $\sim$ 0.98, corresponding to a sub-critical multiplication of 50. After checking the shutdown capability and radiation fields in and around the building the system

would be taken up to critical. Before the facility is cleared for routine experimental operation, test will be carried out to confirm that the start-up, safety and control systems are performing satisfactorily.

The main purpose of the good geometry experiments (Phase A) is to generate experimental data for the purpose of checking the calculational codes used in the design of the critical facility and also the proposed pulsed fast reactor. Measurements to be performed include critical mass, prompt neutron life-time, spectral density ratios, reactivity coefficients of various materials etc. The PFR geometry experiments (Phase B) to optimise the design of the pulsed fast reactor proper would follow later.

A challenging problem currently under study is the determination of the absolute degree of subcriticality of the system before it is made critical. Several elegant reactor noise techniques developed during the past few years are being evaluated. A major effort has been launched to understand the kinetic behaviour of fast neutron systems. This would form the basis of a detailed analysis of the pulsed fast reactor pulsing mechanism.

(ii) Pulsed Fast Reactor

A prototype core assembly of seven dummy fuel elements has been fabricated to conduct heat transfer experiments and optimise the coolant circuit. A detailed design of a prototype mild steel rotor simulating PFR specifications has been worked out. Stress analysis of the rotor has been carried out using photoelastic models. These studies have been carried out by the Reactor Engineering Division.

Detailed cost estimates of the civil works, and air conditioning/ventilation system for the proposed building to house the pulsed fast reactor in Kalpakkam near Madras have been prepared.

D. SEISMOLOGY

1. Operation and Maintenance of Seismic Array and Microbarographs.

The Gauribidanur seismic array as well as long period seismograph system have been in continuous operation throughout the year. Almost all the underground nuclear explosions from the Russian region as well as the major ones from the Nevada test site of USA were detected. The network of microbarographs run by the section has also been recording continuously. It has enabled the latest Chinese atmospheric explosion of 14th October 1970 to be detected and analysed so fast that the first announcement of its location, time and yield was made by this section.

2. Data Transcription and Dissemination

The seismic bulletin service, was continued in order to provide the seismological community in the country with the array-determined epicentral parameters of major earthquakes. High quality array seismograms of selected events were also supplied on request to different organisations. By a systematic process of editing and machine digitization, the data corresponding to interesting seismic events was converted into discrete form on magnetic tape as computer compatible library records.

3. Research Programme

(i) Experimental Seismology

Studies of the structure of the earth's crust surrounding the Gauribidanur array was continued on the basis of the local seismic events recorded clearly by the array. This has enabled a plausible, two-layer structure to be evolved on the basis of which a set of travel times has been calculated for the different crustal phases of body waves.

Auto-correlation and spectral methods were successfully used to pick out depth phase from Koyna seismograms. Systematic application of correlation filtering methods has indicated the possibility of increasing the precision with which the array could detect and locate seismic sources in the core shadow region, and to reduce the threshold of detection.

Details of focal mechanisms of the recent major Indian earthquakes (Koyna and Bhadrachalam) were worked out.

(ii) Theoretical Seismology

The analytical study for assessing the influence of surface irregularities near the surface on the structure of the seismic signal for low frequency excitations has been completed. The problem of phase change of surface waves propagated around the spherical earth was also investigated.

(iii) Study of Atomospheric Pressure Waves

The technique of locating atomospheric explosions, from the pressure waves recorded by the microbarograph net work was improved by gaining a better understanding of the mode of propagation of these waves in the real atmosphere. Dispersion relations based on the recorded pressure wave signals from atmospheric explosions were obtained for the average atmosphere between Central Asia and the microbarograph stations. Interesting correlation between internal gravity wave signals and meteorological disturbances was found.

4. Systems Development

Preliminary work on site selection, field engineering and other details connected with the installation of a triangular array of high gain vertical seismometers at Gauribidanur was completed. The system, which is expected to be installed by the middle of next year, will provide simultaneous recording of the vertical component of earth motion in the period range from 6 seconds, at the centre as well as the two extremities of the existing array. Field studies at Gauribidanur have established the feasibility of telemetering reliably long period seismic signals over distances of upto 40 kms. using systems built around indigenous wireless transreceiver equipment.

Considerable progress was made in prototypes studies of the subassemblies required for an array of geophones meant to be installed in the Kolar Gold Mines for the purpose of locating precisely the focii of rockbursts.

E. DEVELOPMENT OF SPECIAL NUCLEAR INSTRUMENTS

I. Isotope Separator

(V.A. Hattangadi, R.P. Anand*, F.R. Bhathena,
K.L. Patel, C.V. Rayarappan and E. Shallom)

A high voltage, regulated power supply has been constructed for use as the ion accelerator supply in the electromagnetic isotope separator, DUMAS which is now under construction. The power supply has two independent outputs providing 55 kV D.C. at 100 mA, stabilised to better than1 in 10^4 . The control circuits are transistorised although the regulation is done through a high voltage series tube (450 TH). The entire circuit, including the low-drift D.C. amplifier and the isolation pulse transformer (with 75 kV primary- to - secondary insulation) was designed and developed in the section using indigenous transistors and components. Preliminary tests have shown the output ripple to be less than 4 in 10^5 at 40 kV D.C., which is indicative of the regulation achieved. Further rigorous tests, under full load conditions are in progress.

An arc current stabiliser, using SCR's for control and a transistorised D.C. ripple filter circuit for the ion-source magnet supply have also been developed and tested on the test bench. The fabrication of the vacuum system for the new separator was also started during the current year. A prototype diffusion pump assembly, with its own by-pass valves, water-failure alarm system etc., was constructed and tested; six more such trolleys are now under construction. The fabrication of the vacuum chambers on the ion-source limb is nearly completed. The"drift chamber" is completed and the construction of the ion-source magnet and chamber is nearing completion. A number of vacuum components required for the system, such as the gate valves, leak tight rotating shaft seals, high current electrical feed-through insulators etc., have also been designed and some of these are under fabrication.

The ion-source itself has been redesigned with a number of improvements and modifications that have suggested themselves from past experience.

The new ion-source boxes are also being fabricated.

The electromagnetic isotope separator at TIFR was also run during the year for production of Mg, Ca, Zn and Cl isotopes in milligram quantities. The on-line chlorination of the charge materials was also tried in one of these separations.

II. Nuclear Detectors

The Section was engaged in (a) production of BF_3 neutron detectors, (b) development and production of Helium-3 neutron detectors, (c) development and production of soft x-ray counters and (d) preliminary investigations in neutron radiography.

a) BF_3 Neutron Detectors

Over a hundred standard counters including four fast neutron detectors were fabricated and supplied to various users in the Division as well as in other divisions and institutions. Some counters were also sent to users in other countries.

Apart from this standard production, development work on (i) a position-sensitive BF_3 counter (ii) fast neutron dosimeters (for the Health Physics Division) and (iii) a spherical fast neutron proportional counter has been carried out.

b) Helium-3 Neutron Detectors

Some more helium-3 detectors have been made in different sizes.

c) Soft X-ray Proportional Counter

Several argon-filled detector for Mossbauer Spectroscopy have been made. The design has been improved considerably and a resolution of 13% for the 14.4 kev photons have been reached. Apart from the divisional needs, 12 counters have been sent to other institutions in the country. The xenon-filled detectors with beryllium windows have been developed and will be put in production

next year. A 15 cm dia., 45 cm long counter is under fabrication. An end-window counter, for better efficiency, is also being designed.

d) Neutron Radiography

Neutron Radiography is fast becoming a very useful tool in the field of non-destructive testing. Preliminary investigations have been undertaken to find suitable applications. Using indium and gadolinium detector foils, various initial parameters such as beam profiles, optimum foil thicknesses and exposure times were determined experimentally. Satisfactory radiographs have been obtained of various test objects like cadmium, natural uranium, uranium oxide, plastics and perspex. Image resolution of better than 0.012 cm has been achieved.

Investigations are now being made to apply this technique for the determination of the helium content in the cobalt absorbers fabricated for RAPP. Initial results show that at least a qualitative determination of the gas present is feasible.

III. Electronic Instrumentation for Automatic Data Collection

(Virender Singh, V.M. Shah, J.N. Joshi, V.G. Gaonkar and R.S. Kothare)

Apart from producing a number of automatic data collecting systems during this period the following special systems have also been developed.

1. Mossbauer Constant Velocity Drive Units

A circuit was developed to achieve good linearity for the loud speaker drive in the Mossbauer Spectrometer described in Section B.VI.2. In this drive, application of a triangular wave form across the voice coil terminals results in constant velocity motion as shown in Fig.42. Keeping the frequency fixed it is possible to change the velocity by changing the amplitude of the triangular waveform. However at the change over point when the velocity goes from positive to negative and negative to positive non linearity in velocity is present. Hence it becomes necessary to inhibit Detector signal entering into data collection system, during this

non linear region. This is achieved by gating the pulses from the counter.

The schematic diagram comprising the

(a) symmetrical saw tooth generator

(b) delay generators and

(c) power amplifier can be seen in Fig.42.

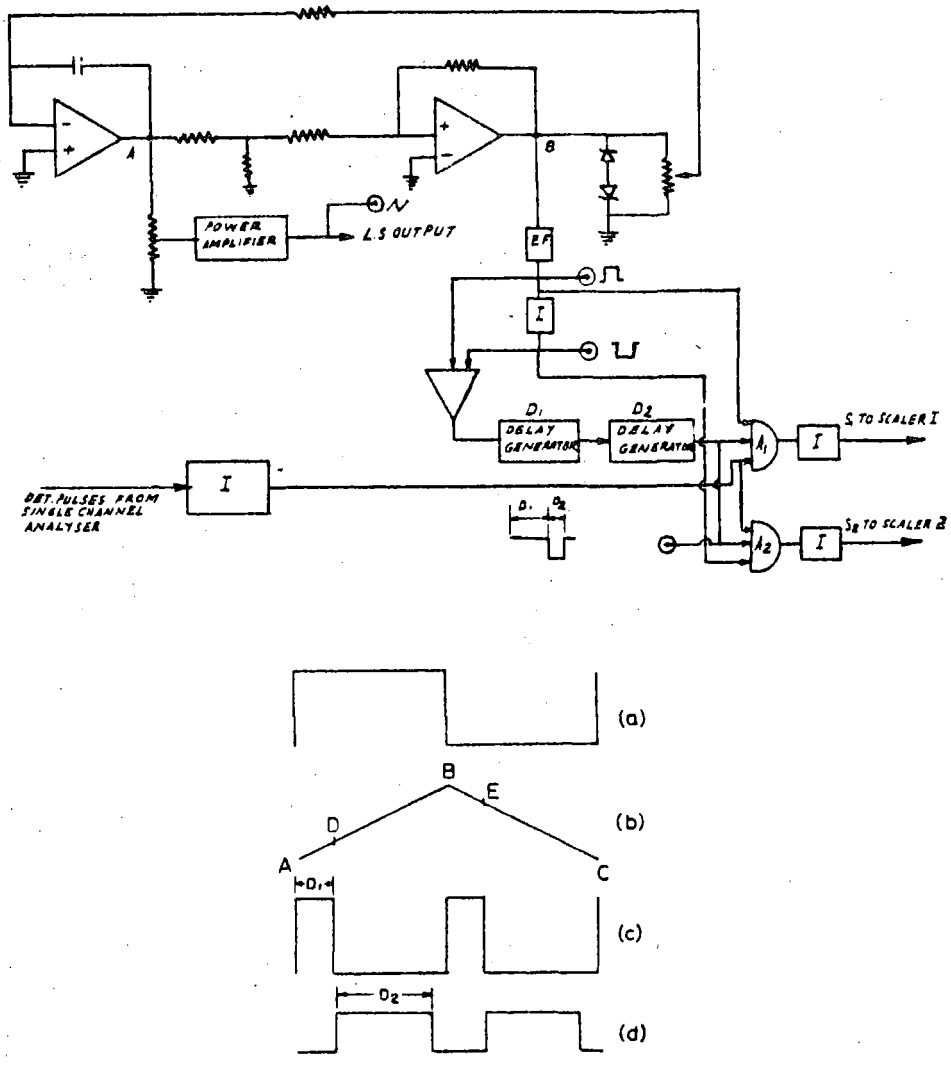

Fig. 42. Logic Diagram of the Mossbauer Drive control unit.

Square waves and triangular waves are generated with the help of two

operational amplifiers. Triangular waves available at point A are connected to the power amplifier through the remote helipot (for velocity selection) and its output made to drive the voice coil.

Delay D_1 is generated with every start of the forward as well as the backward motion of the source by delay generator D_1. During this period the detector signal is inhibited from entering the scalers. After the termination of D_1 another gate is generated by the delay generator D_2.

A coincidence gate A_1 formed by the detector signal, the square wave and D_2 is used to route the detector pulses to enter the first scaler, during a part of the motion, say, forward; similarly the coincidence gate A_2 formed by the detector signal, the complementary square wave and D_2 is used to route pulses to the other scaler during the backward motion.

2. Time-to-Pulse Height Converter Unit

This unit in modular style is for accurate time measurement between any successive pair of pulses and storing such information on a pulse height analyser. This is achieved by initiating a ramp by the first pulse and terminating it by the second pulse. Thus the height of the ramp thus generated is directly proportional to the time delay between these two pulses. A time span of 0-1, 0-10, 0-100 μ sec. is achieved by selecting different time constants in the ramp generator.

3. Dead Time Controller

This instrument also in modular style has two modes of operation.

(i) Fixed dead time controller

(ii) Variable dead time controller

In its fixed dead time controller mode of operation pulses of input signal are formed into pairs. Output is available only when the time interval between these pair of pulses is more than the selected time which is from 1 to 100 μ sec in steps of 1 μ sec.

In the second mode of operation pulses are not formed in pairs but output is available only when the time difference between any two successive pulses is more than the selected time.

4. Modular Interface Unit for Solenoid Operated Printer

After successful operation of an interface unit for teletype page printer[1], the system logic was modified to suit a solenoid operated printing machine as shown in Fig. 43.

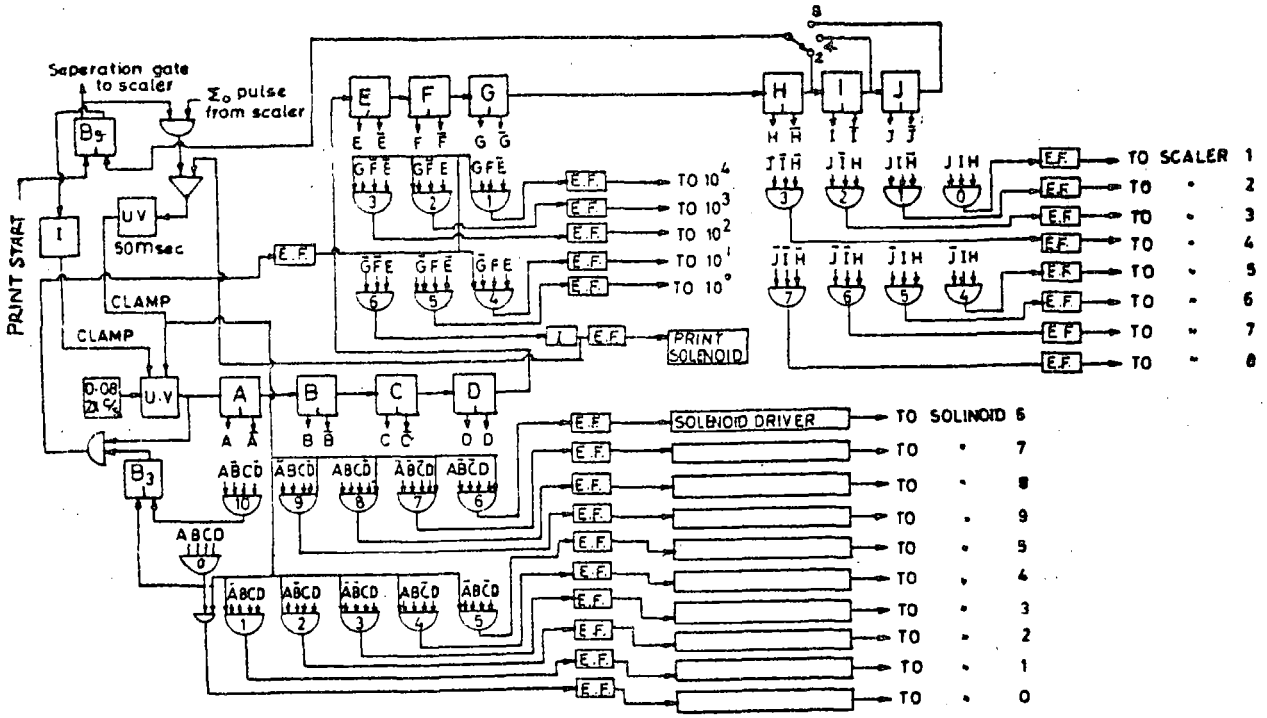

Fig. 43. Logic of the interface unit for Solenoid Printer.

The principle of data transfer from the external to the internal scaler is the same as before. However, signals like space command, parity, line feed and carriage return are not required in this case but only a print command signal is required once all the decades of each scaler have been scanned and the number is stored in the machine. The system logic has been successfully tested on a solenoid operated printer.

---

1. BARC-501 Annual Report of the Nuclear Physics Division, 1969-70, p.88.

PUBLICATIONS

I. PAPERS PUBLISHED DURING 1970

1. Intermediate Structure Effects in the Fission of some Actinide Nuclei: D.K. Sood and N. Sarma, Nucl. Phys. A151, 532-548 (1970)
2. The Reaction $^{19}F(d, \alpha)^{17}O$: M.G. Betigeri, C.M. Lamba, N. Sarma, D.K. Sood and N.S. Thampi, Energica Nucleare, Vol. 17, Numero 4 (1970)
3. Distorted Wave Analysis of Deuteron knock-out from ^{6}Li: A.K. Jain, N. Sarma and B. Banerjee, Nucl. Phys. A 142, 330 (1970)
4. Charge Form Factor and Quadrupole Moment of ^{6}Li: A.K. Jain and N. Sarma, Phys Letters 33 B, 271 (1970)
5. Super Heavy Nuclei - The Present Status: S.S. Kapoor, Physics News Vol. No. 1, 17 (1970)
6. Precise Measurements of the Average Total Kinetic Energy of in the Fast Neutron Fission of ^{235}U: N.N. Ajitanand, Nucl. Phys. A 144, 1, (1970)
7. Fundamental Studies of Fission Process in Heavy Nuclei: S.S. Kapoor, S.K. Kataria, S.R.S. Murthy, D.M. Nadkarni, V.S. Ramamurthy, P.N. Rama Rao and R. Ramanna, Report on work performed on Research Contract No. 535 RB/IAEA
8. K x-ray yields in 0-1 μs from ^{236}U Fragments: S.K. Kataria, S.S. Kapoor, S.R.S. Murthy and P.N. Rama Rao, Nucl. Phys. A 154, 458-466 (1970)
9. Excitation Energy Dependence of Shell Effects on Nuclear Level Densities: V.S. Ramamurthy, S.S. Kapoor and S.K. Kataria, Phys. Rev. Letters Vol. 5, No. 6, p. 386 (1970)
10. Excitation Energy Dependence of Shell Effects on Nuclear Level Densities: V.S. Ramamurthy, S.S. Kapoor and S.K. Kataria, Phys. Rev. Letters Vol. 5, No. 6, 386 (1970)
11. O-H.....S bonds in $Na_2S_2O_5$, $5H_2O$: V.M. Padmanabhan and V.S. Yadava, Curr. Sci. 39, 181, (1970)
12. Potential Functions for Hydrogen Bond Interactions I. A Modified Lippincott - Schroeder Potential Function for N-H....O Interaction Between Peptide Groups: R. Chidambaram, R. Balasubramanian and G.N. Ramachandran, Biochem. Bio Phys. Acta, 221, 182 (1970)

13. Potential Function for Hydrogen Bond Interactions II. Formulations of an Emperical Potential Functions: R. Balásubramanian, R. Chidambaram and G.N. Ramachandran, Biochem. Bio. Phys. Acta, 221, 196 (1970)

14. Application of the Symbolic Addition Procedure in Neutron Diffraction for Non-Centrosymmetric crystals, S.K. Sikka, Acta cryst. A26, 662, (1970)

15. Neutron Diffraction Refinement of the Crystal Structure of Potassium Copper Chloride Dihydrate: R. Chidambaram, A. Sequeira and S. Srikanta Acta Cryst. B 26, 827 (1970)

16. Atomic and Magnetic Structure of the Heusler Alloys: M.G. Natera, M.R.L.N. Murthy, R.J. Begum and N.S. Satya Murthy, Phy. Stat. Sol. (a) 3, 959 (1970)

17. Observation of Librational Modes of Water Molecules in Single Crystal Hydrates by Neutron Scattering: C.L. Thaper, B.A. Dasannacharya, A. Sequeira and P.K. Iyengar, Solid State comm. 8, 497 (1970)

18. Study of Molecular Reorientation in Solids by Slow Neutron Scattering: H.J. Kim, P.S. Goyal, G. Venkataraman, B.A. Dasannacharya and C.L. Thaper, Solid State comm. 8, 889 (1970)

19. Lattice Dynamics of $NaNo_3$ - A group theoretical analysis: K.R. Rao, S.F. Trevino and K.W. Logan, J. Chem. Phys. 53, 4645 (1970)

20. Lattice Dynamics of KN_3 - A group theoretical analysis: K.R. Rao and S.F. Trevino, J. Chem. Phys. 53, 4661 (1970)

21. External Vibrations in Complex Crystals: G. Venkataraman and V.C. Sahni, Rev. Mod. Phys. 42, 409-470 (1970)

22. On a method of Constructing Irreducible Multiplier Representations: V.C. Sahni and G. Venkarataman, Phys. Kondens. Materic 11, 199-211 (1970)

23. Irreducible Multiplier Representations for some points in the Brillouin zone of D_6^4: V.C. Sahni and G. Venkataraman, Phys. Kondens. Materie 11, 212-219 (1970)

24. Method of Short-Range Potentials in Quantum Mechanics - Bound States: R. Subramanian and Vestnik Leningradskogo, Universiteta, 10(2) 10(1970)

25. Detection and Location of Atmospheric Nuclear Explosions by Microbarograph Arrays: T.G. Varghese and Vijai Kumar, Nature 225, 259-261 (1970)

26. Some Aspects of Structure of Southern India Based on Recent Bhadrachalam Earthquakes: S.K. Arora, T.G. Varghese and C.A. Krishnan, Nature 225, 261-262, (1970)

27. New Approaches to Study of Local Seismic Phenomena: T.G. Varghese, Journal of Indian Geophysical Union, Vol. 7, No.(1), 29 (1970)

28. New Tables of Angles of Incidence of P waves as a Function of Epicentral Distance: A.R. Banghar, Earthquake Notes Vol. XLI, No. 2, 45 (1970)

29. Dispersion of SH body wave in a continuously Stratified Half Space: A.R. Banghar, Pure and Applied Geophysics Vol. 82, 46 (1970)

30. A. Surface Reflected Phase from Koyna After Shocks: G.S. Murthy, Indian Journal of Meteorology and Geophysics. Vol. 21, 479 (1970)

31. Calculation of K_{eff} for a bare Pu sphere by Collision Probability Method: M.P. Navalkar and S.B.D. Iyengar, Atomkernergie. Bd(1970)

II. PAPERS PRESENTED AT CONFERENCES DURING 1970

1. A Doorway State Observed as a Resonance in the ^{35}Cl (p,po) Reaction: S.K. Gupta, S.S. Kerekatte, S. Swami, M.R. Dwarakanath, K.K.Sekharan and A.S. Divatia, (N-13)*, 1970
2. A Study of $^{64}Ni(p,n)^{64}Cu$ Reaction: S.S. Kerekatte, S.K. Gupta and A.S. Divatia, (N-14),1970
3. Evidence of Doorway State in $^{29}Si(\alpha,n)^{32}S$ Reaction: M. Balakrishnan, M.K. Mehta and A.S. Divatia, (N-15),1970
4. A Pre-Injection e/m Analyzer System for use with Van de Graaff Ion Sources: S.N. Misra and M.R. Dwarakanath, (N-90), 1970
5. Lowest T = 3/2 State in ^{33}Cl observed as Resonance in $^{32}S(p,\gamma)^{33}Cl$ Reactions: M.A. Eswaran, M. Ismail and N.C. Ragoowansi, (N-12) 1970
6. Isobaric Analogue States in ^{67}Ga: M.G. Betigeri, C.M. Lamba, N. Sarma D.K. Sood and N.S. Thampi, (N-16), 1970
7. Study of the Two Hole States in ^{12}C Nucleus with the (π^-,nn) Reaction: B.K. Jain, (N-52), 1970
8. Triton Knock out from ^{7}Li Nucleus: A.K. Jain and N. Sarma, (N-53), 1970
9. Analysis of (p,2p) and (e,e'p) Reactions of ^{12}C Nucleus: R. Shanta and B.K. Jain, (N-56), 1970
10. Dynamic Correlations in Atomic Nuclei: B.K. Jain, (I-4), 1970
11. Ion-Optics of a Split - Pole Magnetic Spectrograph by method of Ray-Tracing: S. Das and N. Sarma (N-101), 1970
12. Half-Life of the 126 KeV Level in ^{124}Te by Beta-Gamma perturbed Angular Correlations: A.P. Agnihotry, M.C. Joshi and K.G. Prasad (N-127), 1970
13. Half Life Magnetic Moment of $(9/2^+)$ State in ^{103}Rh: C.V.K. Baba, S.K. Bhattacherjee and H.C. Jain, International Conference on 'Hyperfine Interactions detected by Nuclear Radiation' Rehovoth, Jerusalem September 1970
14. Transient Field on Rh in Fe at Low Recoil Energies: S.K. Bhattacherjee, H.G. Devare, H.C. Jain, M.C. Joshi and C.V.K. Baba, International Conference on 'Hyperfine Interactions detected by Nuclear Radiation' Rehovoth, Jerusalem

*The numbers I-, N-, and S- refer to the Serial numbers of abstracts of papers presented at the Nuclear Physics and Solid State Physics Symposium of the Department of Atomic Energy held at Madurai University December 28-31, 1970.

15. Nuclear Moments and Hyperfine Fields: C.V.K. Baba, (I-7) 1970

16. Half Life of the 126 KeV State in ^{109}Ag: H.C. Jain, S.K. Bhattacherjee and C.V.K. Baba, (N-127), 1970

17. An unified Theory on the Structure of Atoms and Nuclei: R. Ramanna and S. Jyothi, (N-80), 1970

18. On Atoms and Nuclei: R. Ramanna, Indian Academy of Science Meetings, Bangalore (1970)

19. Shell Effects on Nuclear Level Densities: V.S. Ramamurthy, S.K. Kataria and S.S. Kapoor, (N-84), 1970 p. 271

20. On the Production Possibility of Superheavy Nuclei: V.S. Ramamurthy and S.S. Kapoor, (N-85), 1970 p. 279

21. Further Studies of K x-ray Emission from ^{252}Cf Fragments: S.S. Kapoor, D.M. Nadkarni, S.R.S. Murthy, V.S. Ramamurthy and P.N. Rama Rao, (N-72), 1970 p. 349

22. Delayed Gamma-Ray Emission in the Spontanious Fission of ^{252}Cf: N.N. Ajitanand, (N-71), 1970 p. 339

23. Excitation Functions for the Neutron Induced Fission of Heavy Nuclei: K.N. Iyengar, R.H. Iyer, S.S. Kapoor, D.M. Nadkarni and M.L. Sagu, (N-18), 1970 p. 67

24. Emission of Long Range Charged Particles in the Fission of ^{235}U by Thermal to 4 MeV Neutrons: D.M. Nadkarni, and S.S. Kapoor, (N-19), 1970 p. 7.

25. Magnetic Structures of Some Spinel Ferrites by Polarised and Unpolarised Neutron Diffraction: N.S. Satya Murthy, M.G. Natera, R.J. Begum and S.I. Youssef (8B 1.2) International Conference on Ferrites, Kyoto, June 1970

26. Exchange Integrals in Some Spinels by Paramagenetic Neutron Scattering: N.S. Satya Murthy, L. Madhav Rao, N.G. Natera and S.I. Youssef, (8B 1.5), International Conference on Ferrites, Kyoto, June 1970

27. Neutron Scattering Studies of Some Spinels: N.S. Satya Murthy, L. Madhav Rao, R.J. Begum, M.G. Natera and S.I. Youssef (MeA-8) International Conference on Magnetism Grenoble, September, 1970

28. Magnetic Structure and Exchange Integral Measurements in $TlMnF_3$: L. Madhav Rao and N.S. Satya Murthy (MeA-12), International Conference on Magnetism, Grenoble, September 1970

29. Neutron Diffraction Studies in some Ternary Alloys: M.R.L.N. Murthy, R.J. Begum and N.S. Satya Murthy, (S-104), 1970

30. The Atomic and Magnetic Structure of Co_2TiO_4: R.J. Begum, L. Madhav Rao and N.S. Satya Murthy, (S-105), 1970
31. Exchange Integrals in Some Spinel Ferrites: R.J. Begum, L. Madhav Rao, S.K. Paranjpe and N.S. Satya Murthy, (S-106), 1970
32. Spin Relaxation of Fe^{3+} Ion in Ferrites using Mossbauer Effect: P.K. Iyengar and S.C. Bhargava, (S-108), 1970
33. Lattice Dynamics of Calcium Oxide: P.R. Vijayaraghavan and P.K. Iyengar (S-133), 1970
34. Polariton Dispersion Relations in Ca WO_4: V.C. Sahni and G. Venkataraman, (S-134), 1970
35. Frequency Distribution and Thermo-dynamic Properties of Solid Ammonia: P.S. Goyal, B.A. Dasannacharya, C.L. Thaper and P.K. Iyengar, (S-136) 1970
36. Group Theoretical Study of Lattice Dynamics of KN_3, NaN_3 and $NaNO_3$: K.R. Rao and S.F. Trevino, (S-158), 1970
37. Dispersion Relations for Phonons in KN_3: K.R. Rao, S.F. Trevino, H. Prask and R. Mical, (S-159), 1970
38. Atomic Correlations in Liquids: K.R. Rao, (I-5), 1970
39. A Special Case of the Saxon-Hunter Theorem for Three Dimensional Potentials: K.V. Bhagwat and R. Subramanian, (S-8), 1970
40. Spin orientation in Magnetic Materials by Neutron Diffraction and Mössbauer Effect: P.K. Iyengar, (I-1), 1970
41. Paramagnetic Scattering of Neutrons from $KMnF_3$ in the Short Range Ordered Region: K. Usha Deniz and P.S. Goyal, International Conference in Magnetism, Grenoble, September, 1970
42. Earthquake data from Gauribidanur: T.G. Varghese, Annual Meeting of Indian Academy of Sciences, Bangalore, September, 1970
43. Role of Seismometer arrays in Rock Burst Studies: Symposium on Rock Mechanics, Kolar Gold Fields, November, 1970.
44. A method of Measurement of Absolute Disintegration Rate of a Radio-Active Source: O.P. Joneja, J.S. Coachman and M.P. Navalkar, (N-99), 1970

III. B.A.R.C. REPORTS PUBLISHED DURING 1970

1. TANIMULA - A Programme for Refinement of Structure Factor Phases by Karle-Hauptman Tangents Formula: S.K. Sikka, BARC-491(1970)
2. Report of the work done at Korean Atomic Energy Research Institute: M.P. Navalkar, BARC/I-98(1970)
3. Computer Screening of Applications for Training School: K. Subbukutty, O.P. Joneja and M.P. Navalkar, BARC/I-101
4. Geographic Locations and Geocentric Direction cosines of Seismograph Stations: A.R. Banghar, BARC-53(1970)
5. Revised Lag Tables for Array Analysis: S.K. Arora, BARC-59(1970)
6. Nuclear Explosion Data from Gauribidanur Array: S.K. Arora and C.A. Krishnan, BARC-64(1970)

IV. THESES SUBMITTED TO UNIVERSITIES DURING 1970

1. Study of Low Energy (p,n) Reactions in Medium-weight Nuclei: S.K. Gupta, (Ph.D) University of Bombay.
2. Study of the Magnetic Properties of some Alloys and Compounds by Neutron Scattering: R.J. Begum (Ph.D) University of Bombay.
3. Neutron Scattering Studies in Some Magnetic Insulators: L. Madhav Rao (Ph.D) University of Bombay.
4. Studies of K x-rays in the Thermal Fission of ^{235}U: S.K. Kataria (M.Sc) University of Bombay.

LECTURES HELD UNDER THE AUSPICES OF THE PHYSICS COLLOQUIM DURING 1970

	Speaker	Title of Lecture	Date
1.	Shri P.S.Parvathanathan	Surface Studies Using Mossbauer Effect	14.4.70
2.	Dr.B.K. Jain	Study of the Atomic Nucleus with New Probes	21.4.70
3.	Shri P.S. Goyal	Molecular Dynamics and the Neutrons	28.4.70
*4.	Dr.Y.R. Waghmare (Indian Institute of Technology, Kanpur)	Effective Interactions in Nuclei	16.6.70
5.	Shri O.P. Joneja	Review of Fast Neutron Spectrum Measurements	23.6.70
6.	Prof.N.Austern (University of Pittsburgh)	Stripping Form Factors	14.7.70
7.	Dr. S.K. Gupta	Systematics of Ground State Spins of Light odd-odd Nuclei	21.7.70
8.	Shri P.R.Vijayaraghavan	Lattice Dynamics of Fluorite Structures	4.8.70
9.	Dr.V.M. Padmanabhan	Study of Dislocations in Crystals	11.8.70
10.	Dr.(Smt.) Usha Deniz	Liquid Crystals	18.8.70
11.	Dr.D.D.Bhawalkar (Electronics Division)	Recent Developments in High Power Lasers	25.8.70
12.	Shri N.N.Ajitanand	Recent Investigations in Fission at Lucas Heights	8.9.70
13.	Shri B.Lal	Compound Inelastic Scattering of Nucleons	15.9.70
14.	Dr. G.P. Phondke (Biology Division)	Physics and Life Sciences	22.9.70
15.	Dr.K.R. Rao	Neutron-Electron Interaction	29.9.70
16.	Dr.S. Ramani (Tata Institute of Fundamental Research)	Third Generation Computers for Data Acquisition and Control	13.10.70
17.	Shri A.K. Jain	Energetically favoured Sub-structures in Nuclei	20.10.70

	Speaker	Title of Lecture	Date
18.	Shri K.V. Bhagwat	Some applications of delta-function potentials to problems in three dimensions	24.11.70
19.	Dr.(Smt.) Jyoti K.Parikh	Structure Calculations in p-f shell nuclei	8.12.70

* The affiliations of speakers not belonging to the Nuclear Physics Division are shown in parantheses.

NUCLEAR PHYSICS DIVISION STAFF

Dr. R. Ramanna	Director, Physics Group
Dr. P.K.Iyengar	Head, Nuclear Physics Division

A. NUCLEAR PHYSICS

I. Nuclear Reactions and Nuclear Spectroscopy

*1. Dr. A.S. Divatia
2. Dr. M.K. Mehta
3. Shri M. Balakrishnan
**4. Dr. M.R. Dwarakanath
5. Shri C.V. Fernandez
6. Dr. S.K. Gupta
7. Shri S.S. Kerekatte
8. Shri S.S. Saini

9. Dr. M.A. Eswaran
10. Shri M. Ismail
11. Shri H.H. Oza
12. Shri N.L. Ragoowansi

13. Dr. N.Sarma
14. Dr.M.G. Betigeri
15. Shri A.K. Jain
16. Dr. B.K. Jain
17. Shri C.M.Lamba
18. Dr. D.K. Sood
19. Shri N.S. Thampi
20. Dr.(Smt.) Jyothi K. Parikh(Visiting Member)
21. Dr.(Kum.) R. Shanta (Visiting Member)

22. Dr. C.V.K. Baba
23. Shri V.S. Ambekar
24. Shri P.J. Bhalerao
25. Shri M.G. Patwardhan
26. Shri M.Y. Vaze

---

* Also attached to Variable Energy Cyclotron Project

** Left the Centre in November 1970

II. Fission Physics

1. Dr. R. Ramanna
2. Dr. S.S. Kapoor
3. Shri N.N. Ajitanand
4. Shri B.R. Ballal
5. Shri S. Jyothi
6. Shri S.K. Kataria
7. Shri Madan Lal
8. Shri S.R.S. Murthy
9. Dr. D.M. Nadkarni
10. Shri V.S. Ramamurthy
11. Shri P. N. Rama Rao
12. Shri S.L. Raote

B. SOLID STATE PHYSICS

I. X-ray Crystallography

1. Dr. V.M. Padmanabhan
2. Shri S. Mehdi Ali
3. Shri V.K. Wadhawan
4. Shri V.S. Yadava

II. Neutron Crystallography

1. Dr. R. Chidambaram
2. Shri S.N. Momin
3. Shri H. Rajagopal
4. Shri M. Ramanadham
5. Dr. A.S. Sequeira
6. Dr. S.K. Sikka
7. Shri R.R. Bugayong (Colombo Plan Fellow from the Philippines)

III. Neutron Diffraction Studies of Magnetic Materials

*1. Dr. N.S. Satya Murthy
2. Dr. (Smt) R.J. Begum
3. Dr. L. Madhav Rao
4. Shri M.R.L.N. Murthy
5. Shri S.K. Paranjpe
6. Shri V.C. Rakhecha
7. Shri C.S. Somanathan
8. Shri B.S. Srinivasan
9. Shri B.G. Yoon (IAEA Fellow from Korea)
10. Shri N.K. Radhakrishnan (Research Student of the Indian Institute of Technology)
11. Shri G.R. Tendulkar (Research Associate from the University of Bombay)

---

* On deputation at AERE, Harwell, U.K. from September, 1970.

IV. Neutron Inelastic Scattering, Lattice Dynamics Molecular Physics

1. Dr. P.K. Iyengar
2. Dr. G. Venkataraman
3. Shri R.N. Aiyer (on loan to Training Division)
4. Shri K.V. Bhagwat
5. Dr. B.A. Dasannacharya
6. Shri P.K. Dayanidhi
7. Dr. (Smt.) Usha Deniz
8. Shri A.S. Deshpande
9. Shri P.S. Goyal
10. Smt. I.Y. Mithani
11. Shri R.V. Nandedkar
12. Smt. A.S. Paranjpe
13. Dr. K.R. Rao
14. Dr. A.P. Roy
15. Shri V.C. Sahni
16. Shri S.N. Siva (on loan to Technical Physics Division)
17. Shri T. Srinivasan
18. Dr. R. Subramanian
19. Shri C.L. Thaper
20. Shri P.R. Vijayaraghavan
21. Shri T.R. Rao (Research student of the University of Bombay)

V. Mossbauer Studies

1. Dr. P.K. Iyengar
2. Shri S.C. Bhargava
3. Shri P.S. Parvathanathan

C. REACTOR NEUTRON PHYSICS

I. Experimental Measurements

1. Dr. M.P. Navalkar
2. Shri J.S. Coachman
3. Shri S.B.D. Iyengar
4. Shri Jagir Singh
5. Shri O.P. Joneja
6. Shri M.R. Phiske
*7. Shri D.V.S. Ramakrishna
8. Shri S.K. Sadavarte
9. Shri K. Subbukutty

---

* On deputation at Institute for Reaktorentuicklung, Julich, West Germany from September 1970.

II. Pulsed Fast Reactor Project

1. Dr.P.K. Iyengar
2. Shri T.K. Basu
3. Shri K. Chandramoleshwar
4. Shri S. Das
5. Dr. V.R. Nargundkar
6. Shri M. Srinivasan
7. Shri K. Subbarao

D. SEISMOLOGY SECTION

Research and Gauribidanur Array Operations

1. Shri T.G. Varghese
2. Shri S.K. Arora
3. Shri A.R. Banghar
4. Shri R.N. Bharthur
5. Shri M.K. Bhat
6. Shri Jayachandran Nair
7. Shri G.V. Kolvankar
8. Shri C.A. Krishnan
9. Shri A.M. Manekar
10. Shri P.C. Mitra
11. Dr. G.S. Murty
12. Shri Ram Datt
13. Shri T. Ramanunny
14. Shri K.K. Sankaran
15. Shri H.S. Seetharama Sharma
16. Shri B.M. Shah
17. Shri S.R. Singh
18. Shri T.V. Sridharan
19. Shri K.R. Subbaramu
20. Shri Vijai Kumar Jain

E. OTHER ACTIVITIES

I. Nuclear Detectors, Isotope Separator etc.

1. Shri Y.D. Dande
2. Shri V.A. Hattangadi
3. Shri R.P. Anand
4. Shri A.P. Bagool
5. Shri F.R. Bhathena
6. Shri S.R. Chinchanikar
7. Shri K.L. Patel
8. Shri C.V. Rayarappan
9. Shri E. Shallom
10. Shri G.V. Shenoy
11. Shri R.S. Udyavar

II. Van de Graaff Operation and Maintenance

1. Shri T.P. David
2. Shri M.S. Bhatia
3. Shri G.V. Bhatt
4. Shri D.S. Bisht
5. Shri M.E. Doctor
6. Shri N. Fernandez
7. Shri R.P. Kulkarni
8. Shri S.J. Mandke
9. Shri S.N. Misra
10. Shri A.V. Mulay
11. Shri R.V. Patkar
12. Shri S.G. Shukla
13. Shri P.R. Sunder Rao

III. Electronics

1. Shri V. Singh
2. Shri V.G. Goankar
3. Shri J.N. Joshi
4. Shri N.D. Kalikar
5. Shri R.S. Kothare
6. Shri V.M. Shah

IV. Workshop

1. Shri J.N. Soni
2. Shri K.R. Dhall
3. Shri J.S. Chawla
4. Shri V.B. Dikshit
5. Shri P. Narayanan
6. Shri C.S. Patil
7. Shri V.D. Sansare
8. Shri S.R. Sawant

F. ADMINISTRATIVE STAFF

1. Shri T. Ramanujam
2. Shri M.M. Nair
3. Shri T. Ajayakumar
4. Smt. M. Aprane
5. Shri D.R. Gaikwad
6. Shri C.C. John
7. Shri C.P. Rajagopal
8. Shri M.T. Thomas